"Brain-Computer Interfaces for patients with Amyotrophic Lateral Sclerosis"

Dissertation

zur Erlangung des Grades eines
Doktors der Naturwissenschaften

der Mathematisch-Naturwissenschaftlichen Fakultät
und
der Medizinischen Fakultät
der Eberhard-Karls-Universität Tübingen

vorgelegt
von Tatiana Fomina

aus Magnitogorsk, Russland

September - 2016

Tag der mündlichen Prüfung: 13.03.2017

Dekan der Math.-Nat. Fakultät: Prof. Dr. W. Rosenstiel
Dekan der Medizinischen Fakultät: Prof. Dr. I. B. Autenrieth

1. Berichterstatter: Dr. Moritz Grosse-Wentrup

2. Berichterstatter: Prof. Dr. Niels Birbaumer

Prüfungskommission: Dr. Moritz Grosse-Wentrup
    Prof. Dr. Niels Birbaumer
    Prof. Bernhard Schölkopf
    Dr. Axel Lindner

Erklärung / Declaration:

I hereby declare that I have produced the work entitled "Brain-Computer Interfaces for patients with Amyotrophic Lateral Sclerosis", submitted for the award of a doctorate, on my own (without external help), have used only the sources and aids indicated and have marked passages included from other works, whether verbatim or in content, as such. I swear upon oath that these statements are true and that I have not concealed anything. I am aware that making a false declaration under oath is punishable by a term of imprisonment of up to three years or by a fine.

Tübingen, den: _____ _____

                           Datum/Date   Unterschrift/Signature

Abstract

Electroencephalographic (EEG) brain-Computer Interfaces (BCIs) hold promise to restore communication with completely locked-in (CLIS) patients with Amyotrophic Lateral Sclerosis (ALS). However, these patients cannot use existing EEG-based BCIs, possibly because such systems rely on brain processes that are impaired in ALS. We propose to use for BCI for ALS patients high cognitive processes connected to consciousness, because ALS patients should be able to use such BCI as long as they are fully conscious. We introduce a BCI based on neurofeedback from precuneus, brain area linked to consciousness. We describe two cases of successful use of the BCI by ALS patients, with stable online performance over the course of disease progression. Additionally, we show that training time can be improved by replacing the neurofeedback with direct instructions, contrasting self-referential and neutral thoughts. We further investigate self-referential thinking in ALS and find differences in the EEG correlates of self-referential thinking between ALS and healthy controls. This finding raises the question of awareness and consciousness in CLIS ALS. We propose a method that may serve as basis for consciousness detection in CLIS ALS patients: EEG-based identification of the Default Mode Network (DMN), brain resting-state network closely linked to consciousness.

Abbreviations

ALS	Amyotrophic Lateral Sclerosis
BCI	Brain-Computer Interface
BOLD	Blood-oxygen-level dependent
CLIS	Completely Locked-In State
DMN	Default Mode Network
EcOG	Electrocorticography
EEG	Electroencephalography
ERP	Event-Related Potential
fMRI	Functional Magnetic Resonance Imaging
FTD	Frontotemporal Dementia
FTND	Frontotemporal Neuron Degeneration
LIS	Locked-In State
MPFC	Medial Prefrontal Cortex
PET	Positron Emission Tomography
REM	Rapid Eye Movement
SMC	Sensorimotor Cortex
SMR	Sensorimotor Ryhthm
SNR	Signal-to-Noise Ratio
SPECT	Single Photon Emission Computer Tomography

Contents

Chapter 1

Synopsis

The Synopsis is structured as follows. First, I describe Amyotrophic Lateral Sclerosis (ALS) and ALS patients' need for Brain-Computer Interfaces (BCI). Then, I introduce electroencephalography as one possible BCI tool and discuss the state of the art in EEG-based BCIs and their performance with ALS patients. In Sections 1.5 – 1.8, I describe an alternative BCI for ALS patients based on neurofeedback, as was suggested in the papers "Toward Cognitive Brain-Computer Interfaces for Patients with Amyotrophic Lateral Sclerosis" (Chapter 2) and "Self-Regulation of Precuneus Brain Rhythms: A Novel Brain Computer Interface for Patients with Amyotrophic Lateral Sclerosis" (Chapter 3). In Section 1.9, I introduce an improved BCI with direct instructions, described in the paper "A Cognitive Brain-Computer Interface for Patients with Amyotrophic Lateral Sclerosis" (Chapter 4). Because such a BCI with direct instructions is based on self-referential thinking, self-referential processing in ALS was investigated. The resulting paper "Self-Referential Processing in Amyotrophic Lateral Sclerosis: an Electroencephalography study" (Chapter 5) is summarized in the section 1.10. These results lead to the question of consciousness in late-stage ALS and I describe a possible approach to answer it ("Identification of the Default Mode Network with Electroencephalography", Chapter 6). In conclusion, I summarize the results and outline the directions for future research.

1.1   Amyotrophic Lateral Sclerosis

Amyotrophic lateral sclerosis (ALS), also known as Lou Gehrig's disease or Motor Neurone Disease (MND), is a neurodegenerative disease, characterized mainly by the loss of motor functions due to motor axon retraction, followed by loss of the motor neuron and finally muscle atrophy [1, 2]. ALS is the most common motor neuron disease. In Europe, about 2.16 people per 100,000 are diagnosed with ALS every year [3]. ALS has been increasingly in the public eye since 2014, when the ALS Ice Bucket Challenge campaign was started in order to raise awareness about ALS.

ALS is a highly inhomogeneous disease with its causes remaining largely unknown. Only 10% of the cases are familial ALS, which is believed to be inherited and caused by genetic mutation in a heterogeneous set of genes [3–5]; the rest of the cases are sporadic. The disease onset usually happens after the age of 40, though rare ALS cases of juvenile ALS have also been reported [3, 5]. Based on the onset region, ALS is divided into bulbar and spinal types. Bulbar ALS, observed in about 25% of the cases, usually starts with difficulty speaking or swallowing. More common spinal ALS presents with difficulty walking or with reduced manual dexterity. Other symptoms include muscle weakness and atrophy, muscle cramps, exaggerated reflexes and muscle twitching. As ALS progresses, neuron and muscle atrophy continuously affects other body parts, leading to the paralysis of all muscles apart from the extraocular muscles (locked-in slate, LIS) and eventually full paralysis (completely locked-in state, CLIS). Life expectancy after disease onset is estimated as 3–5 years, but the actual life length varies greatly, spanning the range from a few months to decades [3, 5]. The disease progression is usually measured with the ALS Functional Rating Scale Revised (ALSFRS-R) [6], a 12-item questionnaire with a score between 48 (normal function) and 0 (severe disability). Most of the patients die from respiratory failure, and only some choose artificial ventilation, which increases the life expectancy. There is no cure for ALS and treatment is mostly limited to supportive care. The only drug that have been shown to slow down the progression of the disease, Rilusole, prolongs median survival by only about two to three months [7].

ALS has long been believed to be confined to motor neural pathways, but recent neurological evidence suggests that ALS is a complex multisystem disorder with cortical and subcortical pathology beyond motor areas. The analysis of the

spreading pattern of pTDP-43 protein associated with ALS [8] showed that ALS is limited to motor cortices only in the early stages of the disease. As the disease progresses, the pathological protein agglomerations spread throughout the cortex, eventually affecting almost the whole brain [8]. The involvement of the whole brain is further supported by the morphological and metabolic studies. Abrahams et al. showed that ALS is associated with changes in the white matter [9] and Schmidt et al. later reported alterations in functional and structural connectivity [10]. Additionally, metabolism is reduced in the entire cortex [11]. Growing evidence points towards even broader effects of ALS, involving in particular disorders of serotonergic systems. Dentel et al. found pathological agglomerates of pTDP-43 protein in the central serotogenic neurons of the brain stem (raphe nuclei) [12], which possibly causes decreased serotonin concentrations in the brain of ALS patients [12, 13] and degeneration of the serotonin projections [12].

The effect of ALS and related physiological alterations on the non-motor functions is not completely clear. Cognitive abnormalities are reported in as many as half of ALS patients [5, 14, 15]. Cognitive decline correlates with the severity of symptoms [16] and affects word generation, immediate free recall, attention, mental control tasks [14, 15] and emotion control [17, 18]. The majority of observed psychological symptoms are considered to be signs of frontotemporal dysfunction [14, 19]. Several studies specifically investigated the connection between frontotemporal dysfunction and cognitive decline in ALS. Ludolph et al. and later Abrahams et al. found with positron emission tomography (PET) that reduced word fluency correlates with reduced metabolism in the medial prefrontal cortex (MPFC) in ALS [11, 20]. Mantovan et al. showed that observed memory deficits in ALS patients are connected to frontal lobe dysfunction detected with single photon emission computer tomography (SPECT) [21]. Furthermore, in 15% of the cases, ALS co-occurs with another neurodegenerative disease - fronto-temporal dementia (FTD) [22, 23], characterized by neuronal death in the frontal and temporal lobes. Clinically, FTD and ALS are usually seen as separate diseases, though recent evidence suggests the two might actually be two parts of the same disease, with symptoms of one or the other being more prevalent in the early disease stages [5, 14, 24].

1.2 Communication in ALS

ALS symptoms include difficulty in articulating words and eventually the inability to talk at all. From that stage till the LIS patients experience communication problems but can still communicate, either with simple eye-movements or with commercial eye-tracking systems. Those who reach CLIS, however, lose the ability to volitionally control any muscle, including oculomotor muscles, and so lose all the means of communication.

Therefore, a system that would allow communication independent from voluntary movements would greatly improve the quality of life of CLIS ALS patients and their relatives. Such a system has to be easy to use, portable and compatible with the patients' life support systems. In the absence of any types of voluntary movements, the system has to rely solely on the remaining signals from the central nervous network - brain signals. Such system is called a Brain-Computer Interface (BCI) and it can be used as an artificial communication channel as long as the patient is able to generate communication messages with his/her brain. Various techniques can be used for non-invasive brain signal recording, however, most of them are not portable (functional magnetic resonance imaging, fMRI, positron emission tomography, PET) or require a special shielded room for the recordings (Magnetoencephalography, MEG). Electroencephalography (EEG) is safe, cheap, portable and can be used easily both at patients' homes and in clinical environments. This makes EEG a suitable technology for building the BCI, that would allow to restore communication with ALS patients.

1.3 Electroencephalography

Electroencephalography (EEG) is a non-invasive method for recording brain activity through electrodes placed on the scalp. Its principle is based on a neuron's property of inducing voltage fluctuations via firing. Neurons communicate to each other by releasing neurotransmitters into the synaptic cleft. Neurotransmitters bind to receptors at dendrites and cause change in the post-synaptic potential through the opening or closing of ion channels in the cell membrane. Ion flux propagates through the brain tissue due to volume conduction and causes a change

of potential in the electrodes. EEG records the activity of groups of neurons spatially oriented in the same way and firing in a synchronous manner, which gives rise to signals strong enough to be recorded on the surface of the head.

At the EEG electrodes, the synchronised activity of neurons is seen as oscillations. These oscillations are often referred to as "neural oscillations" or "brain rhythms". They occur in different frequencies and are usually analysed as power spectrum in the frequency domain. The EEG spectrum is separated into several frequency bands: δ (0.1 – 4 Hz), θ (4 – 7 Hz), α (8 – 15 Hz), β (16 – 30 Hz), γ (30 – 100 Hz). Normally, EEG power spectrum has a characteristic α peak. It is usually observed around 10–14 Hz. The peak frequency is different in different people, and even for the same person, it changes throughout lifetime [25]. This peak increases in rest in the absence of any input [25]. Another peak is the μ peak registered over the motor cortices. It also increases in rest state, as the neurons start firing in synchronous manner in the absence of any input. The peak decreases as a response to tasks or events - an effect known as the event-related desynchronisation.

A wide range of cognitive processes are associated with neuronal oscillations in different frequencies easily detectable by EEG [25–29]. For example, θ is connected with spatial orientation, workload, episodic memory, memory encoding and selective attention (for reviews on θ see [25–27]); α correlates with episodic memory, workload and sensory processing [25, 28]; and γ is involved in auditory and visual processing and selective attention [28, 30]. Despite a large body of EEG research, the exact match between cognitive processes and neuronal oscillations is still not known for several reasons. First, most of the studies are based on a low density EEG, which makes source localization highly inaccurate. Second, lack of established paradigms makes meta-analysis difficult and leads to ambiguous results of non-unique mapping between oscillations and cognitive processes [28, 29].

1.4   EEG-based BCI for ALS: state of the art

EEG-based brain-computer interfaces (BCIs) are communication channels that do not depend on the peripheral nerves and muscles [31] and thus may allow completely locked-in (CLIS) patients in late stages of ALS to communicate with the world. So far, different implementations of EEG-based BCIs have been proposed, that work reasonably well with healthy subjects and paralyzed patients; however it

remains difficult to use them with CLIS ALS patients [32]. Birbaumer et al. have suggested that long term paralysis in ALS patients causes a dream-like state [32], making communication impossible. They based their hypothesis on a theory of ideomotor silence and the similarity between the ALS CLIS, in which patients are not able to interact with the world and can only simulate such interaction in their mind, and the REM sleep state, in which similar simulations happen in dreams. Another possible explanation was suggested by Grosse-Wentrup et al. : that existing BCIs are not suitable for ALS patients, because they rely on processes impaired in ALS [33].

In particular, paradigms dependent on low-level sensory- and/or motor processes are unlikely to be available to ALS CLIS patients due to the degeneration of sensorimotor cortex. For example, BCIs based on modulation of sensorimotor-rhythms (SMRs) [34] are probably not suitable for CLIS patients since ALS causes a degeneration of neurons in primary motor cortex [1]. The same is true for tactile BCIs [35] as sensory neurons are also largely affected by ALS [36]. Other BCIs such as P300 speller systems [37, 38] or BCIs based on steady state visual evoked potentials [39] require gaze fixation, which is difficult for patients in late stages of ALS due to impaired oculomotor control [40]. Auditory Event-Related Potential [41] do not require eye fixations, but do not work well with CLIS ALS patients either, due to abnormal ERPs and reduced selective attention in late stage ALS patients [14, 42].

Grosse-Wentrup et al. suggested to avoid impaired low-level sensory- and/or motor processes, and to use instead high cognitive processes, that correlate with posterior γ [28, 30] as a BCI signal [33]. This way they avoided both the brain area and the processes primarily affected by ALS. Grosse-Wentrup et al. employed operant conditioning, a type of learning in which changes in the behaviour happen as a result of observing the feedback, to train the participants to self-regulate the brain oscillations. They achieved an average decoding accuracy of 70.2% with healthy participants, however performance of the LIS ALS patient was barely above the chance level.

1.5 Towards Cognitive BCI for CLIS ALS

In the paper "Towards Cognitive BCI for patients with ALS" (Chapter 2), it was hypothesised that low performance of ALS patient in the previous study on neurofeedback-based BCI [33] might be caused by a decreased learning rate in late stages ALS [43] and thus may be improved by starting the training earlier in the disease. Thus, the neurofeedback BCI study of Grosse-Wentrup et al. [33] was replicated with a moderately impaired ALS patient.

Similarly to Grosse-Wentrup et al., operant conditioning in combination with neurofeedback was employed. The subject was provided with feedback on the amount of parietal γ power he generated and asked to either up- or down-regulate it in pseudo-randomized manner. No instructions were provided on how to achieve the modulations, instead the subject was asked to try different mental strategies. As expected, significant modulations in γ frequency range were observed and resulted in two-class decoding accuracy of 79,2%. Unfortunately, despite Independent Component Analysis (ICA) - based artefact attenuation, it was not possible to exclude muscle contaminations for two reasons. First, the modulation was not specific to the feedback frequency band (55 – 85 Hz), but rather spanned the whole γ range (40 – 85 Hz), which is characteristic for muscle activity. Second, the modulation was spatially spread over the whole cortex, with the maximum of modulation outside the feedback area. At the same time, modulation in the individual θ range was highly localized, both in space and in the frequency domain. The θ range, while still being connected to high cognitive processes [25–27], is less likely to be contaminated by muscle artefacts than γ band. Importantly, the maximum of modulation was observed in between the two hemispheres in the precuneus, the brain area involved in a number of cognitive processes [44] and a hub of the Default Mode Network (DMN), linked to consciousness [45].

1.6 The Default Mode Network, the Precuneus and Consciousness

The Default Mode Network is the brain's resting state network. It has been initially discovered by comparing BOLD signal during rest to that during task performance [46]. Raichle et al. have noticed that while task-specific regions and

networks are more activated when participants are performing correspondent tasks, the DMN regions are activated when participants are task-free, in wakeful rest, or daydreaming and mind-wandering. The DMN consists of the medial prefrontal cortex (MPFC), posterior cingulate cortex/precuneus, inferior parietal lobe, lateral temporal cortex and hippocampal formation. Later research has discovered that DMN regions have a property of functional connectivity: the BOLD signal from different DMN parts detected by fMRI is highly correlated, while being anti-correlated to the task-positive networks [47]. This highlights the co-activation and probably communication between different parts of the DMN and is widely used for fast and reliable identification of the DMN from resting state only. Instead of comparing resting state activations to task activations, the DMN is identified by putting a seed in the precuneus and finding all the regions with activations correlating with the seed's activity.

Despite the DMN is deactivated during the majority of tasks, some tasks have the opposite effect of DMN activation. Those are mostly tasks in some way related to the concept of "self": remembering one's past experiences, envisioning the future, or making moral judgements (for a detailed review see [48]). Thus, self-referential activity is considered to be one of the main DMN functions [48].

The DMN seems to be involved in promoting the state of consciousness. Crone et al. compared DMN deactivations during auditory stimuli presentation in healthy participants, minimally conscious patients and patients in a vegetative state. They found that the level of the DMN deactivation correlates with the level of consciousness [45]. Another study demonstrated a correlation between level of consciousness and connectivity within the DMN [49]. DMN activation alterations have been observed in a number of disorders of consciousness [48, 50]. Additionally, the DMN shows reduced connectivity in sleep [51, 52], when the level of consciousness is reduced. All these arguments taken together point towards the DMN playing a vital role in consciousness.

The precuneus, being a functional core of the DMN [53, 54], is also closely connected with consciousness and high cognitive processes. In particular, it is involved in visuo-spatial imagery, episodic memory retrieval and self-processing (for a review see [44]). Precuneus function is reduced in vegetative state [55] and anaesthesia [56]. It is also one of the first regions to restore its activity when vegetative state patients recover consciousness [57, 58].

The important role of the precuneus in consciousness makes precuneus activity a suitable target for a BCI for ALS patients. As long as patients are fully conscious, the DMN and precuneus in particular are likely to function similarly to a healthy brain. Once the DMN function is disrupted, patients are likely to enter a state of altered consciousness [45, 49], in which meaningful communication is not possible any more.

1.7   BCI based on neurofeedback

The optimal neurofeedback signal for a BCI for ALS patients should arise from the brain area that is minimally affected by ALS and be associated with processes that are not impaired by ALS. For example, the oscillations in the motor cortex are suboptimal due to degeneration of the pyramidal motor neurons in ALS. It is not clear what cognitive functions are available to CLIS ALS patients given the cortex-wide morphological alterations (discussed in Section 1.1). Thus, it is beneficial to use the precuneus, a brain area linked to consciousness, for the BCI for patients with ALS, because consciousness is a fundamental pre-requisite for communication. While successful communication is possible with patients who cannot talk, or cannot move, or cannot see, no communication is possible with unconscious patients, no matter how advance the technology is.

"Self-Regulation of Brain Rhythms in the Precuneus: A Novel BCI Paradigm for Patients with ALS" introduces the new BCI based on modulation of precuneus oscillations in θ and γ frequency bands. The choice of frequency bands was based on the previous studies. Grosse-Wentrup et al. showed that healthy subjects can learn to modulate γ in parietal areas [33] and the following study (Section 1.5, Chapter 2) confirmed that an early stage ALS patient can learn it too. At the same time, even stronger modulations in the θ range were observed in the precuneus. Additionally, θ and γ are coupled [59], associated with multiple cognitive processes [26–29] and correlate with the DMN activity [60, 61], which makes those frequency bands a suitable choice for the BCI. Bandpower modulations can provide a basis for simple binary BCI communication: for example, a volitional increase in the amplitude of neuronal oscillations may be used to communicate a "yes", while a decrease may signal a "no" response to a question.

The BCI was introduced to the patients in several steps. As the first step, two ALS patients were trained to modulate the brain oscillations: one in θ and one in γ frequency range. They were provided with a setup that asked them in a pseudo-randomized manner to either up- or down-regulate the oscillations in the precuneus (for more technical details on the method, see Chapter 3). After each training session, the performance and the pattern of modulations were evaluated. Once a consistent modulation was observed over several sessions and it was possible to successfully decode it, an online state classifier was introduced and the classifier decision was added to the feedback at the end of each trial. Finally, the patient could use the BCI to answer simple "yes/no" personal questions. It is of high importance to do transitions gradually and to increase the complexity slowly. First, the BCI system has to remain understandable, predictable and intuitive for the patients. Second, the advance to the next step should be done only when the system performance gets stable enough, to avoid patient's frustration and loss of trust in the system.

Within all these steps, the neurofeedback signal was adjusted. The BCI training loop consists of a computer and a human and both parts of the loop have to adjust to each other in order to achieve optimal performance [62]. While in online neurofeedback sessions the patient have been trained to modulate brain activity; offline the setup was adjusted in order for it to be able to pickup the modulations that the patient created. Furthermore, the brain is a non-stationary system and an ALS patient's brain even more so due to the disease progress. Constant system adjustment allows to compensate for the alterations in the brain's state. For the same reasons the classifier was re-trained several times during the study.

Both of the patients learned to control the neurofeedback BCI and did not lose this skill in the progress of their disease. One of the patients reported using self-referential memories to control BCI and the other could not formulate the strategy, and reported being able to control the BCI by simply "wanting" the neurofeedback signal to change in one direction or the other. The post hoc analysis confirmed that the observed modulations arise from the precuneus and do not happen due to artifacts (such as muscle or eye movements, that can be also detected in θ and γ frequency bands). The precuneus origin of the signal was further supported by a fMRI experiment, in which one of the patients was asked to up- or down-regulate the oscillations inside an fMRI scanner.

The proposed BCI has yet to be tested with CLIS ALS patients. (It was not possible to test the BCI with patients in CLIS, because neither of the two patients lived until the CLIS.) However, the stability of GH's performance despite the dramatic progress of his disease and the use of consciousness-related processes for the BCI hold a promise that such a system should be suitable for ALS patients in all disease stages. Unfortunately, the long training time makes it difficult to test. Due to the decline in learning abilities in ALS [43], training has to start in an early disease stage and has to continue on regular basis while the disease is progressing. This is difficult to achieve on a large scale. Progression of ALS from the diagnosis to CLIS can take up to tens of years [5], and not all ALS patients survive until the CLIS. Thus, the proposed paradigm, despite being promising from the scientific point of view, might be economically infeasible. In further research this issue was addressed by replacing the operant conditioning with another method: direct instructions, which shortened the training time.

1.8 Operant conditioning and direct instructions

During the training, the patients were provided with real-time information about their precuneus activity and asked to try different mental strategies in order to change the activity in the desired direction. The operant conditioning in combination with neurofeedback training is widely used in therapies aiming to up- or down-regulate neural oscillations to improve cognitive functions or well-being. For example, α and θ neurofeedback training was used first for treatment of alcoholics [63] and later for creative performance enhancement [64] and Attention-Deficit Hyperactivity Disorder (ADHD) treatment [65]. Most patients cannot explain how they achieve the modulations, but Niv et al. suggested that DMN modulations is a primary mechanism of the neurofeedback training [66]. For BCI, the operant conditioning with neurofeedback was first used by Birbaumer et al. and was later proven successful in multiple studies [33, 67, 68]. Operant conditioning offers an intuitive BCI, that - once it is learned - can be used naturally without additional cognitive effort, similar to the way we use hands or legs, or learn to talk or ride a bicycle. The problem highlighted by previous studies is the long training time required before patients can reliably use the BCI. Additionally, controlling such a BCI is a skill that should be acquired early in the disease due to decreased learning rates in late stage ALS [43].

A cognitive non-motor BCI with direct instructions is an alternative approach to BCI. It was first suggested by Anderson et al., who successfully classified brain activations during five different mental tasks: the baseline resting state task, the mental letter composing task, the non-trivial multiplication task, the visual counting task and the geometric figure rotation task [69]. The cognitive BCI with direct instructions offers the benefits of being ready to use without the need for a long period of initial training, at the cost of being less intuitive and high in mental effort required to keep the thoughts on the required task.

1.9 BCI based on direct Instructions

To improve the training time for the BCI, the previously used operant-conditioning was replaced by direct instructions. Following the strategy of one of the ALS patients from the neurofeedback BCI study (Chapter 3), participants were instructed to use self-referential memories to control the BCI. Self-referential thinking is a high cognitive process that is not likely to be impaired in ALS. It is known to correlate positively with θ bandpower [70] and thus can be detected with EEG. Self-referential thinking is also known to engage the DMN, thus one can expect more activity in the precuneus for self-referential than for not self-referential thoughts. Additionally, self-referential thinking is an easy intuitive task that requires moderate mental effort to perform.

In the study "A Cognitive Brain-Computer Interface for Patients with Amyotrophic Lateral Sclerosis" (Chapter 4), participants were asked to remember positive self-referential memory to up-regulate the precuneus activity and to concentrate on their breathing to down regulate it. No neurofeedback was provided in order to simplify the setup and avoid distraction. Twelve healthy participants and five ALS patients were able to generate distinct patterns in the θ and α frequency bands, allowing classification rates of above 60%. The source localization performed on the data of healthy participants (Chapter 6) confirmed that the modulation arose from the DMN.

In the next stages, such a cognitive BCI can be integrated with neurofeedback on the current θ and α over the precuneus, which would allow for combining the benefits from the direct instructions with those from operant conditioning. Integration with neurofeedback training might also further improve the performance.

Later, an online classifier should be introduced to provide an online BCI. Nevertheless, before further improvements are incorporated, it is necessary to validate the chosen processes and to ensure that self-referential processes are unaffected by ALS. Otherwise, such a BCI would not offer ALS patients any advantage over a motor-imagery BCI or any other BCI type.

1.10   Self-referential processing in ALS

Self-referential thinking can be used as a basis for EEG-based BCI for ALS patients, because self-referential thinking, being a main cognitive process, is unlikely to be impaired in ALS patients. "Self-referential thinking in Amyotrophic Lateral Sclerosis: an Electroencephalography study" examined whether self-referential thinking is indeed spared in ALS. In particular, the self-referential processing in ALS was investigated by comparing the EEG correlates of it in ALS patients and healthy controls. For that ten healthy participants and ten ALS patients in different disease stages (ranging from the very first symptoms to LIS and CLIS) were recruited. The EEG data were collected while participants were making judgements about themselves, their close friends and celebrities (for more details see chapter 5). To exclude confounding effects, such as not understanding the task, not following the instructions, or falling asleep, a fourth non-self-referential condition was introduced as control condition. In this condition participants were asked to count the syllabuses in the word they hear.

Following previous fMRI studies with a similar setup [71], modulations in the medial prefrontal cortex (MPFC) were expected. To test this, an ANOVA was performed on bandpowers in θ, α, β, low and high γ frequency bands for both groups of subjects. For healthy participants, there was a significant difference between the four conditions with different degree of self-referential processing. The difference remained significant after removing the control (counting) condition from the analysis and analysing only the three self-referential conditions (judgements about oneself, friend or celebrity). For ALS patients, there was a significant difference between the four conditions with different degree of self-referential processing as well. However, after removing the control (counting) condition, the difference in bandpowers between the remaining three self-referential conditions was not significant any more. The results showed that EEG correlates of self-referential processing differ between healthy participants and ALS patients.

It was not possible to separate the effect of ALS from that of the long-term paralysis or the medication. Most of the ALS patients take rilusole and/or painkillers. To the best of my knowledge, none of those medicine has been reported to induce changes in self-referential thinking. Nevertheless, it is not possible to say whether the observed differences in MPFC activations between ALS patients and healthy controls are directly connected with ALS. Irrespective of the cause of alterations in self-referential thinking, the results suggest that self-referential processing is a suboptimal process for the BCI for ALS patients.

Altered self-referential processing is one of the major FTD symptoms [72]. This further supports the connection between ALS and FTD and the hypothesis of an ALS-FTD disease continuum [5, 14, 24]. However, none of the patients were diagnosed with FTD and all of the patients who were able to communicate appeared fully conscious and mentally healthy. Due to the lack of communication, nothing can be said about the two CLIS ALS who participated in the study. Other neuroimaging studies also found ALS related alterations in patients without cognitive disorders [4]. In particular, Portet et al. reported abnormal event-related potentials (ERPs) in patients without cognitive impairement [14]. Similar results were reported by Pinkhardt [42], who found an increased ERP response to non-relevant stimuli in all examined ALS patients, even those who did not show any symptoms of attention disorder. In an attempt to explain these observations, Tsermentseli et al. suggested that neuroimaging might detect alterations preceding the clinical symptoms. The results on altered self-referential processing in ALS (chapter 5) align well with this hypothesis. Cognitive deficits progress slower than motor [43] and it might be that for many ALS patients, cognitive symptoms never get detected and diagnosed because by the time such symptoms develop, motor symptoms advance to CLIS, making further psychological testing impossible.

Furthermore, alterations in self-referential processing have important implications for understanding of the CLIS ALS state of consciousness. Laureys et al. suggested a 2-D scale of consciousness with one axis being wakefulness, and the other being awareness [73]. There are different levels of consciousness on both axes, ranging from fully conscious state (awake,aware) to coma (not awake, not aware), to vegetative state (awake, not aware) and lucid dreaming (not awake, aware). As of now, CLIS patients are shown on the scheme with a doted line overlapping with fully conscious state, because CLIS patients' consciousness cannot be measured with conventional behavioural methods. The results of the study on self-referential

processing in ALS suggest that CLIS ALS patients are probably awake (since they produced different activity in counting and self-referential conditions), but possibly not fully aware, or at least not fully self-aware. Thus, CLIS ALS patients may reside in altered state of consciousness. Further studies have to investigate level of consciousness in CLIS ALS patients.

1.11   EEG DMN for consciousness estimation

Alterations of self-referential processing in ALS suggest that ALS patients might have an altered state of consciousness. The Coma Recovery Scale (revised) (CRS-R) [74] is routinely used for examining patients with disorders of consciousness, as well as for differentiating between vegetative state and minimally conscious state. CRS-R is based on tests for auditory, motor and oromotor functions. Unfortunately, all those functions are impaired in CLIS ALS and cannot be used as a measure of consciousness. No other behavioural testing can be performed due to the absence of communication means. Thus, neuroimaging techniques are the only feasible option for consciousness estimation in CLIS ALS.

FMRI can be used for consciousness estimation in paralyzed patients, since the connectivity of the DMN correlates with the level of consciousness [49]. The DMN is known to be less active in sleep, including the REM sleep [51, 52] and thus could be used for verification of the thought extinction theory, suggesting that ALS patients reside in a REM-like state [68]. Unfortunately, fMRI is difficult to use with CLIS patients. CLIS ALS patients are dependent on artificial ventilation systems and their transportation into fMRI scanner can be difficult and potentially dangerous.

EEG, being cheap, easy to use, and highly portable, serves as a promising alternative. EEG-based entropy monitors are widely used in clinical settings for anaesthesia depth estimation [75]. However, they are likely to rely primarily on the EMG component of the data and muscle tone relaxation and are probably not suitable for consciousness estimation in CLIS ALS patients due to muscle atrophy in late stage ALS. Other studies showed that EEG entropy might correlate with the levels of consciousness, but entropy estimation from the EEG data remains difficult [76] and does not allow to reliably differentiate REM steep from the awake state [77].

EEG-based identification of the DMN might offer an alternative approach to consciousness estimation in CLIS ALS as it might allow to combine the benefits of using EEG with the DMN sensitivity to the state of consciousness. Previously, Knyazev et al. has attempted to localize DMN with EEG [78], however they managed to recover only one node of the DMN. In "Identification of the DMN with the EEG" (Chapter 6) an alternative method for DMN localization with EEG was proposed. Using the data collected in the BCI study (Chapter 4), I compared the EEG power in α and θ frequency bands in two conditions: recalling positive self-referential memories and concentrating on breathing. I employed the fact that self-referential thinking activates the DMN, while tasks that are not connected with self-referential processing deactivate it. With this approach, I was able to localize the MPFC, precuneus/posterior cingulate, and left temporal node.

In the future, this approach can lead to a method for consciousness estimation in CLIS ALS. However, it has to be validated first: one possibility is to do simultaneous EEG/fMRI recordings and compare the DMN recovered with traditional methods with the EEG DMN. Unfortunately, the simultaneous EEG/fMRI recordings are normally done with smaller number of electrodes (16-64), which can affect the source localization resolution. Another possibility is reproducing the study on the DMN in minimally conscious and vegetative state patients [49] with EEG and direct evaluation of whether the EEG DMN correlates with the levels of consciousness in the same way that the fMRI DMN does.

1.12   Future research

Future research should focus primarily on consciousness characterization in CLIS ALS. The level of consciousness in CLIS ALS should define the type of communication that is needed for such patients and the type of BCI that can be used in order to achieve it. If CLIS ALS patients are unconscious, maybe they do not need any BCI at all. On the other hand, if they are in an altered state of consciousness which still allows basic communication, then they would need an easy to use BCI with a very simple, intuitive interface. The latter can be achieved by developing a BCI that would either not require training or allow for training earlier in the disease.

ALS patients' level of consciousness might also restrict the types of questions ALS patients can be asked. This is especially relevant for BCI validation. ALS patients might not be able to retrieve memories or recognize others, while still being able to answer simple questions about the present moment, i.e. "Are you in pain?", "Is it night now?", "Do you hear me?".

If ALS patients' consciousness is altered in the late stages, the neurofeedback BCI might be an optimal solution. Such a BCI is based on processes tightly connected with consciousness and thus holds the promise to remain functional as long as consciousness is preserved. Training time can be improved, as proposed above, with direct instructions. However, it might be beneficial to use for the direct instructions other DMN functions not related to self-referential processing, as other processes might be less affected by ALS. Other functions of the DMN in ALS patients, such as future envision and theory of mind [48], should be addressed in future studies. If those functions are not altered in ALS, they can be used as a basis for a cognitive BCI with direct instructions. Another way to facilitate training is to use transfer learning [79]. It would allow to make use of the data collected from other patients, thus shortening the time between the start of the training and delivering the system that allows for online communication.

Other nodes of the DMN and other frequency bands should be investigated. It has been shown that DMN correlates with θ [60]. Other studies found the DMN to be closely connected with α frequency range, and even used that as a basis for DMN identification [78, 80]. In "Self-Regulation of Brain Rhythms in the Precuneus: A Novel BCI Paradigm for Patients with ALS" θ and γ frequency ranges were compared. Both candidate bands were found suitable, however, θ seems to be more stable across sessions. Frequency bands might have to be adjusted individually for every patient. In this case, such an adjustment should be automated, so that the BCI can be made independent from researchers and patients can use it on their own.

Consciousness is not stationary and can change over time. It is likely that late stage ALS patients have periods with more and less consciousness or that they fall asleep for short time periods [81]. In this case, it would be beneficial to build a system that can constantly monitor the patient's consciousness state and offer communication only when the patient enters the brain state suitable for communication.

Even if ALS patients' consciousness is not altered, their attention is reduced [42]. It has to be taken into account when designing the BCI for ALS patients. The interface has to be as simple as possible and the use of the BCI should be intuitive. This can be achieved with operant conditioning and neurofeedback. Such a BCI, once learned, does not require additional mental effort and patients can use the BCI even in late stages of the disease.

To be able to deliver this system to more patients, the system has to be made more independent: patients should be able to train on their own, without the need for a researcher to intervene. It can be achieved by switching to a commercially available BCI system with dry electrodes or to a system with smaller numbers of electrodes. It has to be noted, however, that in the latter case accurate source localization might not be possible.

Another way to make such a BCI system more independent is by using invasive methods instead of EEG. Electrocorticography (ECoG) is a small electrode array that is implanted between scalp and dura. It is less invasive than microelectrodes arrays implanted directly into the brain, and allows to get better signal quality than EEG. ECoG data is less contaminated by muscle artefacts and has a better signal-to-noise ratio (SNR) due to the absence of bone and skin signal attenuation. My BCI studies can serve as preliminary studies for implementing such a system. In that sense, the main result of my research is the proof-of-concept and the identification of the region, on which ECoG should be placed. Once it has been shown that precuneus oscillations can be used for BCI, the next step would be to implant an ECoG array on the precuneus area in between the two hemispheres. Then, patients can be trained in a similar manner as they were trained with the EEG-based BCI. Frequency bands can be adjusted dynamically and individually. Since the SNR is better for ECoG, it is reasonable to expect even higher classification accuracy. Putting the array directly on the precuneus would also allow to avoid possible mistakes in source localisation due to individual differences in cortex folding.

Bibliography

[1] K Nihei, A C McKee, and N W Kowall. Patterns of neuronal degeneration in the motor cortex of amyotrophic lateral sclerosis patients. *Acta Neuropathologica*, 86(1):55–64, June 1993. ISSN 0001-6322. doi: 10.1007/BF00454899. URL `http://link.springer.com/10.1007/BF00454899`.

[2] L R Fischer, D G Culver, P Tennant, A A Davis, M Wang, A Castellano-Sanchez, J Khan, M A Polak, and J D Glass. Amyotrophic lateral sclerosis is a distal axonopathy: Evidence in mice and man. *Experimental Neurology*, 185(2):232–240, 2004.

[3] M C Kiernan, S Vucic, B C Cheah, M R Turner, A Eisen, O Hardiman, J R Burrell, and M C Zoing. Amyotrophic lateral sclerosis. *Lancet*, 377(9769): 942–55, 2011. ISSN 1474-547X. doi: 10.1016/S0140-6736(10)61156-7. URL `http://www.ncbi.nlm.nih.gov/pubmed/21296405`.

[4] S Tsermentseli, P N Leigh, and L H Goldstein. The anatomy of cognitive impairment in amyotrophic lateral sclerosis: More than frontal lobe dysfunction. 48(2):166–182, 2012.

[5] W Robberecht and T Philips. The changing scene of amyotrophic lateral sclerosis. *Nature reviews. Neuroscience*, 14(4):248–64, 2013. URL `http://www.ncbi.nlm.nih.gov/pubmed/23463272`.

[6] J M. Cedarbaum, N Stambler, E Malta, C Fuller, D Hilt, B Thurmond, and A Nakanishi. The ALSFRS-R: A revised ALS functional rating scale that incorporates assessments of respiratory function. *Journal of the Neurological Sciences*, 169(1-2):13–21, 1999.

[7] R G Miller, J D Mitchell, M Lyon, and D H Moore. Riluzole for amyotrophic lateral sclerosis (ALS)/motor neuron disease (MND), 2007.

[8] H Braak, J Brettschneider, A C Ludolph, V M Lee, J Q Trojanowski, and K Del Tredici. Amyotrophic lateral sclerosis–a model of corticofugal axonal spread. *Nature reviews. Neurology*, 9(12):708–14, 2013. URL `http://www.pubmedcentral.nih.gov/articlerender.fcgi?artid=3943211&tool=pmcentrez&rendertype=abstract`.

[9] S Abrahams, L H Goldstein, J Suckling, V Ng, A Simmons, X Chitnis, L Atkins, S C R Williams, and P N Leigh. Frontotemporal white matter changes in amyotrophic lateral sclerosis. *Journal of Neurology*, 252(3):321–331, 2005.

[10] R Schmidt, E Verstraete, M A de Reus, J H Veldink, L H van den Berg, and M P van den Heuvel. Correlation between structural and functional connectivity impairment in amyotrophic lateral sclerosis. *Human Brain Mapping*, 35(9):4386–4395, 2014.

[11] A C Ludolph, K J Langen, M Regard, H Herzog, B Kemper, T Kuwert, I G Böttger, and L Feinendegen. Frontal lobe function in amyotrophic lateral sclerosis: a neuropsychologic and positron emission tomography study. *Acta neurologica Scandinavica*, 85(2):81–9, 1992. URL `http://www.ncbi.nlm.nih.gov/pubmed/1574993`.

[12] C Dentel, L Palamiuc, A Henriques, B Lannes, O Spreux-Varoquaux, L Gutknecht, F René, A Echaniz-Laguna, J L Gonzalez De Aguilar, K P Lesch, V Meininger, J P Loeffler, and L Dupuis. Degeneration of serotonergic neurons in amyotrophic lateral sclerosis: A link to spasticity. *Brain*, 136(2): 483–493, 2013. ISSN 00068950. doi: 10.1093/brain/aws274.

[13] L Dupuis, O Spreux-Varoquaux, G Bensimon, P Jullien, L Lacomblez, F Salachas, G Bruneteau, P F Pradat, J P Loeffler, and V Meininger. Platelet serotonin level predicts survival in amyotrophic lateral sclerosis. *PLoS ONE*, 5(10), 2010.

[14] F Portet, C Cadilhac, J Touchon, and W Camu. Cognitive impairment in motor neuron disease with bulbar onset. *Amyotrophic lateral sclerosis and other motor neuron disorders : official publication of the World Federation of Neurology, Research Group on Motor Neuron Diseases*, 2(1):23–9, 2001. URL `http://www.ncbi.nlm.nih.gov/pubmed/11465929`.

[15] G M Ringholz, S H Appel, M Bradshaw, N A Cooke, D M Mosnik, and P E Schulz. Prevalence and patterns of cognitive impairment in sporadic ALS. *Neurology*, 65(4):586–590, 2005.

[16] P J Massman, J Sims, N Cooke, L J Haverkamp, V Appel, and S H Appel. Prevalence and correlates of neuropsychological deficits in amyotrophic lateral sclerosis. *Journal of neurology, neurosurgery, and psychiatry*, 61(5):450–5, 1996. ISSN 0022-3050. doi: 10.1136/jnnp.61.5.450. URL `http://www.pubmedcentral.nih.gov/articlerender.fcgi?artid=1074039&tool=pmcentrez&rendertype=abstract`.

[17] S McCullagh, M Moore, M Gawel, and A Feinstein. Pathological laughing and crying in amyotrophic lateral sclerosis: An association with prefrontal cognitive dysfunction. *Journal of the Neurological Sciences*, 169(1-2):43–48, 1999.

[18] N T Olney, M S Goodkind, C Lomen-Hoerth, P K Whalen, C A Williamson, D E Holley, A Verstaen, L M Brown, B L Miller, J Kornak, R W Levenson, and H J Rosen. Behaviour, physiology and experience of pathological laughing and crying in amyotrophic lateral sclerosis. In *Brain*, volume 134, pages 3455–3466. Oxford University Press, 2011.

[19] C Lomen-Hoerth, J Murphy, S Langmore, J H Kramer, R K Olney, and B Miller. Are amyotrophic lateral sclerosis patients cognitively normal? *Neurology*, 60(7):1094–1097, 2003. URL `http://www.neurology.org/cgi/doi/10.1212/01.WNL.0000055861.95202.8D`.

[20] S Abrahams, L H Goldstein, J J Kew, D J Brooks, C M Lloyd, C D Frith, and P N Leigh. Frontal lobe dysfunction in amyotrophic lateral sclerosis. A PET study. *Brain : a journal of neurology*, 119 (Pt 6:2105–20, 1996. ISSN 0006-8950. URL `http://www.ncbi.nlm.nih.gov/pubmed/9010014`.

[21] M C Mantovan, L Baggio, G Dalla Barba, P Smith, E Pegoraro, G Soraru, P Bonometto, and C Angelini. Memory deficits and retrieval processes in ALS. In *European Journal of Neurology*, volume 10, pages 221–227, 2003.

[22] Y Mitsuyama. Presenile dementia with motor neuron disease in Japan: clinico-pathological review of 26 cases. *Journal of neurology, neurosurgery, and psychiatry*, 47(9):953–959, 1984. URL `http://jnnp.bmj.com/cgi/doi/10.1136/jnnp.47.9.953`.

[23] D Neary, J S Snowden, D M Mann, B Northen, P J Goulding, and N Mac-dermott. Frontal lobe dementia and motor neuron disease. *Journal of neurology, neurosurgery, and psychiatry*, 53(1):23–32, 1990. ISSN 0022-3050. URL `http://www.pubmedcentral.nih.gov/articlerender.fcgi?artid=1014093{&}tool=pmcentrez{&}rendertype=abstract`.

[24] M J Strong, C Lomen-Hoerth, R J Caselli, E H Bigio, and W Yang. Cognitive impairment, frontotemporal dementia, and the motor neuron diseases. In *Annals of Neurology*, volume 54, 2003.

[25] W Klimesch. EEG alpha and theta oscillations reflect cognitive and memory performance: a review and analysis. *Brain Research Reviews*, 29(2–3):169–95, 1999. URL `http://www.ncbi.nlm.nih.gov/pubmed/10209231`.

[26] M J. Kahana, D Seelig, and J R. Madsen. Theta returns. *Current Opinion in Neurobiology*, 11(6):739–744, 2001.

[27] M J Kahana. The cognitive correlates of human brain oscillations. *Journal of Neuroscience*, 26(6):1669–1672, 2006. ISSN 1529-2401. doi: 10.1523/JNEUROSCI.3737-05c.2006. URL `http://www.ncbi.nlm.nih.gov/pubmed/16467513`.

[28] E Başar, C Başar-Eroglu, S Karakaş, and M Schürmann. Gamma, alpha, delta, and theta oscillations govern cognitive processes. *International Journal of Psychophysiology*, 39(2-3):241–248, 2001. ISSN 01678760. doi: 10.1016/S0167-8760(00)00145-8. URL `http://www.sciencedirect.com/science/article/pii/S0167876000001458`.

[29] E Başar. Brain oscillations in neuropsychiatric disease. *Dialogues in Clinical Neuroscience*, 15(3):291–300, 2013.

[30] S Ray, E Niebur, S S Hsiao, A Sinai, and N E Crone. High-frequency gamma activity (80-150Hz) is increased in human cortex during selective attention. *Clinical Neurophysiology*, 119(1):116–33, January 2008. ISSN 1388-2457. doi: 10.1016/j.clinph.2007.09.136. URL `http://www.pubmedcentral.nih.gov/articlerender.fcgi?artid=2444052&tool=pmcentrez&rendertype=abstract`.

[31] J R Wolpaw, N Birbaumer, W J Heetderks, D J McFarland, P H Peckham, G Schalk, E Donchin, L A Quatrano, C J Robinson, and T M Vaughan. Brain-computer interface technology: a review of the first international meeting.

IEEE Transactions on Rehabilitation Engineering, 8(2):164–73, 2000. ISSN 10636528. doi: 10.1109/TNSRE.2003.814799. URL `http://www.ncbi.nlm.nih.gov/pubmed/10896178`.

[32] N Birbaumer, F Piccione, S Silvoni, and M Wildgruber. Ideomotor silence: the case of complete paralysis and brain-computer interfaces (BCI). *Psychological Research*, 76(2):183–91, 2012. ISSN 14302772. doi: 10.1007/s00426-012-0412-5. URL `http://www.ncbi.nlm.nih.gov/pubmed/22252304`.

[33] M Grosse-Wentrup and B Schölkopf. A brain-computer interface based on self-regulation of gamma-oscillations in the superior parietal cortex. *Journal of neural engineering*, 11(5):056015, 2014. URL `http://www.ncbi.nlm.nih.gov/pubmed/25125446`.

[34] G Pfurtscheller, D Flotzinger, and J Kalcher. Brain-Computer Interface– a new communication device for handicapped persons. *Journal of Microcomputer Applications*, 16(3):293–299, 1993. ISSN 07457138. doi: 10.1006/jmca.1993.1030. URL `http://www.sciencedirect.com/science/article/B6WK5-45PKMWB-M/2/af82b899dde1d6e3ef776373739ade7c`.

[35] A Brouwer and J B F Van Erp. A Tactile P300 Brain-Computer Interface. *Frontiers in neuroscience*, 4(May):11, 2010. URL `http://www.pubmedcentral.nih.gov/articlerender.fcgi?artid=2871714&tool=pmcentrez&rendertype=abstract`.

[36] M Gasparini, V Bonifati, E Fabrizio, G Fabbrini, L Brusa, G L Lenzi, and G Meco. Progressive sensory nerve dysfunction in amyotrophic lateral sclerosis: a prospective clinical and neurophysiological study. *Journal of Neurology*, 240(5):399–402, 2001. URL `http://www.springerlink.com/openurl.asp?genre=article&id=doi:10.1007/s004150170181`.

[37] E Donchin, K M Spencer, and R Wijesinghe. The mental prosthesis: assessing the speed of a P300-based brain-computer interface. *IEEE Transactions on Rehabilitation Engineering*, 8(2):174–179, 2000. URL `http://www.ncbi.nlm.nih.gov/pubmed/10896179`.

[38] M Salvaris and F Sepulveda. Visual modifications on the P300 speller BCI paradigm. *Journal of Neural Engineering*, 6(4):046011, 2009. URL `http://discovery.ucl.ac.uk/1322362/`.

[39] E E. Sutter. The brain response interface: communication through visually-induced electrical brain responses. 15(1):31–45, 1992. ISSN 07457138. doi: 10.1016/0745-7138(92)90045-7.

[40] C Donaghy, M J Thurtell, E P Pioro, J M Gibson, and R J Leigh. Eye movements in amyotrophic lateral sclerosis and its mimics: a review with illustrative cases. *Journal of Neurology, Neurosurgery & Psychiatry*, 82(1): 110–116, 2011. URL `http://www.ncbi.nlm.nih.gov/pubmed/21097546`.

[41] A Kübler, A Furdea, S HaIder, E M Hammer, F Nijboer, and B Kotchoubey. A Brain-Computer Interface Controlled Auditory Event-Related Potential (P300) Spelling System for Locked-In Patients. *Disorders of Consciousness*, 1157:90–100, 2009. ISSN 00778923.

[42] E H Pinkhardt, R Jürgens, W Becker, M Mölle, J Born, A C Ludolph, and H Schreiber. Signs of impaired selective attention in patients with amyotrophic lateral sclerosis. *Journal of neurology*, 255(4):532–8, 2008. ISSN 0340-5354. doi: 10.1007/s00415-008-0734-9. URL `http://www.ncbi.nlm.nih.gov/pubmed/18274808`.

[43] H Schreier, T Gaigalat, U Wiedemuth-Catrinescu, M Graf, I Uttner, R Muche, and A C Ludolph. Cognitive function in bulbar- and spinal-onset amyotrophic lateral sclerosis: A longitudinal study in 52 patients. *Journal of Neurology*, 252(7):772–781, 2005. ISSN 03405354.

[44] A E Cavanna and M R Trimble. The precuneus: A review of its functional anatomy and behavioural correlates. *Brain*, 129(3):564–583, 2006.

[45] J S Crone, G Ladurner, Y Höller, S Golaszewski, E Trinka, and M Kronbichler. Deactivation of the default mode network as a marker of impaired consciousness: An fmri study. *PLoS ONE*, 6(10), 2011.

[46] M E Raichle, A M MacLeod, A Z Snyder, W J Powers, D A Gusnard, and G L Shulman. A default mode of brain function. *Proceedings of the National Academy of Sciences of the United States of America*, 98(2):676–682, 2001. ISSN 0027-8424.

[47] M D Fox, A Z Snyder, J L Vincent, M Corbetta, D C Van Essen, and M E Raichle. The human brain is intrinsically organized

into dynamic, anticorrelated functional networks. *Proceedings of the National Academy of Sciences of the United States of America*, 102(27): 9673–8, July 2005. ISSN 0027-8424. doi: 10.1073/pnas.0504136102. URL `http://www.pubmedcentral.nih.gov/articlerender.fcgi?artid=1157105&tool=pmcentrez&rendertype=abstract`.

[48] R L Buckner, J R Andrews-Hanna, and D L Schacter. The Brain's Default Network. *Annals of the New York Academy of Sciences*, 1124(1):1–38, 2008. ISSN 1749-6632. doi: 10.1196/annals.1440.011. URL `http://dx.doi.org/10.1196/annals.1440.011`.

[49] A Vanhaudenhuyse, Q Noirhomme, L J F Tshibanda, M A Bruno, P Boveroux, C Schnakers, A Soddu, V Perlbarg, D Ledoux, J F Brichant, G Moonen, P Maquet, M D. Greicius, S Laureys, and M Boly. Default network connectivity reflects the level of consciousness in non-communicative brain-damaged patients. *Brain*, 133(1):161–171, 2010.

[50] A G Garrity, G D Pearlson, K McKiernan, D Lloyd, K A Kiehl, and V D Calhoun. Aberrant "default mode" functional connectivity in schizophrenia. *American Journal of Psychiatry*, 164(3):450–457, 2007.

[51] T Koike, S Kan, M Misaki, and S Miyauchi. Connectivity pattern changes in default-mode network with deep non-REM and REM sleep. *Neuroscience Research*, 69(4):322–330, 2011.

[52] S G Horovitz, A R Braun, W S Carr, D Picchioni, T J Balkin, M Fukunaga, and J H Duyn. Decoupling of the brain's default mode network during deep sleep. *Proceedings of the National Academy of Sciences of the United States of America*, 106(27):11376–11381, 2009.

[53] A V Utevsky, D V Smith, and S Huettel. Precuneus is a functional core of the default-mode network. *The Journal of neuroscience : the official journal of the Society for Neuroscience*, 34(3):932–40, 2014. URL `http://www.pubmedcentral.nih.gov/articlerender.fcgi?artid=3891968&tool=pmcentrez&rendertype=abstract`.

[54] P Fransson and G Marrelec. The precuneus/posterior cingulate cortex plays a pivotal role in the default mode network: Evidence from a partial correlation network analysis. *NeuroImage*, 42(3):1178–1184, 2008. ISSN 10538119.

[55] S Laureys, S Goldman, C Phillips, P Van Bogaert, J Aerts, a Luxen, G Franck, and P Maquet. Impaired effective cortical connectivity in vegetative state: preliminary investigation using PET. *NeuroImage*, 9(4):377–382, 1999.

[56] P Fiset, T Daloze, G Plourde, P Meuret, V Bonhomme, N Hajj-ali, S B Backman, and A C Evans. Brain Mechanisms of Propofol-Induced Loss of Consciousness in Humans: a Positron Emission Tomographic Study. *The Journal of Neuroscience*, 19(13):5506–5513, 1999. ISSN 0270-6474.

[57] S. LAUREYS, C. LEMAIRE, P. MAQUET, C. PHILLIPS, and G. FRANCK. Cerebral metabolism during vegetative state and after recovery to consciousness. *Journal of Neurology, Neurosurgery & Psychiatry*, 67(1):121–122, July 1999. ISSN 0022-3050. doi: 10.1136/jnnp.67.1.121. URL `http://jnnp.bmj.com/cgi/content/long/67/1/121`.

[58] S Laureys, A M Owen, and N D Schiff. Brain function in coma, vegetative state, and related disorders, 2004.

[59] R T Canolty, E Edwards, S S Dalal, M Soltani, S S Nagarajan, M S Berger, N M Barbaro, and R T Knight. High gamma power is phase-locked to theta oscillations in human n eocortex. *Science*, 313:1626–1628, 2009.

[60] R Scheeringa, M C M Bastiaansen, K M Petersson, R Oostenveld, D G Norris, and P Hagoort. Frontal theta EEG activity correlates negatively with the default mode network in resting state. *International journal of psychophysiology : official journal of the International Organization of Psychophysiology*, 67(3): 242–51, March 2008. ISSN 0167-8760. doi: 10.1016/j.ijpsycho.2007.05.017. URL `http://www.ncbi.nlm.nih.gov/pubmed/17707538`.

[61] A Berkovich-Ohana, J Glicksohn, and A Goldstein. Mindfulness-induced changes in gamma band activity - Implications for the default mode network, self-reference and attention. *Clinical Neurophysiology*, 123(4):700–710, 2012.

[62] M van Gerven, J Farquhar, R Schaefer, R Vlek, J Geuze, A Nijholt, N Ramsey, P Haselager, L Vuurpijl, S Gielen, and P Desain. The brain-computer interface cycle. *Journal of neural engineering*, 6(4):041001, 2009.

[63] E G Peniston and P J Kulkosky. Alpha-theta brainwave training and beta-endorphin levels in alcoholics. *Alcoholism, clinical and experimental research*, 13:271–279, 1989. ISSN 0145-6008. doi: 0145-6008/89/1302-0271\$2.00/0.

[64] J H Gruzelier. EEG-neurofeedback for optimising performance. I: A review of cognitive and affective outcome in healthy participants. *Neuroscience and Biobehavioral Reviews*, October 2013. ISSN 1873-7528. doi: 10.1016/j.neubiorev.2013.09.015. URL `http://www.sciencedirect.com/science/article/pii/S0149763413002248`.

[65] J M Williams. Does Neurofeedback Help Reduce Attention-Deficit Hyperactivity Disorder? *Journal of Neurotherapy*, 14(4):261–279, 2010. URL `http://www.tandfonline.com/doi/abs/10.1080/10874208.2010.523331`.

[66] S Niv. Clinical efficacy and potential mechanisms of neurofeedback. 54(6): 676–686, 2013.

[67] A Kuebler, B Kotchoubey, H P Salzmann, N Ghanayim, J Perelmouter, V Hömberg, and N Birbaumer. Self-regulation of slow cortical potentials in completely paralyzed human patients. *Neuroscience Letters*, 252(3):171–4, 1998. ISSN 03043940. URL `http://www.ncbi.nlm.nih.gov/pubmed/9739988`.

[68] N Birbaumer, N Ghanayim, T Hinterberger, I Iversen, B Kotchoubey, A Kübler, J Perelmouter, E Taub, and H Flor. A spelling device for the paralysed. *Nature*, 398(6725):297–298, 1999. URL `http://www.ncbi.nlm.nih.gov/pubmed/10192330`.

[69] C W Anderson and Z Sijercic. Classification of EEG signals from four subjects during five mental tasks. *Advances*, pages 407–414, 1996. URL `http://sce.uhcl.edu/boetticher/CSCI5931ComputerHumanInteraction/ClassificationofEEGsignalsfromfoursubjectsduringfivementaltasks.pdf`.

[70] Y Mu and S Han. Neural oscillations involved in self-referential processing. *NeuroImage*, 53(2):757–768, 2010.

[71] T F Heatherton, C L Wyland, C N Macrae, K E Demos, B T Denny, and W M Kelley. Medial prefrontal activity differentiates self from close others. *Social cognitive and affective neuroscience*, 1(1):18–25, 2006.

[72] D Neary, J S Snowden, L Gustafson, U Passant, D Stuss, S Black, M Freedman, A Kertesz, P H Robert, M Albert, K Boone, B L Miller, J Cummings, and D F Benson. Frontotemporal lobar degeneration: a consensus on

clinical diagnostic criteria. *Neurology*, 51(6):1546–1554, 1998. URL `http://eutils.ncbi.nlm.nih.gov/entrez/eutils/elink.fcgi?dbfrom=pubmed&id=9855500&retmode=ref&cmd=prlinks$\delimiter"026E30F$npapers3://publication/uuid/5585A7A8-6AAF-4056-A34B-6FB202BC70D2`.

[73] S Laureys, M Boly, G Moonen, and P Maquet. Two Dimensions of Consciousness: Arousal and Awareness. *Neuroscience*, 2:1133–1142, 2009. doi: 10.1016/B978-0-12-375073-0.50025-7. URL `http://www.coma.ulg.ac.be/papers/vs/EncConsc_coma_2009.pdf`.

[74] K Kalmar and J T Giacino. The JFK Coma Recovery Scale–Revised. *Neuropsychological rehabilitation*, 15(3-4):454–460, 2005.

[75] P Mahon, R G. Kowalski, A P Fitzgerald, E M Lynch, G B Boylan, B McNamara, and G D Shorten. Spectral entropy as a monitor of depth of propofol induced sedation. *Journal of Clinical Monitoring and Computing*, 22(2):87–93, 2008.

[76] J D Sitt, J R King, I El Karoui, B Rohaut, F Faugeras, A Gramfort, L Cohen, M Sigman, S Dehaene, and L Naccache. Large scale screening of neural signatures of consciousness in patients in a vegetative or minimally conscious state. *Brain*, 137(8):2258–2270, 2014.

[77] N Burioka, M Miyata, G Cornélissen, F Halberg, T Takeshima, D T Kaplan, H Suyama, M Endo, Y Maegaki, T Nomura, Y Tomita, K Nakashima, and E Shimizu. Approximate entropy in the electroencephalogram during wake and sleep. *Clin. EEG Neurosci.*, 36(1):21–24, 2005. URL `http://eeg.sagepub.com/lookup/doi/10.1177/155005940503600106`.

[78] G G Knyazev, J Y Slobodskoj-Plusnin, A V Bocharov, and L V Pylkova. The default mode network and EEG alpha oscillations: An independent component analysis. *Brain Research*, 1402:67–79, 2011. ISSN 00068993.

[79] V Jayaram, M Alamgir, Y Altun, B Schölkopf, and M Grosse-Wentrup. Transfer learning in brain-computer interfaces. *IEEE Computational Intelligence Magazine*, 11(1):20–31, 2016.

[80] J Mo, Y Liu, H Huang, and M Ding. Coupling between visual alpha oscillations and default mode activity. *NeuroImage*, 68:112–118, 2013.

[81] S R. Soekadar, J Born, N Birbaumer, M Bensch, S Halder, A R Murguialday, A Gharabaghi, F Nijboer, B Scholkopf, and S Martens. Fragmentation of slow wave sleep after onset of complete locked-in state. *Journal of Clinical Sleep Medicine*, 9(9):951–953, 2013.

Contributions

Chapter 2.

Towards Cognitive Brain-Computer Interfaces for Patients with Amyotrophic Lateral Sclerosis

Tatiana Fomina (TF), Bernhard Schölkopf (BS), Moritz Grosse-Wentrup (MGW)

Published in 7th Computer Science and Electronic Engineering Conference, pages: 77-80, Curran Associates, Inc., CEEC, 2015

MGW suggested, designed the study and supervised the work. TF performed a literature review, analyzed the data, wrote the paper. BS provided advice on study design and data analysis.

Chapter 3.

Self-Regulation of Precuneus Brain Rhythms: A Novel Brain–Computer Interface for Patients with Amyotrophic Lateral Sclerosis

Tatiana Fomina (TF), Gabriele Lohmann (GL), Michael Erb (ME), Thomas Ethofer (TE), Bernhard Schölkopf (BS), Moritz Grosse-Wentrup (MGW)

Under review in Journal of Neural Engineering

MGW and TF designed the study, conducted experiments. TF performed a literature review, conducted EEG experiments with LS and partially with GH, analyzed the data, wrote the paper. ME and TE performed an fMRI experiment. GL provided advice on fMRI analysis. MGW and BS provided advice on study design and data analysis. MGW supervised the work.

Chapter 4.

A Cognitive Brain–Computer Interface for Patients with Amyotrophic Lateral Sclerosis

Matthias Hohmann (MH), Tatiana Fomina (TF), Vinay Jayaram (VJ), Natalie Widmann (NW), Cristian Förster (CF), Jennifer Just (JJ), Matthis Synofzik

(MS), Bernhard Schölkopf (BS), Ludger Schöls (LS), Moritz Grosse-Wentrup (MGW)
Accepted to Progress in Brain Research journal

MGW, MH and TF designed the study. MH, NW, CF, VJ, TF conducted experiments with ALS patients. MH performed a literature review, designed the study, conducted experiments with healthy participants, analyzed the data, wrote the paper. TF assisted MH with experiments with healthy participants and data analysis. VJ provided code for pattern classification. LS, JJ and MS provided advice on ALS. MGW and BS provided advice on study design and data analysis. MGW supervised the work.

Chapter 5.

Self-referential processing in Amyotrophic Lateral Sclerosis: an Electroencephalography study
Tatiana Fomina (TF), Sebastian Weichwald (SW), Ludger Schöls (LS), Bernhard Schölkopf (BS), Moritz Grosse-Wentrup (MGW)
In preparation for Brain

TF performed a literature review, designed the study, conducted experiments with healthy and ALS patients, analyzed the data, wrote the paper. SW provided advice on data analysis. LS provided advice on ALS. MGW and BS provided advice on study design and data analysis. MGW supervised the work.

Chapter 6.

Identification of the Default Mode Network with Electroencephalography
Tatiana Fomina (TF), Matthias Hohmann (MH), Bernhard Schölkopf (BS), Moritz Grosse-Wentrup (MGW)
Published in Proceedings of the 37th IEEE Conference for Engineering in Medicine and Biology, pages: 7566-7569, EMBC, 2015

TF performed a literature review, designed the study, analyzed the data, wrote the paper. SW provided advice on data analysis. MGW and BS provided advice on study design and data analysis. MGW supervised the work.

Chapter 2

Towards Cognitive BCI for Patients with ALS

Towards Cognitive Brain-Computer Interfaces for Patients with Amyotrophic Lateral Sclerosis

Tatiana Fomina*[†], Bernhard Schölkopf[†] and Moritz Grosse-Wentrup[†]
*IMPRS for Cognitive and Systems Neuroscience, University of Tübingen, Tübingen, Germany
[†] Department Empirical Inference, Max Planck Institute for Intelligent Systems, Tübingen, Germany
Email: tatiana.fomina@tuebingen.mpg.de, moritzgw@tuebingen.mpg.de

Abstract—**Brain-Computer Interfaces (BCIs) often rely on low-level cognitive processes known to be impaired in late stages of amyotrophic lateral sclerosis (ALS). We propose a BCI for ALS patients based on self-regulation of neuronal oscillations in the superior parietal lobule, which is less affected by ALS than motor and sensory cortices. We describe a case of self-regulation of band power in gamma range (55–85 Hz) based on feedback from the parietal cortex by an ALS patient, resulting in a mean offline two-class decoding accuracy of 79.2% across four sessions. Despite a good offline decoding accuracy, a source localisation analysis revealed that gamma-power modulation was not spatially localized, suggesting confounding by non-cortical artifacts. Theta-power in contrast, showed a strong localized response in the precuneus. As such, this may be an alternative possibility of using self-regulation of neuronal oscillations for cognitive BCI.**

I. Introduction

Brain-computer interfaces (BCIs) based on electroencephalography (EEG) promise to provide an alternative communication channel to locked-in patients in late stages of amyotrophic lateral sclerosis (ALS). Up to date, different implementations of EEG-based BCI have been proposed, though, none of them has been shown to be available to completely locked-in state (CLIS) patients [1]. Many existing BCI paradigms use processes that are likely to be impaired in ALS. For example, BCIs based on volitional modulation of sensorimotor-rhythms (SMRs) [2] are probably not suitable for CLIS patients since ALS is associated with a degeneration of neurons in the primary motor cortex [3]. The same is true for tactile BCIs [4] as sensory neurons are also largely affected by ALS [5]. Other BCIs such as P300 speller systems [6], [7] are based on gaze fixation on a target letter, which is hard to achieve in late stages of ALS due to impaired oculomotor control [8]. Thus, paradigms dependent on low-level sensory and/or motor processes are unlikely to be available to CLIS ALS patients.

CLIS ALS patients may be able to use cognitive BCIs based on higher cognitive processes, such as attention, memory or emotions, associated with brain areas that are less affected by ALS. One of such brain areas is the superior parietal cortex [9], [10]. Previously, we have successfully used neurofeedback to train 11 healthy subjects and one ALS patient to self-regulate the power of γ (55–85 Hz) oscillations in the superior parietal cortex [11]. However, the classification accuracy achieved by the locked-in ALS patient was not sufficient for online communication. The low performance of the ALS patient may

have been caused by a decline in learning abilities in the late stage of ALS [12]: the patient had scored 0 out of 48 in the revised ALS functional rating scale (ALSFRS-R) at the beginning of the training. We hence hypothesized, first, that ALS patients in earlier disease stages are able to gain better control of neuronal oscillations in the superior parietal cortex, and, second, that these patients can maintain this skill when progressing into the completely locked-in state.

In the present work, we report on a pilot-study to test the first hypothesis. We trained an early-stage ALS patient with an ALSFRS-R score of 33 to self-regulate γ-power (55–85 Hz) in the superior parietal cortex. While the patient achieved an offline decoding accuracy 79.2% across four training sessions, a source level analysis revealed that the patient generated γ-modulations over almost the entire cortex, which may be an artifact of contamination of the γ-range by muscular (EMG) signals. However, we additionally found a strong modulation in θ-range (2–5 Hz) in the precuneus and the occipital lobe that was anti-correlated with bandpower changes in the γ-range. The precuneus, being part of the default mode network (DMN) [13], is tightly linked to high cognitive processes and consciousness [13]. Because θ-oscillations are less confounded by EMG signals, θ-power in the precuneus may be a promising target for building a cognitive BCI for patients in late stages of ALS.

II. Methods

A. Patient data and the individual frequency bands

We recruited one ALS patient for the present study. At the beginning of the study this male patient was 59 years old, had been diagnosed with bulbar ALS eight months before, and scored 33 out of 48 points on the revised ALS functional rating scale (ALSFRS-R). We conducted four training sessions over the course of one month in the patient's home. The patient gave informed consent to participate in this study according to guidelines set by the Max Planck Society. The study was approved by an ethics committee of the Max Planck Society.

As the EEG rhythms in ALS patients may slow down, we identified the patient's individual frequency bands [14]. For that, we recorded a five-minute eyes-closed and a five-minute eyes-open resting-state EEG of the patient. The individual α peak was located at 10 Hz; the lower border of the individual α band / upper border of the individual θ band was determined by the intersection of the spectral power of channel Oz

between eyes-open and eyes-closed resting states [14]. The individual lower border of θ was set at 2 Hz.

B. Neurofeedback training

The patient performed four neurofeedback sessions over the course of one month. Training was identical to the one described in [11]. During every training session we recorded an EEG with 121 active electrodes at 500 Hz sampling frequency using a QuickAmp amplifier (BrainProducts GmbH, Gilching, Germany). Prior to each training session, a five-minute eyes-open resting-state baseline was recorded. This data were used to calibrate a beamformer aimed at the right superior parietal cortex [15]. The scalp topography (identical to [11]) for the beamformer was obtained by distributing 300 dipoles in the superior parietal cortex and computing their projection to the EEG electrodes using a three-shell spherical head model. During the neurofeedback training, the recorded data were spatially filtered with the precomputed beamformer. Next, γ-power (55–85 Hz) of the beamformed signal was computed with FFT in combination with a Hanning window on the last 5s of data. This estimate was standardized by the mean and standard deviation of resting-state γ-power.

Feedback was provided both in the visual and auditory domains. The current estimate of γ-power was mapped to the vertical position of a white ball displayed centrally on a computer screen in front of the subject (Fig. 1). The screen's center position was chosen to represent median resting-state γ-power (baseline), and the top and bottom of the screen represented plus and minus two standard deviations, respectively. Concurrently, auditory feedback was provided. If the feedback signal exceeded the baseline, a humming sound was played; otherwise - a wind sound was played. The volume of each sound was scaled linearly with the distance of the current γ power signal from the baseline. The feedback signal was updated at 25 Hz. All online signal processing was carried out with BCI2000 [16] and its extension BCPy2000.

Every session consisted of three blocks of 10 one minute trials per condition in pseudorandomized order with 10 s inter-trial breaks. In every trial, a yellow block at the top or bottom of the screen indicated the current target for the white ball. The patient did not receive any instructions on how to control the feedback signal. Following each session, he was asked to write down the thoughts and feelings associated with up- and down regulation of the feedback signal. We have evaluated the performance during the neurofeedback training by computing the median of the standardized beamformed signal over each trial and comparing the sign of it with the target direction of the correspondent trial.

To ensure the safety of the neurofeedback procedure for the patient, we did not further reward up- or down regulatation of γ-power beyond plus/minus two standard deviations of resting-state γ-power. Additionally, after every session the patient was asked if he had noticed any negative effect of the training procedure.
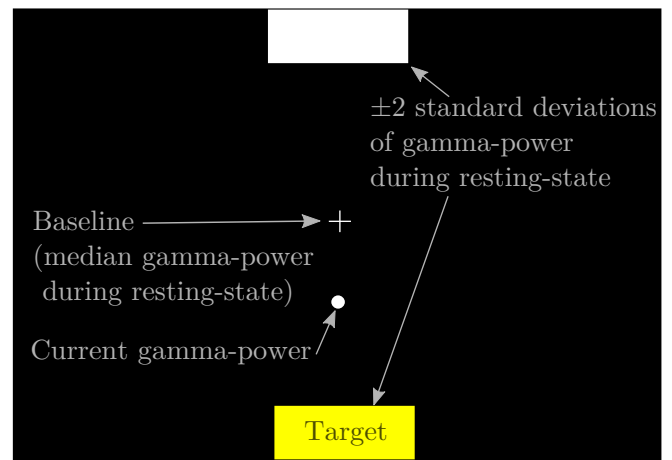

Fig. 1. Visual feedback shown to the patient during the neurofeedback training.

C. Offline analysis

1) Preprocessing: The raw EEG data of each session was cleaned from artifactual components by an independent component analysis (ICA), as described in [11].

2) Offline classification: The beamformer, that was also used for the online feedback, was then applied to the cleaned data, followed by log-bandpower estimation. The resulting one-dimentional vector was used for offline leave-one-trial-out classification with a support vector machine (SVM).

3) Frequency specificity: To investigate the frequency specificity of the beamformed signal, we computed the signed coefficient of determination R^2 for trial-averaged bandpower in frequencies ranging from 1–249 Hz.

4) Dynamic statistical parametric maps (dSPM): To investigate source-level modulations of bandpower, we applied dSPM, a noise-normalized minimum norm estimate [17], to the preprocessed data filtered in the γ (55 – 85 Hz) band as well as to the pre-processed data filtered in the θ (2–5 Hz) band with 3rd order Butterworth filter. First, the forward model $\mathbf{x}[t] = A\mathbf{s}[t]$ was computed, with the matrix A specifying the projection of $K = 3 \cdot 15028$ current dipoles spread over the 15028 cortex locations $\mathbf{s}[t] \in R^K$ on the $N = 124$ electrodes $\mathbf{x}[t] \in R^N$. We generated the forward model with the BrainStorm toolbox [18], using standardized electrode locations and a standardized three-shell spherical head model. Then, the activity of each source was estimated from the measurements of the electrical potential on the surface of the scalp at N electrode locations as described in [17]:

$$\tilde{\mathbf{s}}[t] = W\mathbf{x}[t], \text{ with } W = \Sigma A^T (A\Sigma A^T + C)^{-1}. \quad (1)$$

Here, Σ is the spatial covariance of the dipole strength vector $\Sigma = \mathbf{s}[t]\mathbf{s}[t]^T$, approximated by the identity matrix, and C is the sensor noise covariance matrix, computed individually for each session from the eyes-open resting-state data We then estimated a noize-normalized current dipole power $\tilde{\mathbf{q}}_{\mathbf{i}}[t]$ at each time point t and location i [17]. We made no assumptions

on dipole orientations and thus averaged the three dipoles for each location,

$$\tilde{\mathbf{q}}_{\mathbf{i}}[t] = \frac{\sum\limits_{j \in G_i} \tilde{\mathbf{s}}_j^2[t]}{\sum\limits_{j \in G_i} \mathbf{w}_j C \mathbf{w}_j^T} \qquad (2)$$

where, $\mathbf{w}_j$ is the jth row of the unmixing matrix W and G_i is the set of indices of dipoles located at i [17]. We averaged the current dipole power over each trial.

To estimate the effect of the neurofeedback training, we then averaged the current dipole power estimate over all trials of each conditions and computed the difference D. To test the null-hypothesis H_0: $D = 0$ that there is no difference between the two conditions, we estimated p-values for each source. For that we randomly permuted the condition labels of the trials 10^3 times. We then counted the instances in which the resulting $|D_{HO}|$ exceeded $|D|$ and estimated the probability that $|D_{HO}| > |D|$. We thereby obtained a p-value for each source location. As a last step, we corrected the significance level using a false discovery rate (FDR) of $\alpha_{\text{FDR}} = 0.05$ [19] to compensate for the multiple comparisons for each of the K cortical sources. To plot the results, we set the $D = 0$ for the sources for which we did not reject the null-hypothesis.

III. EXPERIMENTAL RESULTS

A. Neurofeedback training

Throughout four sessions, the ALS patient has modulated median γ (55 – 85 Hz) power in the required direction in 197 trials out of 240 (Fig. 2). The patient reported that he achieved up-regulation of parietal γ-power by inducing positive emotions. He reported that he down-regulated the feedback signal by inducing negative emotions. The patient reported no negative side-effects of this strategy or of the training procedure as a whole.

B. Offline classification

The patient achieved the following offline decoding accuracies in the four sessions: 86.7%, 80.0%, 88.3%, 61.7%. This results in a mean offline decoding accuracy of 79.2%. For each individual session a decoding accuracy of 60.0% is required to reject the null-hypothesis of chance-level performance at significance level $\alpha = 0.05$ [20]. The patient performed above this threshold in all four sessions.

C. Frequency specificity

The modulation of the beamformed signal averaged over all sessions is the most prominent in the γ band (Fig. 3). Additionally, there is a modulation in the opposite direction in the individual θ band.

D. Dynamic statistical parametric maps (dSPM)

On source level, we found a significant modulation in γ band (55 – 85 Hz) over almost entire cortex (Fig. 4A) and in the individual θ (2 – 5 Hz) band over the precuneus and occipital lobe (Fig. 4B).
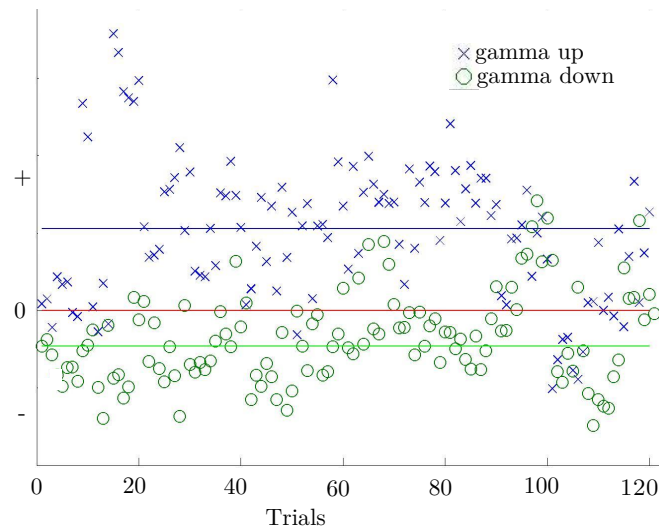

Fig. 2. Neurofeedback performance: median standartized γ power in the superior parietal cortex computed for each trial: green circles represent the trials where the patient was asked to down-regulate his γ power; blue crosses mark the trials where he was asked to up-regulate it. Green line shows the mean of down-regulation trials; blue line – mean of up-regulation trials. Red line marks the baseline.
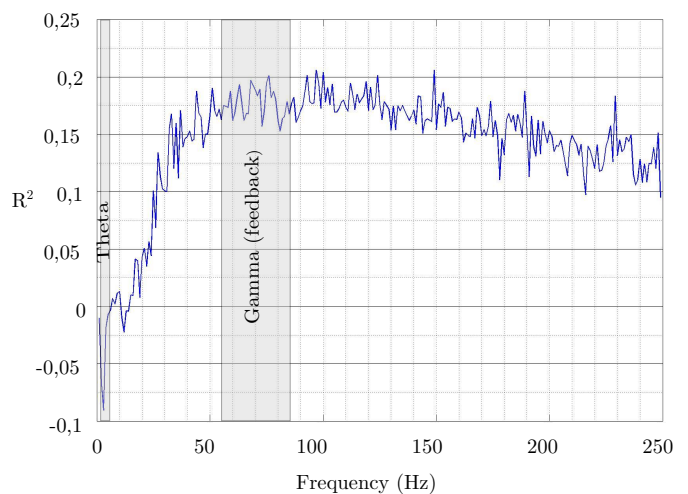

Fig. 3. Mean neurofeedback spectral specificity. Gray area mark the individual θ band and the feedback γ band.

IV. DISCUSSION

We have trained one ALS patient to self-regulate band power in the γ range using neurofeedback. Such self-regulation can potentially serve as a basis for BCI for CLIS ALS patients. However, modulation in γ band was not localized in the area targeted by the feedback, but spread over the entire cortex. While in general spacial specificity is not crucial for controlling the BCI, it is essential for ensuring the cortical nature of the modulation. In this case, lack of spatial specificity of the modulation does not allow us to exclude potential contamination of the feedback signal by the EMG activity.
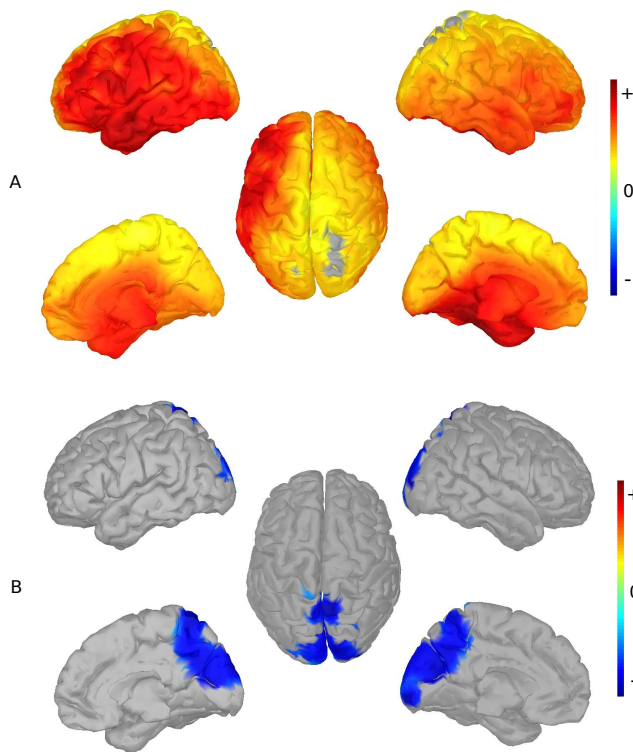
Fig. 4. Brain areas showing significant modulation in A) γ range ($55 - 85$ Hz); B) θ range ($2 - 5$ Hz), both FDR corrected at $\alpha = 0.05$.

We found higher spatial specificity of the modulation in the individual θ band. Even though the feedback was limited to the γ range, the patient also significantly modulated the θ power in the precuneus. The posterior θ has been previously connected with emotional processing (for review see [21]). It agrees with the the strategy used by the patient and further supports the hypothesis that observed self-regulation of parietal oscillations arouses from a high-level cognitive process. Θ band is also less likely to be affected by the EMG signals.

It can be beneficial to further explore the modulation in the individual θ band over the precuneus. Precuneus is considered to be a hub of the Default Mode Network and is tightly linked to the consciousness [13]. Neural oscillations associated with the consciousness can be an interesting alternative approach to the problem of developing BCI for CLIS ALS based on high cognitive processes.

Our study is limited to only one ALS patient. It has still to be studied whether other ALS patients in various stages of the disease are able to learn to control their neural oscillation in superior parietal cortex. It is possible that feedback frequencies or even aimed sources of activity have to be adjusted individually for each subject.

ACKNOWLEDGMENT

REFERENCES

[1] N Birbaumer, F Piccione, S Silvoni, and M Wildgruber. Ideomotor silence: the case of complete paralysis and brain-computer interfaces (BCI). *Psychological Research*, 76(2):183–91, 2012.

[2] G Pfurtscheller, D Flotzinger, and J Kalcher. Brain-Computer Interface– a new communication device for handicapped persons. *Journal of Microcomputer Applications*, 16(3):293–299, 1993.

[3] K Nihei, A C McKee, and N W Kowall. Patterns of neuronal degeneration in the motor cortex of amyotrophic lateral sclerosis patients. *Acta Neuropathologica*, 86(1):55–64, 1993.

[4] A-M Brouwer and J B F van Erp. A Tactile P300 Brain-Computer Interface. *Frontiers in Neuroscience*, 4(5):11, 2010.

[5] M Gasparini, V Bonifati, E Fabrizio, G Fabbrini, L Brusa, G L Lenzi, and G Meco. Progressive sensory nerve dysfunction in amyotrophic lateral sclerosis: a prospective clinical and neurophysiological study. *Journal of Neurology*, 240(5):399–402, 2001.

[6] E Donchin, K M Spencer, and R Wijesinghe. The mental prosthesis: assessing the speed of a P300-based brain-computer interface. *IEEE Transactions on Rehabilitation Engineering*, 8(2):174–179, 2000.

[7] M Salvaris and F Sepulveda. Visual modifications on the P300 speller BCI paradigm. *Journal of Neural Engineering*, 6(4):046011, 2009.

[8] C Donaghy, M J Thurtell, E P Pioro, J M Gibson, and R J Leigh. Eye movements in amyotrophic lateral sclerosis and its mimics: a review with illustrative cases. *Journal of Neurology, Neurosurgery & Psychiatry*, 82(1):110–116, 2011.

[9] R Schmidt, E Verstraete, M A de Reus, J H Veldink, L H van den Berg, and M P van den Heuvel. Correlation between structural and functional connectivity impairment in amyotrophic lateral sclerosis. *Human Brain Mapping*, 35(9):4386–4395, 2014.

[10] H Braak, J Brettschneider, A C Ludolph, V M Lee, J Q Trojanowski, and K Del Tredici. Amyotrophic lateral sclerosis–a model of corticofugal axonal spread. *Nature reviews. Neurology*, 9(12):708–14, 2013.

[11] M Grosse-Wentrup and B Schölkopf. A brain-computer interface based on self-regulation of gamma-oscillations in the superior parietal cortex. *Journal of neural engineering*, 11(5):056015, 2014.

[12] H Schreiber, T Gaigalat, U Wiedemuth-Catrinescu, M Graf, I Uttner, R Muche, and A C Ludolph. Cognitive function in bulbar- and spinal-onset amyotrophic lateral sclerosis: A longitudinal study in 52 patients. *Journal of Neurology*, 252(7):772–781, 2005.

[13] A V Utevsky, D V Smith, and S Huettel. Precuneus is a functional core of the default-mode network. *The Journal of neuroscience : the official journal of the Society for Neuroscience*, 34(3):932–40, 2014.

[14] W Klimesch. EEG alpha and theta oscillations reflect cognitive and memory performance: a review and analysis. *Brain Research Reviews*, 29(2-3):169–95, 1999.

[15] B D van Veen, W van Drongelen, M Yuchtman, and A Suzuki. Localization of brain electrical activity via linearly constrained minimum variance spatial filtering. *IEEE Transactions on Bio-Medical Engineering*, 44(9):867–880, 1997.

[16] G Schalk, D J McFarland, T Hinterberger, N Birbaumer, and J R Wolpaw. BCI2000: A general-purpose brain-computer interface (BCI) system. *IEEE Transactions on Biomedical Engineering*, 51(6):1034–1043, 2004.

[17] A M Dale, A K Liu, B R Fischl, R L Buckner, J W Belliveau, J D Lewine, and E Halgren. Dynamic Statistical Parametric Mapping. 26(1):55–67, 2000.

[18] J.C. Mosher, S. Baillet, F. Darvas, D. Pantazis, E.K. Yildirim, and R.M. Leahy. Brainstorm electromagnetic imaging software. In *5th International Symposium on Noninvasive Functional Source Imaging within the Human Brain and Heart (NFSI 2005)*, 2005.

[19] Y Benjamini and Y Hochberg. Controlling the False Discovery Rate: A Practical and Powerful Approach to Multiple Testing. *Journal of the Royal Statistical Society. Series B (Methodological)*, 57(1):289 – 300, 1995.

[20] G R Müller-Putz, R Scherer, C Brunner, R Leeb, and G Pfurtscheller. Better than random ? A closer look on BCI results. *International Jouranl of Bioelectromagnetism*, 10(1):52–55, 2008.

[21] B Güntekin and E Baar. A review of brain oscillations in perception of faces and emotional pictures. *Neuropsychologia*, 58:33–51, 2014.

Chapter 3

Self-Regulation of Brain Rhythms in the Precuneus: A Novel BCI for Patients with ALS

Self-Regulation of Brain Rhythms in the Precuneus: A Novel BCI Paradigm for Patients with ALS

Tatiana Fomina[1,2], Gabriele Lohmann[3,4], Michael Erb[4], Thomas Ethofer[4], Bernhard Schölkopf[1], and Moritz Grosse-Wentrup[1]

[1] Department of Empirical Inference, Max Planck Institute for Intelligent Systems, Tübingen, Germany

[2] IMPRS for Cognitive and Systems Neuroscience, University of Tübingen, Tübingen, Germany

[3] Max Planck Institute for Biological Cybernetics, Tübingen, Germany

[4] Department of Biomedical Magnetic Resonance, University of Tübingen, Tübingen, Germany

E-mail: `tfomina@tuebingen.mpg.de`, `gabriele.lohmann@tuebingen.mpg.de`, `michael.erb@med.uni-tuebingen.de`, `thomas.ethofer@med.uni-tuebingen.de`, `bs@tuebingen.mpg.de`, `moritzgw@tuebingen.mpg.de`

December 2015

Abstract. Electroencephalographic (EEG) brain-computer interfaces (BCIs) hold promise in restoring communication for patients with completely locked-in stage (CLIS) amyotrophic lateral sclerosis (ALS). However, these patients cannot use existing EEG-based BCIs, arguably because such systems rely on brain processes that are impaired in the late stages of ALS. Here, we propose a BCI for ALS patients based on self-regulation of brain rhythms in the precuneus, as measured by high-density EEG in combination with online source localization. Because there is a tight connection between the precuneus and consciousness, precuneus oscillations are likely generated by high-level cognitive processes, which are less likely to be affected by ALS than processes linked to the peripheral nervous system. We describe two cases of successful self-regulation of precuneus oscillations (one in the theta range and one in the gamma range) by ALS patients, with stable online performance over the course of disease progression. One patient achieved a mean online decoding accuracy in a binary decision task of 70.55% across 26 training sessions, and the other patient achieved 59.44% across 16 training sessions. We provide empirical evidence that these oscillations were cortical in nature and originated from the intersection of the precuneus, cuneus, and posterior cingulate.

1. Introduction

Amyotrophic lateral sclerosis (ALS) is a neurodegenerative disease that is mainly characterized by loss of motor neurons [1]. As the disease progresses, patients gradually lose the ability to move their limbs, talk, swallow, move their eyes and eyelids, and breathe. Eventually, the patients enter a completely locked-in state (CLIS) in which they cannot communicate. It has long been believed that ALS is purely a motor

disease, but recent evidence suggests that ALS eventually affects the whole brain. Schmidt et al. found that, even in early ALS, the alterations in functional and structural connectivity are spread beyond the motor cortices, with the degree of those alterations decreasing with distance from the motor cortex [2]. Braak et al. connected ALS with misfolding of the pTDP-43 protein [3]. They also found that agglomerates of the misfolded proteins are spread beyond the motor cortex with disease progression. It is not clear how these structural alterations affect cognitive functions and whether patients residing in a CLIS for a prolonged time are still conscious. Kübler and Birbaumer have suggested that long-term paralysis might disable a patient's ability for goal-directed thinking [4] and that CLIS patients reside in a state of mind similar to REM sleep [5]. If an ALS patient in a CLIS is conscious, such patient would benefit from restoring communication. To communicate, such ALS patient would need a method that does not depend on peripheral nerves or muscles. One such method could be a brain-computer interface (BCI) [6].

In clinical settings, BCI systems based on an electroencephalogram (EEG) are particularly advantageous due to their mobility, safety, and low price. Various EEG-based BCI-systems have been proposed, yet none has been shown to enable communication with CLIS ALS patients [5]. Current BCI paradigms are often based on low-level cognitive processes that are likely impaired in ALS. For example, BCIs based on volitional modulation of sensorimotor-rhythms (SMRs) in motor and sensory cortices or tactile BCIs [7] are unsuitable for CLIS ALS patients because of the degenerated neurons in their primary motor [1] and sensory [8] cortices. P300 speller systems [9,10] are also unsuitable for these patients because of their impaired gaze fixation [11]. However, some BCIs are based on low-level processes that are likely unaffected by ALS [12], including auditory BCIs [13,14], but they do not yet provide decoding accuracies sufficient for communication when used by severely paralyzed patients [15].

Communication is needed only as long as patients remain conscious. If they are conscious, their brain structures supporting consciousness are probably not yet affected by ALS. We propose to use activity in those brain structures for communication with CLIS ALS patients. One brain area connected with consciousness and self-referential processing is the precuneus, a part of the superior parietal cortex [16]. Activation of the precuneus has been shown to correlate with one's degree of self-relevance of retrieved judgements [17], and connectivity in the precuneus has been shown to correlate with one's degree of consciousness [18]. In contrast, precuneus deactivation has been observed in various stages of sleep [19,20] and in vegetative states [21]. These correlations suggest that altering the precuneus would likely alter one's conscious state to a state close to sleep or a vegetative state, making communication impossible. Though we do not know to what extent ALS affects the precuneus, previous research suggests that a conscious patient who has the capacity for communication might have normal precuneus function. Thus, we propose to communicate with CLIS ALS patients by using the neural oscillations in their precuneus.

In this work, we investigate the possibility of basic communication with ALS

patients by using self-regulation of brain rhythms in the precuneus. We have two hypotheses: First, ALS patients in early disease stages are able to gain control of brain rhythms in the precuneus. Second, they can maintain this skill as their disease progresses.

We tested these hypotheses by training two ALS patients (with a revised ALS functional rating scale (ALSFRS-R [22]) of 33 and 36 out of 48 in the beginning and 10 and 33 by the end of the study) to self-regulate their precuneus oscillations. One patient used the θ frequency range (2–5 Hz), building on our previous work with the same patient [23]. The other patient used the γ frequency range (55–85 Hz), as motivated by our previous work with another subject [24]). We trained them by neurofeedback, which was derived by beamforming from high-density EEG recordings. With the resulting BCI the two patients achieved a mean online accuracy of 70.55% (over 26 sessions) and 59.44% (over 16 sessions), respectively.

We were not able to assess the performance of our BCI in the CLIS: One of the patients died before entering the CLIS. The other patient moved away, making further training infeasible.

2. Methods

Section 2.1 provides information on the ALS patients who participated in the study. Section 2.2 explains the neurofeedback training procedure. In Section 2.3, we describe the online BCI. The evaluation of patients' performance is explained in Section 2.4, including an investigation of the spectral- and spatial specificity of brain rhythm modulation.

2.1. Subjects

Two male ALS patients were recruited from the local community. At the beginning of the training, the first patient, GH, was 59 years old. He was diagnosed with bulbar ALS eight months before, with his first symptoms appearing 18 months prior to the study. Throughout the study, his ALSFRS-R score decreased from 33 to 10. We conducted 29 training sessions with GH over 18 months. GH had been trained to modulate his posterior γ (55–85 Hz) power in an earlier study [23]. At the beginning of the training, the second patient, LS, was 63 years old. He was diagnosed with bulbar ALS four years before. Throughout the study, his ALSFRS-R score decreased from 36 to 33. We conducted 22 training sessions with LS over 8 months. Prior to the training, LS participated in a pilot study that was unrelated to the paradigm reported in the present work. On sessions 12 and 13, LS had a broken rib. All recordings were carried out in the patients' homes. Both patients gave informed consent. The study was approved by the Max Planck Society's ethics committee.

2.2. Neurofeedback training

2.2.1. Hardware EEG recordings were done with an EEG cap with 121 actiCAP active electrodes at a sampling frequency of 500 Hz with a QuickAmp amplifier (BrainProducts GmbH, Gilching, Germany). Electrodes were placed according to the extended 10-20 system, using electrode P7P as the initial reference. All recordings were converted to a common average reference.

2.2.2. Experimental paradigm Every training session consisted of three blocks. Each block started with a five-minute resting phase, during which the subject was instructed to focus on a cross in the middle of a computer screen and let his mind wander. The data acquired in this phase were used to calibrate a beamformer that we aimed at the precuneus. The details of the beamforming procedure are described in Section 2.2.4. These data were also used to estimate the natural variations of resting log-bandpower over the ranges of 2–5 Hz for GH and 55–85 Hz for LS. To do so, we spatially filtered the recorded data with the precomputed beamformer (as described in Section 2.2.4) and applied a fast Fourier transform (FFT) with a sliding Hanning window of 5 s with a step length of 40 ms. We used this estimate to calibrate the feedback, as described below.

In each of the three blocks, the resting phase was followed by the neurofeedback training phase, which consisted of 20 trials, each lasting 1 min with a pause of 5 ± 0.5 s between one and the next. In every trial the patient was asked in pseudorandom order either to up-regulate or to down-regulate his θ (GH) or γ (LS) log-bandpower in his precuneus. The number of trials per condition was balanced in each block. The patient received continuous feedback on the current state of the log-bandpower in his precuneus (the log-bandpower computations are described in Sections 2.2.3 and 2.2.4).

In this training, the patient received simultaneous visual and auditory feedback. While visual feedback is more intuitive, patients with progressing ALS eventually lose oculomotor control, making visual feedback useless. Once this happens, patients must rely only on auditory feedback. The patient received both types of feedback to allow for a smooth transition. For visual feedback, the estimated log-bandpower was mapped to the vertical position of a white ball displayed on the computer screen in front of the subject (Figure 1). The screen's center position represented the median resting-state bandpower (baseline), and the blocks in the top and bottom of the screen represented the median minus two and plus two standard deviations, respectively. For auditory feedback, we used two distinct sounds from a publicly available sound repository (`http://freesound.org`): If the estimated log-bandpower exceeded the baseline, a humming sound played continuously (`http://freesound.org/people/freesound/sounds/50168`); otherwise, a wind sound played continuously (`http://freesound.org/people/homejrande/sounds/17383`). The volume of each sound increased linearly as the difference increased between the current log-bandpower and the baseline. The feedback signal was updated at 25 Hz. All online signal processing and stimuli presentation was performed with BCI2000 [25] and its extension BCPy2000.
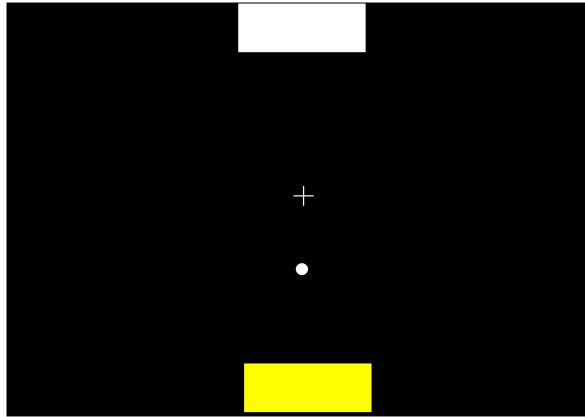
Figure 1. Example of the feedback screen. The vertically moving white ball corresponds to the estimated log-bandpower. The fixation cross in the center represents the median resting-state bandpower (baseline); the boxes at the top and bottom represent the median resting-state bandpower minus two and plus two standard deviations, respectively. Subjects were instructed to move the white ball to the yellow box (either top or bottom).

The patient was prompted to up- and down-regulate with both auditory and visual instructions. Auditory instructions were given at the beginning of each trial: The name of the sound corresponding to the trial task was read out in German by a male voice ("Summen" for up-regulation; "Windrauschen" for down-regulation). Visual instructions were shown throughout the trial: A yellow box at the top or the bottom of the screen indicated the target for up- or down-regulation, as shown in Figure 1.

Beginning in session 14, we did not provide GH with targets, but instead asked him questions, which he answered with our BCI. A decrease in θ bandpower meant "yes", and an increase in θ bandpower meant "no". GH had provided twenty personal questions (ten with a "yes" answer and ten with a "no" answer), which we presented to him in each block in pseudorandom order.

In the training trials, every time the ball was in the target area (log-bandpower of two standard deviations or more away from the baseline in the desired direction for three cumulative seconds, a "winning" sound was played (`http://freesound.org/people/fins/sounds/171670/`) and one point was awarded. The patient's number of collected points was shown on the screen throughout training. At the end of the trial, additional points were awarded for successful online classification (Section 2.3).

The patients did not receive any instructions on how to control the feedback signal. Following each session, they were asked to write down their thoughts and feelings associated with up- and down-regulation of the feedback signal.

Due to technical problems, only two blocks of the experiment are available for GH's sessions 1, 6, 12, 25, 28 and LS' sessions 3, 11, 22, resulting in 20 trials for each condition; only one block of experiment is available for LS' session 12, resulting in 10 trials per condition.
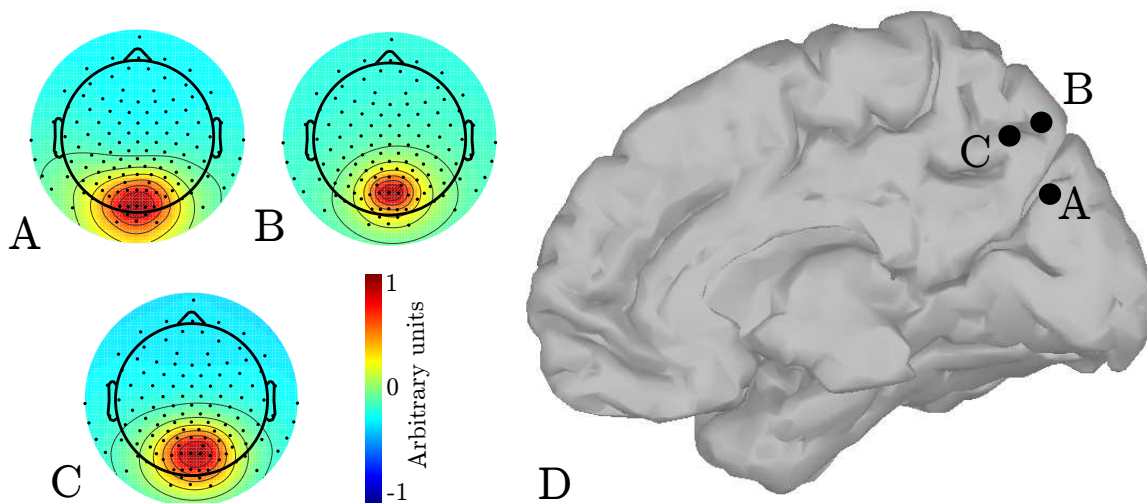
Figure 2. A) Initial beamformer topography for GH (sessions 1–12); B) Final beamformer topography for GH (sessions 13–29); C) Beamformer topography for LS. D) Medial view of the brain right hemisphere with the dipoles (marked with black dots) fitted to the topographies A–C.

2.2.3. Online feedback We provided online feedback in the γ band to LS and in the θ band to GH. The γ feedback frequency band for LS was set to 55–85 Hz to avoid contamination by 50 Hz line noise. For GH, we identified his personal θ band by recording EEG data during two resting states: eyes closed for 5 min and eyes open for 5 min. GH's individual α peak was located at 10 Hz; the lower border of the GH individual α band / upper border of the GH individual θ band was determined as the intersection of the spectral power of channel Oz between the eyes-open and eyes-closed resting states [26], which we determined to be at 5 Hz. The individual lower border of θ was initially set at 2 Hz, resulting in an initial feedback range of 2–5 Hz. We adjusted the feedback frequency band, in order to capture the strongest observed modulations, first to 2–4 Hz (sessions 4–12) and then to 1–5 Hz (sessions 13–29).

To estimate the current log-bandpower, we spatially filtered the recorded data with the precomputed beamformer (as described in Section 2.2.4) and applied a FFT with a sliding Hanning window of 5 s with a step length of 40 ms. The estimate was standardized by using the median and standard deviation of the estimated log-bandpower from the resting state.

2.2.4. Beamforming To estimate the bandpower in the precuneus, we used linearly constrained minimum-variance (LCMV) beamforming [27]. LCMV beamforming is an adaptive spatial filter that attenuates the activity of sources outside the region of interest (ROI), while preserving the activity from sources within the ROI. The ROI activity $y[t]$ is estimated as the dot product between the spatial filter $\mathbf{w}^*$ and measurements of the electrical potential on the surface of the scalp at N electrode locations $\mathbf{x}[t] \in R^N$:

$y[t] = \mathbf{w}^{*T}\mathbf{x}[t]$. The spatial filter is obtained by solving the optimization problem

$$\mathbf{w}^* = \underset{\mathbf{w}}{\operatorname{argmin}}\{\mathbf{w}^T \Sigma_{EEG} \mathbf{w}\} \text{ s.t. } \mathbf{w}^T \mathbf{a} = 1, \tag{1}$$

which has the analytic solution [27]

$$\mathbf{w}^* = (\mathbf{a}^T \Sigma_{EEG}^{-1} \mathbf{a})^{-1} \mathbf{a}^T \Sigma_{EEG}^{-1}. \tag{2}$$

Here, $\Sigma_{EEG} \in R^{N \times N}$ is a spatial covariance matrix of EEG data computed for every subject and session from the resting-state data (pre-filtered for 1–100 Hz with 3-rd order Butterworth filter); $\mathbf{a} \in \mathbb{R}^N$ is the topography of the ROI dipole projection on the scalp.

As an initial beamformer topography $\mathbf{a} \in \mathbb{R}^N$ for GH (Figure 2A), we took the topography of the independent component (IC, for the details see Section 2.4.1) that showed significant modulation in the individual θ (2–5 Hz) range in our previous study with GH [23]. On session 13, we updated the topography by performing and independent component analysis (ICA) on the concatenated data from all previous sessions and selecting the non-artefactual IC with the highest modulation (as measured by the R^2). The final beamformer topography is shown in Figure 2B.

For LS, we selected the IC topography that was visually similar to GH topographies (Figure 2C) from ICA decomposition computed (as explained in Section 2.4.1) for the data collected for the pilot study unrelated to the paradigm reported in the present work. The LS beamformer topography remained constant throughout the study.

For each beamformer topography, we localized a corresponding dipole. We spread $K = 3 \cdot 15028$ current dipoles over 15028 cortical locations, with three dipoles at every location being mutually orthogonal. Then, we generated the leadfield matrix A, specifying the projection of dipole activity $\mathbf{s}[t] \in R^K$ on the $N = 121$ electrodes $\mathbf{x}[t] \in R^N$. The leadfield matrix was generated with the BrainStorm toolbox [28] for standardized electrode locations and a standardized three-shell spherical head model. For each topography and dipole position, we then fitted the linear combinations of three mutually orthogonal dipole topographies to the beamformer topographies and, for each topography, selected the dipole with the lowest square error. The resulting dipole locations for all three beamformer topographies are shown in (Figure 2D). We note that dipole A (corresponding to the initial GH beamformer topography) lies slightly outside the precuneus. During the first 12 sessions, GH thus received feedback from the intersection of the cuneus and the precuneus. We investigate the effects of this change in feedback topography in Section 3.3

2.2.5. Safety There are no studies on how neurofeedback affects ALS progression. To avoid abnormal θ and γ powers, and to ensure the safety of the neurofeedback procedure for the patients, we did not reward the patients for up- or down-regulating bandpower beyond plus or minus two standard deviations of their resting-state bandpower. This way patients were trained to modulate oscillations within their natural range of variations. Additionally, after every session the patients were asked if they had noticed any negative effects of the training. None of the patients reported any negative effects of the study.

2.3. BCI: Online classification

Beginning in session four for GH and in session nine for LS, we performed online classification. The data corresponding to each trial were classified online with a pre-trained classifier, providing one bit of information per trial.

To accomplish this, a linear ν-support vector machine (ν-SVM) classifier [29] was trained on all previously collected data by using the lib-svm toolbox [30]. To prevent the classifier from focusing on artefacts, we pre-processed the data prior to the classifier training. We performed ICA (as explained in Section 2.4.1), manually selected the artefactual ICs, and then randomly permuted these ICs across the trials within each session. Then, we re-projected the ICs back on on the scalp and used this data to train the classifier. In this way, we ensured that artefactual ICs did not carry any information on the class labels without altering the overall power of the EEG. We used the trial-averaged θ (GH) or γ (LS) log-bandpower on all channels as the 121-dimensional feature vector. The optimal ν-parameter was estimated by ten-fold crossvalidation (CV): The ν-parameter was changed from 0.05 to 1 in steps of 0.05 and the mean CV classification accuracy was estimated for every value. The ν-parameter yielding maximal CV accuracy was used for training the final ν-SVM.

Feedback on online classification was provided to the patient after each trial. For a successful classification, a "winning" sound (`http://freesound.org/people/fins/sounds/171670/`) was played and 10 points were added to the final score.

For GH, prior to session 15 the classifier was retrained using the three most-recent sessions. For LS, prior to session 11 the classifier was retrained using his five most successful previous sessions. From session 18 onward we classified the trial by the sign of the difference between the baseline and the median γ bandpower in the precuneus (as estimated by the beamformer). The details of the classifier change are discussed in Section 3.3.

2.4. Offline analysis

2.4.1. ICA-based artefact attenuation EEG recordings are often contaminated by muscle (EMG) [31] and ocular (EOG) artefacts [32]. To attenuate the effects of these artefacts, we used second-order blind identification (SOBI) independent component analysis (ICA) [33]. Specifically, the data from each session were first high-pass filtered with a third-order Butterworth filter with cutoff frequency of 0.1 Hz, then reduced to 64 dimensions by principle component analysis (PCA), and finally separated into independent components (ICs). The ICs were then visually inspected and rejected as artefactual if they fulfilled any of the following criteria [34]: (1) The IC spectrum did not follow the cortical $\frac{1}{f}$-behaviour; (2) The IC topography was not dipolar; (3) The IC time series contained EOG-like activity (eyelid blinks, eye movements); (4) The IC time series contained any other artefacts (50-Hz line noise, large spikes). The remaining ICs were re-projected on the scalp to obtain the data cleaned from artefacts of muscular and ocular activity.

2.4.2. Topography of bandpower modulation To investigate the topographies of the bandpower modulations, we computed the signed R^2 for every EEG channel. First, we estimated log-bandpower for each trial by using a FFT with a Hanning window of 1 min (trial length). Then we averaged the log-bandpower over the feedback frequency range. Lastly, we computed signed R^2, i.e., the percentage of variance in the data that is explained by the class labels, for every channel in every session and then averaged it over sessions.

2.4.3. Offline classification To estimate how discriminable the up- and down-regulated states are, we employed a linear discriminant analysis (LDA). For every session, the block-specific precomputed beamformer was applied to the ICA-cleaned data, and then the log-bandpower for each trial was estimated by using a FFT with a Hanning window of 1 min (trial length). We then averaged the log-bandpower over the frequency range of the feedback. The resulting one-dimensional vector was used for offline leave-one-trial-out crossvalidation (LOOCV) accuracy estimation with the LDA classifier.

2.4.4. Spectral specificity of bandpower modulation We analyzed the spectral specificity of the neurofeedback training using both the ICA-cleaned data and the raw data. For that, we first applied the block-specific precomputed beamformer to the data and then computed the log-bandpower for each trial by using a FFT with a Hanning window of 1 min (trial length). Then, we computed the signed R^2 for all training sessions and all frequencies from 1 Hz to 250 Hz in non-overlapping windows of 1 Hz width. Lastly, we averaged the signed R^2 across all training sessions.

2.4.5. Spatial specificity of the bandpower modulation: Dynamic statistical parametric maps and statistical testing To test whether the bandpower modulation arose from the precuneus, we employed noise-normalized minimum norm estimate dynamic statistical parametric maps (dSPM) [35]. We spread $K = 3 \cdot 15028$ current dipoles over 15028 cortical locations, with three dipoles at every location being mutually orthogonal. Then, we generated the leadfield matrix A specifying the projection of dipole activity $\mathbf{s}[t] \in R^K$ on the $N = 121$ electrodes $\mathbf{x}[t] \in R^N$. The leadfield matrix was generated with the BrainStorm toolbox [28] for standardized electrode locations and a standardized three-shell spherical head model. The ICA-cleaned data was filtered in the γ (55–85 Hz, LS) or θ (2–5 Hz, GH) band. Then the activity of each source was estimated from the ICA-cleaned EEG measurements at N electrode locations, as described in [35]:

$$\tilde{\mathbf{s}}[t] = W\mathbf{x}[t], \text{ with } W = \Sigma_d A^T (A\Sigma_d A^T + C)^{-1}. \tag{3}$$

Here, Σ_d is the spatial covariance of the dipole strength vector, approximated by the identity matrix, and C is the sensor noise covariance matrix, computed for each session from the resting-state data. We then estimated a noise-normalized current dipole power $\tilde{\mathbf{q_i}}[t]$ at each time point t and location i [35] by averaging the three dipoles for each location,

$$\tilde{\mathbf{q}}_{\mathbf{i}}[t] = \frac{\sum\limits_{j \in G_i} \tilde{\mathbf{s}}_j^2[t]}{\sum\limits_{j \in G_i} \mathbf{w}_j C \mathbf{w}_j^T} \tag{4}$$

where $\mathbf{w}_j$ is the jth row of the unmixing matrix W and G_i is the set of dipole indices located at i [35].

To estimate the effect of the neurofeedback training, we then averaged the current dipole power estimate over all trials from all sessions of each condition and computed the difference D between the up- and down-regulation conditions. To test the null hypothesis H_0: $D = 0$ that there is no difference in activity between the two conditions, we estimated a p-value for each cortical location. To do this, we randomly permuted the condition labels of the trials 10^3 times. We then counted the number of times the resulting $|D_{H0}|$ exceeded $|D|$ and divided this number by the number of permutations to obtain a p-value for each source location. Lastly, we corrected the significance level by using a false discovery rate (FDR) of $\alpha_{\mathrm{FDR}} = 0.05$ [36] to compensate for the multiple comparisons at each of the 15028 cortical locations. To plot the results, we set $D = 0$ for the locations at which we did not reject the null hypothesis.

2.4.6. Spatial specificity of the bandpower modulation: Functional magnetic resonance imaging (fMRI) Following the fifth neurofeedback session, patient GH participated in an additional fMRI study. This fMRI study followed the same design as the neurofeedback training, except that no feedback was provided. Instead, GH was asked to carry out the same thought patterns he previously used to control the EEG-based neurofeedback. Eighteen trials per condition were recorded in pseudorandomized order in a 3T Siemens TRIO (Erlangen, Germany), using a multi-band gradient echo planar sequence with 48 slices (3 mm isotropic voxel, MB 3, TR 1500 ms, TE 30 ms). The BOLD data was then motion-corrected, high-pass filtered at 0.01 Hz, and spatially smoothed with a kernel of 7 mm using the LIPSIA software package [37]. We then employed a linear SVM with leave-one-trial-out cross-validation to compute voxel-wise decoding accuracy in differentiating the experimental conditions that correspond to up- and down-regulation of precuneus θ power in the neurofeedback sessions. Here, trial-averaged BOLD signals of the center voxel and its six adjacent voxels were used as features. Parameter tuning of the SVM was carried out by an inner-loop cross-validation. We tested each voxel for a decoding accuracy significantly above chance-level by a binomial test [38], using a false discovery rate (FDR) of $\alpha_{\mathrm{FDR}} = 0.01$. We could not do the fMRI study with LS, because he could not formulate an explicit strategy for controlling the BCI and was thus unable to control his precuneus γ in the absense of continuous feedback.

3. Experimental Results

The results section is structured as follows. First, we report the general results: average neurofeedback training performance (offline classification accuracy), BCI performance (online classification accuracy), patients' strategies and the resulting bandpower modulation topographies. Then, we describe changes in performance across sessions. We note that our setup does not enable us to distinguish between effects that are due to disease progression and those that result from repeated training. In sections 3.4– 3.5, we provide further evidence of the precuneus origin of the modulations by analysing spectral and spacial specificity of the modulations.

3.1. Neurofeedback training and BCI performances

GH and LS achieved an average online decoding accuracy of 70.55% and 59.44% across all sessions, respectively. Their offline decoding accuracies across all sessions are 70.09% and 75.87%, respectively. GH performed 29 sessions (820 trials per condition), with 26 sessions (710 trials per condition) classified online. LS performed 29 sessions (610 trials per condition), with 26 sessions (440 trials per condition) classified online. For both patients we rejected the null hypothesis of chance-level performance at the significance level $\alpha < 0.01$ [38] offline as well as online.

3.2. Patients' reports and topographies of bandpower modulation

GH reported that he could control his precuneus θ bandpower by alternating pleasant and sad thoughts, with exception of session 12, when he tried to repeat words "yes" or "no" in his head. GH's strategy is in agreement with previous studies connecting emotional processing with posterior θ modulations (for a review, see [39]). LS could not precisely describe how he controlled his precuneus γ bandpower, but he reported that he controlled the ball by thinking "yes" or "no" or by wanting the ball to go in the desired direction.

   Despite different strategies and different feedback frequency bands, the average signed R^2 topographies are similar for both patients (Figure 3). Both topographies resemble the beamformer topographies used for training (Figure 2), indicating successful neurofeedback training. Note that for GH channels in central areas show slight negative correlation, while for LS all the channels are positively correlated with the condition (required direction of precuneus bandpower modulation).

3.3. Performance variations and training effects

For each individual session, an online decoding accuracy of 60.0% is required to reject the null hypothesis of chance-level performance at the significance level $\alpha = 0.05$ [38]. GH performed above this threshold in 22 out of 26 BCI sessions (Figure 4). We note here the difference between online and offline classification accuracies. Online classification accuracy depends on the ability of the pre-trained nu-SVM classifier to generalize from
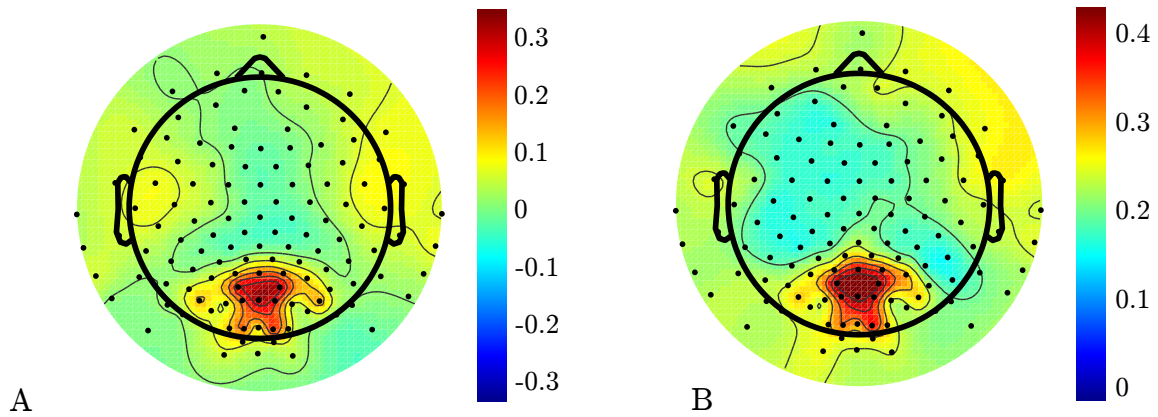
Figure 3. A. Signed R^2 topography for the θ bandpower modulations of patient GH averaged over all training sessions. B. Signed R^2 topography for the γ bandpower modulations of patient LS averaged over all training sessions. Note the different colour scales.
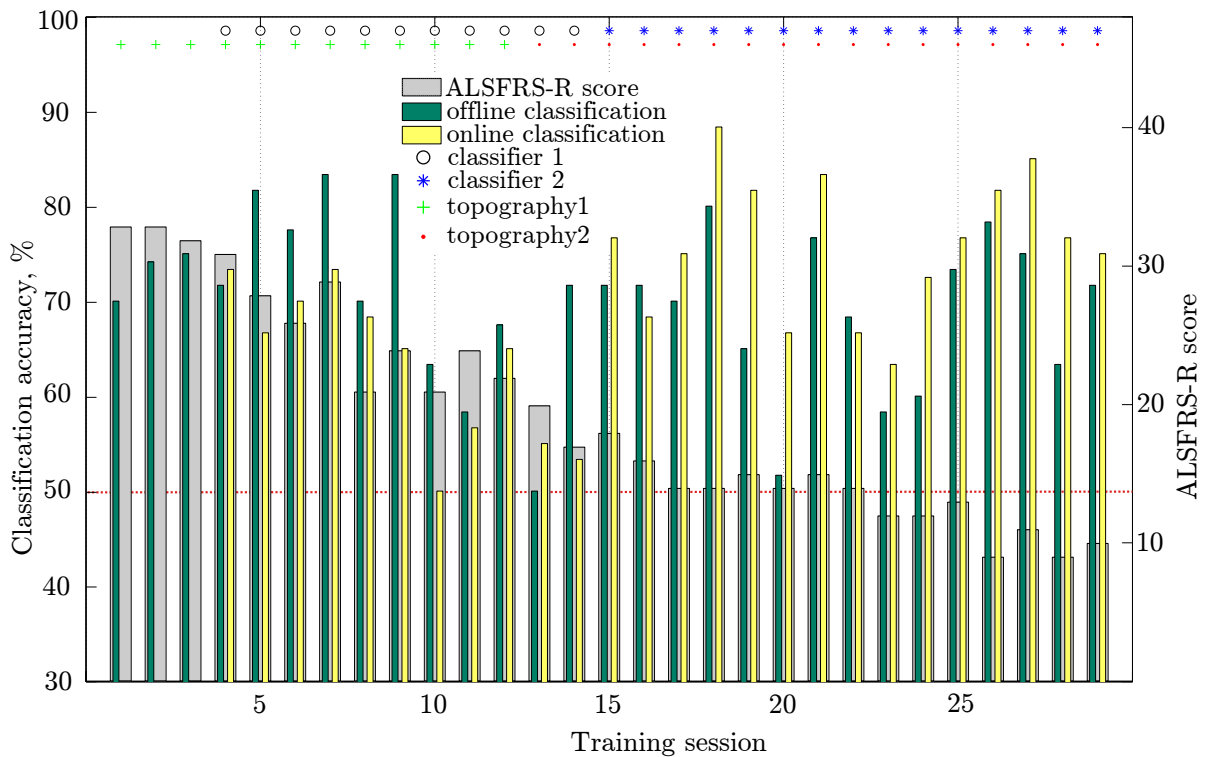

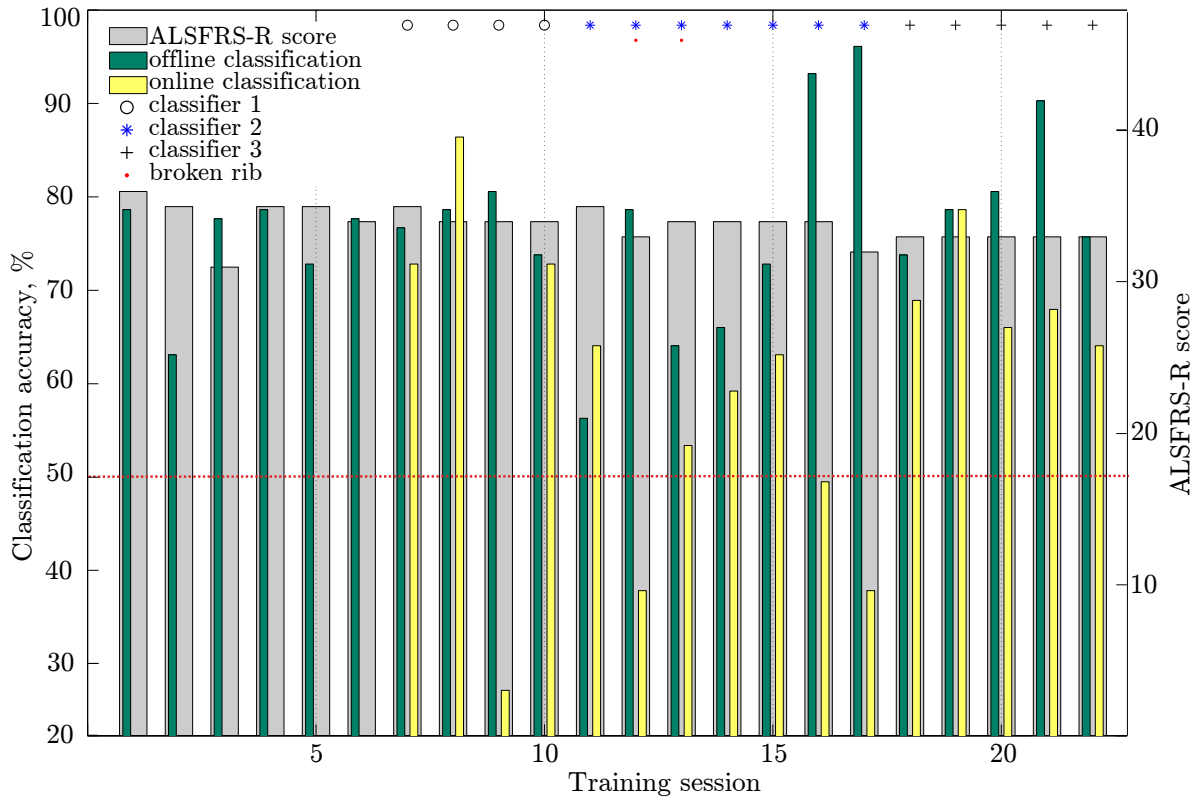**Figure 4.** BCI online (yellow) and offline (green) performance and ALSFR-R score (gray) for patient GH. Circles and asterisks mark the two classifiers; crosses and dots mark the two feedback topographies. Red line corresponds to chance level classification accuracy (two-class classification).

previous sessions to the current one. Offline classification accuracy is always computed only for the data from one session and serves as a measure of neurofeedback training efficiency. Thus, high offline accuracies do not necessary result in high online accuracies, as it is possible that the patient induces activation patterns that are discriminable within
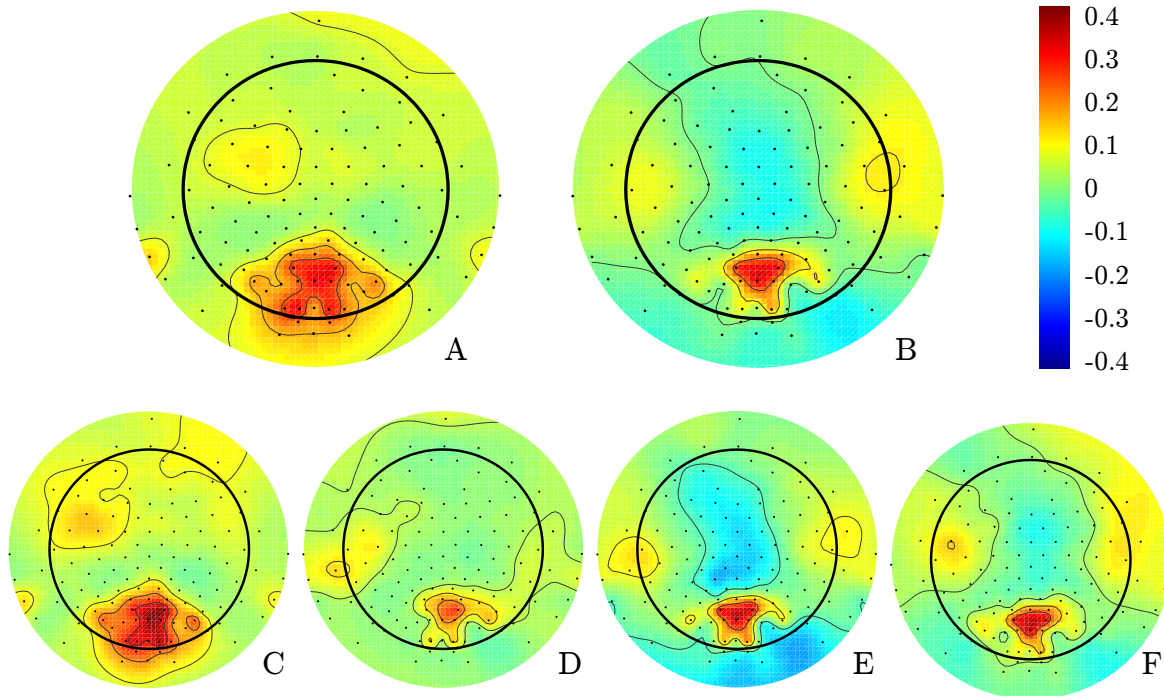
Figure 5. Training effects. Signed R^2 topography for the θ bandpower modulations of patient GH averaged over: A) Sessions 1–12 (topography 1); B) Sessions 13–29 (topography 2); C) Sessions 4–8 (first sessions classified online); D) Sessions 10–14 (before classifier update); E) Sessions 15–19 (after classifier update); F). Sessions 25–29 (final sessions)

one session, but are changing from session to session (for example due to strategy changes or ALS-related changes). Despite a fast disease progression, as indicated by a decline of the ALSFRS-S score by 23 points over the course of the study, GH's offline accuracy remained roughly stable across the whole study. His initially high online accuracy declined to chance-level performace in sessions 14 and 15, but recovered after updating the online classifier in session 15.

The pattern of bandpower modulation also remained stable, becoming more localized and converging to Figure 3 after an update of the beamformer topography (Figure 5 A–B). The central electrodes showed initially positive correlation with the condition and changed to negative after an update of the beamformer. Changes in the modulations topography motivated the classifier update, that led to increase in online classification accuracies (Figure 5 C–F). Despite the progress of ALS, the modulations topography remained consistent (Figure 5 F).

LS performed above the decoding accuracy of 60.0%, that is required to reject the null hypothesis of chance-level performance at the significance level $\alpha = 0.05$ [38], in 10 out of 16 online decoding sessions (Figure 6). LS also showed convergence to the beamformer topography as a result of training (Figure 7, A, B, and D). However, LS' performance was likely impaired in several sessions by pain from a broken rib. LS broke a rib before session 12, but expressed the desire to continue the training. This event

Figure 6. BCI online (yellow) and offline (green) performance and ALSFR-R score (gray) for patient LS. Circles, asterisks, and crosses mark the three classifiers; the red dot marks the sessions when LS had a broken rib. Red line corresponds to chance level classification accuracy (two-class classification).
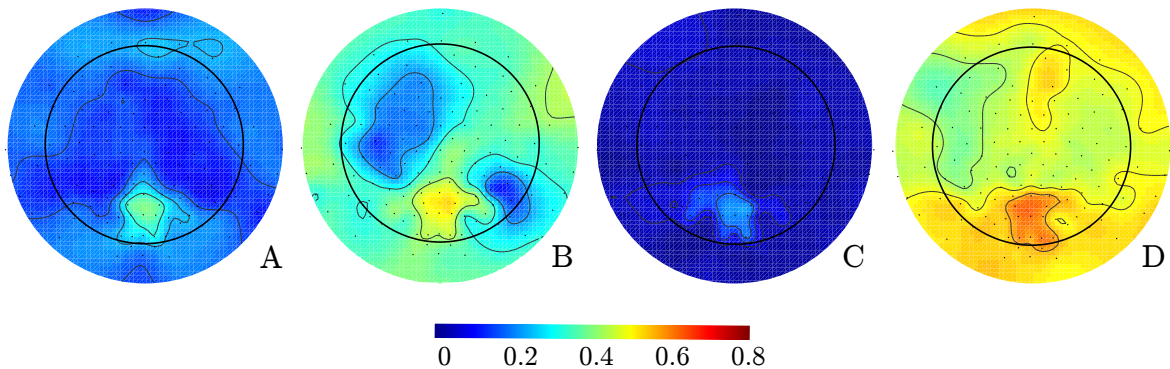

Figure 7. Training effects: Signed R^2 topography for the γ bandpower modulations of patient LS averaged over A) Sessions 1-5; B) Sessions 7–10 (first sessions classified online); C) Session 12–13 (broken rib); D) Sessions 15–22 (recovery).

coincided with a drop in online decoding accuracy to chance-level. The averaged R^2 topography over those two sessions showed almost no modulation (Figure 7, C). LS performance only recovered after we updated the online decoding algorithm in session 18 (cf. Section 2.3).

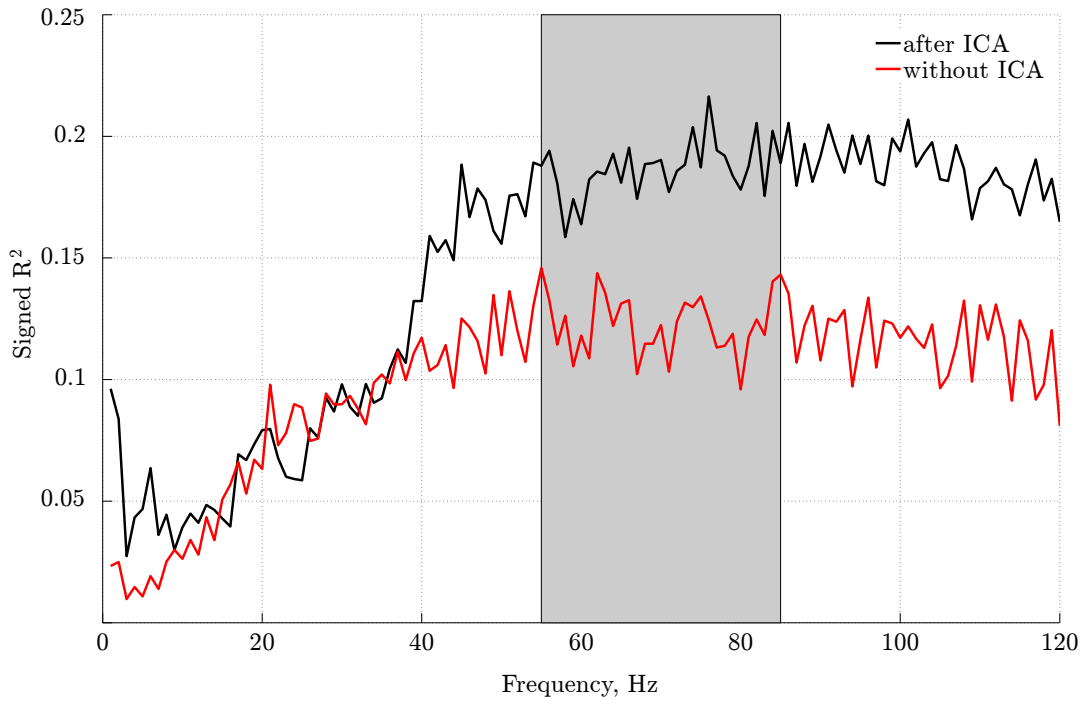## 3.4. Spectral specificity of the bandpower modulation
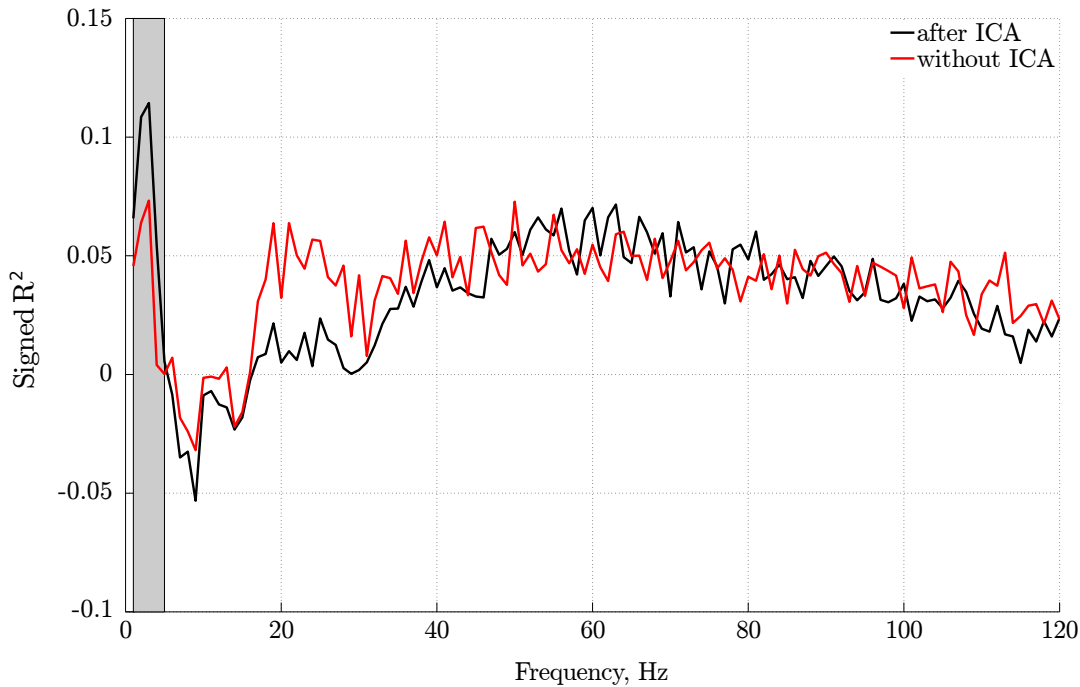
Figure 8. Spectral specificity of the neurofeedback training for patient GH: signed R^2 averaged over all training sessions before and after the ICA artefact attenuation. The shaded area shows the frequency range of the online neurofeedback (1–5 Hz).

Here, we compare modulations of precuneus activation for different frequencies before and after ICA artefact attenuation. Such comparison allows us to estimate the contribution of artefacts to the neurofeedback training.

For both patients the maximum of R^2 lies within the feedback frequency range (Figures 8 & 9, shaded area), indicating successful neurofeedback training. Furthermore, ICA-based attenuation of the artefacts increases the R^2 within the feedback frequency range. This suggests that the induced modulations are primarily of cortical nature.

We note that GH also shows a modulation in the γ range and LS exhibits, to a lesser extent and only visible after ICA-based artefact reduction, regulation of brain rhythms in the θ range. This finding is consistent with previously reported relations between the θ and the γ band [40].

For GH, we also observe a negative correlation between theta ($2 - 5$ Hz) and alpha ($6 - 12$ Hz) rhythms, which is in agreement with previous findings [26]. We do not observe such a negative correlation for LS.

3.5. Spatial specificity of the bandpower modulation: dSPM

For both patients, the maximum bandpower modulation (Figures 10 & 11) coincides with the precuneus and extends to the cuneus and the posterior cingulate. According to GH's reports, he controlled his θ bandpower by alternating pleasant and sad thoughts.

Figure 9. Spectral specificity of the neurofeedback training for patient LS: signed R^2 averaged over all training sessions before and after the ICA artefact attenuation. The shaded area shows the frequency range of the online neurofeedback ($55 - 85$ Hz).
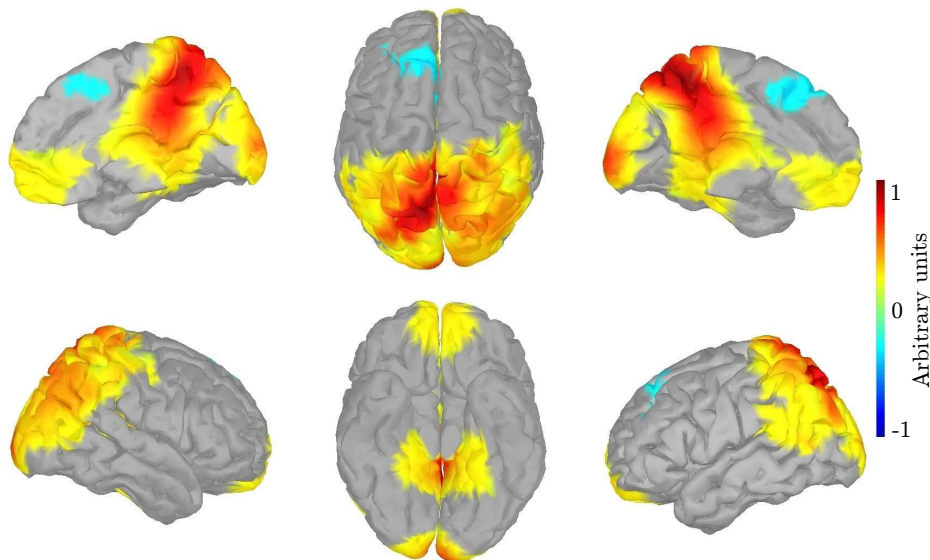

Figure 10. Significant bandpower differences, averaged over all of GH's training sessions.

These reports agree with previous studies that found the posterior cingulate cortex to be activated during emotional evaluation [41]. Positively correlated regions in the precuneus and the frontal medial cortex are parts of the Default Mode Network (DMN) [42]. The DMN is known to be activated by self-referential thoughts [43, 44].
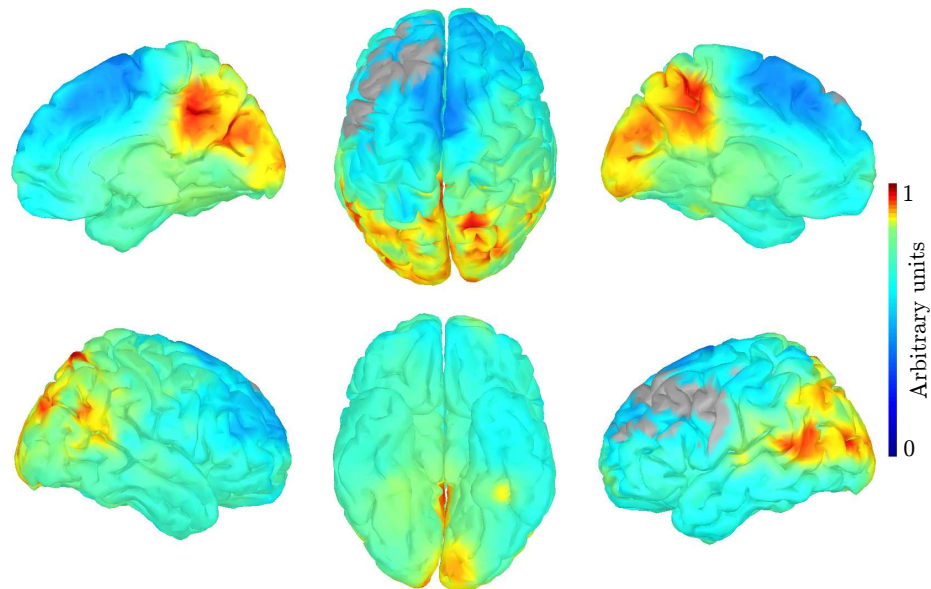
Figure 11. Significant bandpower differences, averaged over all of LS' training sessions.

Deactivation in the pre-motor areas indicates an involvement of the task positive network, which is known to be anticorrelated with the DMN [45].

LS' γ bandpower modulation pattern (Figure 11) is in general similar to GH's, with the strongest modulation found in the precuneus. However, it is much less localized: almost the entire cortex shows a significant modulation. While spatial specificity is generally not crucial for controlling a BCI, the broad modulation suggests a spatially unspecific contamination by residual EMG activity.
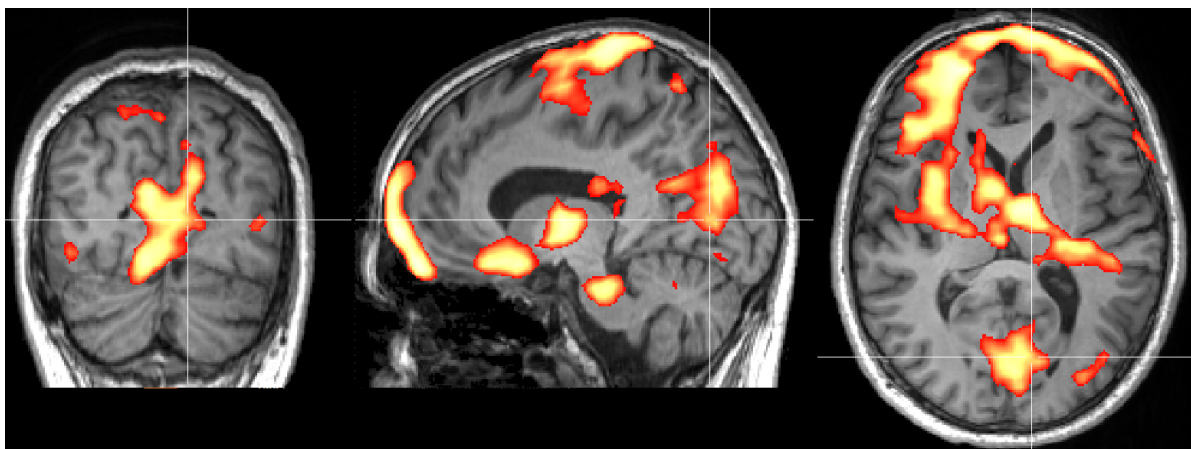
Figure 12. fMRI decoding results of patient GH.

3.5.1. Spatial specificity of the bandpower modulation: fMRI The fMRI decoding results (Figure 12) agree with those of the dSPM source localization, with a statistically significant modulation at the intersection of the precuneus, cuneus, and posterior

cingulate as well as in the medial prefrontal cortex. Deeper brain structures are unlikely to be detectable by EEG.

4. Discussion

In this work, we proposed a novel BCI for ALS patients based on self-regulation of brain rhythms in the precuneus. In particular, we tested two hypotheses: First, ALS patients in early disease stages are able to gain control of neuronal oscillations in the precuneus. Second, they can maintain this skill as the disease progresses. The available evidence supports both hypotheses. Both patients were able to modulate the posterior brain rhythms and use these modulations to control the BCI online. These modulations originated from the intersection of the precuneus, cuneus, and posterior cingulate and were specific to the frequency band in which the patients were trained (θ or γ). Patient GH was able to maintain this skill despite the dramatic decrease in his ALSFRS-R score throughout the training. Patient LS showed almost no disease progression throughout training, shortly lost the ability to control the BCI due to a broken rib, but was able to rapidly recover the skill.

Other EEG-based BCIs have been reported to work well for ALS patients in early to moderate disease stages [4, 5, 46]. However, as the disease progresses, LIS and CLIS patients appear to gradually loose the ability to control conventional BCIs [4, 46]. We were not able to test our novel approach in the CLIS because of the death of one of the patients and a relocation of the other.

ALS gradually affects the whole brain [3, 18]. Because the precuneus is linked to consciousness [21] and consciousness is required for any type of communication, we argue that BCIs based on brain activity in the precuneus have the best chance of maintaining communication with CLIS patients for as long as this is supported by their degree of consciousness. More specifically, the intersection of the precuneus, cuneus, and posterior cingulate is one of the nodes of the DMN [42]. The DMN, comprising the precuneus/posterior cingulate cortex, medial prefrontal cortex, and the temporoparietal junction, is a resting-state network that is active in the absence of any tasks with high cognitive demand. It has been linked to autobiographical memory, envisioning the future, theory of mind and moral decision making (for a review see [47]). Abnormalities in the DMN have been linked to various neuropsychiatric disorders [48]. Failure of precuneus-based BCI in CLIS may indicate alterations in the state of consciousness that prohibit communication.

For conscious CLIS patients, BCIs based on self-regulation of brain rhythms in the precuneus still hold the promise of restoring communication and thus improving ALS patients' life quality [49]. Thus, further investigation is needed on the performance of BCIs based on self-regulation of brain rhythms in the precuneus in CLIS ALS. Because our study is limited to two patients with bulbar ALS, it will also be important to investigate whether other patients can control this type of BCI. Training should be started early, because patients' learning abilities can decline as ALS progresses [50]. In

the future, longitudinal studies with ALS patients could be made easier by developing simple and robust EEG-based neurofeedback systems that can be used by patients and patient's caretakers and do not require the constant presence of a researcher.

5. Acknowledgements

6. References

[1] K Nihei, A C McKee, and N W Kowall. Patterns of neuronal degeneration in the motor cortex of amyotrophic lateral sclerosis patients. *Acta Neuropathologica*, 86(1):55–64, June 1993.

[2] R Schmidt, E Verstraete, M A de Reus, J H Veldink, L H van den Berg, and M P van den Heuvel. Correlation between structural and functional connectivity impairment in amyotrophic lateral sclerosis. *Human Brain Mapping*, 35(9):4386–4395, 2014.

[3] H Braak, J Brettschneider, A C Ludolph, V M Lee, J Q Trojanowski, and K Del Tredici. Amyotrophic lateral sclerosis–a model of corticofugal axonal spread. *Nature reviews. Neurology*, 9(12):708–14, 2013.

[4] A Kübler and N Birbaumer. Brain-computer interfaces and communication in paralysis: extinction of goal directed thinking in completely paralysed patients? *Clinical Neurophysiology*, 119(11):2658–2666, 2008.

[5] N Birbaumer, F Piccione, S Silvoni, and M Wildgruber. Ideomotor silence: the case of complete paralysis and brain-computer interfaces (BCI). *Psychological Research*, 76(2):183–91, 2012.

[6] J R Wolpaw, N Birbaumer, W J Heetderks, D J McFarland, P H Peckham, G Schalk, E Donchin, L A Quatrano, C J Robinson, and T M Vaughan. Brain-computer interface technology: a review of the first international meeting. *IEEE Transactions on Rehabilitation Engineering*, 8(2):164–73, 2000.

[7] A Brouwer and Jan B F Van Erp. A Tactile P300 Brain-Computer Interface. *Frontiers in neuroscience*, 4(May):11, 2010.

[8] G Pfurtscheller, D Flotzinger, and J Kalcher. Brain-Computer Interface–a new communication device for handicapped persons. *Journal of Microcomputer Applications*, 16(3):293–299, 1993.

[9] E Donchin, K M Spencer, and R Wijesinghe. The mental prosthesis: assessing the speed of a P300-based brain-computer interface. *IEEE Transactions on Rehabilitation Engineering*, 8(2):174–179, 2000.

[10] M Salvaris and F Sepulveda. Visual modifications on the P300 speller BCI paradigm. *Journal of Neural Engineering*, 6(4):046011, 2009.

[11] C Donaghy, M J Thurtell, E P Pioro, J M Gibson, and R J Leigh. Eye movements in amyotrophic lateral sclerosis and its mimics: a review with illustrative cases. *Journal of Neurology, Neurosurgery & Psychiatry*, 82(1):110–116, 2011.

[12] A Ramos Murguialday, J Hill, M Bensch, S Martens, S Halder, F Nijboer, B Schölkopf, N Birbaumer, and A Gharabaghi. Transition from the locked in to the completely locked-in state: A physiological analysis. *Clinical Neurophysiology*, 122(5):925–933, 2011.

[13] M Schreuder, B Blankertz, and M Tangermann. A New Auditory Multi-Class Brain-Computer Interface Paradigm: Spatial Hearing as an Informative Cue. *PLoS ONE*, 5(4):14, 2010.

[14] N J Hill and B Schölkopf. An online brain-computer interface based on shifting attention to concurrent streams of auditory stimuli. *Journal of Neural Engineering*, 9(2):026011, April 2012.

[15] A Kübler, A Furdea, S HaIder, E M Hammer, F Nijboer, and B Kotchoubey. A Brain-Computer

Interface Controlled Auditory Event-Related Potential (P300) Spelling System for Locked-In Patients. *Disorders of Consciousness*, 1157:90–100, 2009.

[16] A E Cavanna and M R Trimble. The precuneus: A review of its functional anatomy and behavioural correlates. *Brain*, 129(3):564–583, 2006.

[17] H C Lou, B Luber, M Crupain, J P Keenan, M Nowak, T W Kjaer, H A Sackeim, and S H Lisanby. Parietal cortex and representation of the mental Self. *Proceedings of the National Academy of Sciences of the United States of America*, 101(17):6827–6832, 2004.

[18] A Vanhaudenhuyse, Q Noirhomme, L J F Tshibanda, M A Bruno, P Boveroux, C Schnakers, A Soddu, V Perlbarg, D Ledoux, J F Brichant, G Moonen, P Maquet, M D. Greicius, S Laureys, and M Boly. Default network connectivity reflects the level of consciousness in non-communicative brain-damaged patients. *Brain*, 133(1):161–171, 2010.

[19] P Maquet, J Péters, J Aerts, G Delfiore, C Degueldre, A Luxen, and G Franck. Functional neuroanatomy of human rapid-eye-movement sleep and dreaming. *Nature*, 383(6596):163–166, 1996.

[20] P Maquet, C Degueldre, G Delfiore, J Aerts, J M Péters, A Luxen, and G Franck. Functional neuroanatomy of human slow wave sleep. *The Journal of Neuroscience : the official journal of the Society for Neuroscience*, 17(8):2807–2812, 1997.

[21] J S Crone, G Ladurner, Y Höller, S Golaszewski, E Trinka, and M Kronbichler. Deactivation of the default mode network as a marker of impaired consciousness: An fmri study. *PLoS ONE*, 6(10), 2011.

[22] J M. Cedarbaum, N Stambler, E Malta, C Fuller, D Hilt, B Thurmond, and A Nakanishi. The ALSFRS-R: A revised ALS functional rating scale that incorporates assessments of respiratory function. *Journal of the Neurological Sciences*, 169(1-2):13–21, 1999.

[23] T Fomina, B Schölkopf, and M Grosse-Wentrup. Towards Cognitive Brain-Computer Interfaces for Patients with Amyotrophic Lateral Sclerosis. *Proceedings of Computer Science and Electronic Engineering Conference (CEEC), 2015 7th*, 2015.

[24] M Grosse-Wentrup and B Schölkopf. A brain-computer interface based on self-regulation of gamma-oscillations in the superior parietal cortex. *Journal of neural engineering*, 11(5):056015, 2014.

[25] G Schalk, D J McFarland, T Hinterberger, N Birbaumer, and J R Wolpaw. BCI2000: A general-purpose brain-computer interface (BCI) system. *IEEE Transactions on Biomedical Engineering*, 51(6):1034–1043, 2004.

[26] W Klimesch. EEG alpha and theta oscillations reflect cognitive and memory performance: a review and analysis. *Brain Research Reviews*, 29(2–3):169–95, 1999.

[27] B D van Veen, W van Drongelen, M Yuchtman, and A Suzuki. Localization of brain electrical activity via linearly constrained minimum variance spatial filtering. *IEEE Transactions on Bio-Medical Engineering*, 44(9):867–880, 1997.

[28] J C Mosher, S Baillet, F Darvas, D Pantazis, E K Yildirim, and R M Leahy. Brainstorm electromagnetic imaging software. In *5th International Symposium on Noninvasive Functional Source Imaging within the Human Brain and Heart (NFSI 2005)*, 2005.

[29] B Schölkopf, A J Smola, R C Williamson, and P L Bartlett. New Support Vector Algorithms. *Neural Computation*, 12(5):1207–1245, 2000.

[30] C Chang and C Lin. LIBSVM: A library for support vector machines. *ACM Transactions on Intelligent Systems and Technology*, 2:27:1–27:27, 2011. Software available at `http://www.csie.ntu.edu.tw/~cjlin/libsvm`.

[31] I I Goncharova, D J McFarland, T M Vaughan, and J R Wolpaw. EMG contamination of EEG: Spectral and topographical characteristics. *Clinical Neurophysiology*, 114(9):1580–1593, 2003.

[32] D Hagemann and E Naumann. The effects of ocular artifacts on (lateralized) broadband power in the EEG. *Clinical Neurophysiology*, 112(2):215–231, 2001.

[33] A Belouchrani, K Abed-Meraim, JF Cardoso, and E Moulines. A blind source separation technique using second-order statistics. *IEEE Transactions on Signal Processing*, 45(2):434–444, 1997.

[34] M Grosse-Wentrup and B Schölkopf. High γ-power predicts performance in sensorimotor-rhythm brain-computer interfaces. *Journal of neural engineering*, 9(4):046001, August 2012.

[35] A M Dale, A K Liu, B R Fischl, R L Buckner, J W Belliveau, J D Lewine, and E Halgren. Dynamic Statistical Parametric Mapping. *Neuron*, 26(1):55–67, 2000.

[36] Y Benjamini and Y Hochberg. Controlling the False Discovery Rate: A Practical and Powerful Approach to Multiple Testing. *Journal of the Royal Statistical Society. Series B (Statistical Methodology)*, 57(1):289 – 300, 1995.

[37] G Lohmann, K Müller, V Bosch, H Mentzel, S Hessler, L Chen, S Zysset, and D Y von Cramon. Lipsiaa new software system for the evaluation of functional magnetic resonance images of the human brain. *Computerized medical imaging and graphics*, 25(6):449–457, 2001.

[38] G R Müller-Putz, R Scherer, C Brunner, R Leeb, and G Pfurtscheller. Better than random? A closer look on BCI results. *International Jouranl of Bioelectromagnetism*, 10(1):52–55, 2008.

[39] B Güntekin and E Baar. A review of brain oscillations in perception of faces and emotional pictures. *Neuropsychologia*, 58:33–51, 2014.

[40] R T Canolty, E Edwards, S S Dalal, M Soltani, S S Nagarajan, H E Kirsch, M S Berger, N M Barbaro, and R T Knight. High gamma power is phase-locked to theta oscillations in human neocortex. *Science*, 313:1626–1628, 2006.

[41] M Cabanis, M Pyka, S Mehl, B W Müller, S Loos-Jankowiak, G Winterer, W Wölwer, F Musso, S Klingberg, A M Rapp, K Langohr, G Wiedemann, J Herrlich, H Walter, M Wagner, K Schnell, K Vogeley, H Kockler, N J Shah, T Stöcker, R Thienel, K Pauly, A Krug, and T Kircher. The precuneus and the insula in self-attributional processes. *Cognitive, Affective & Behavioral Neuroscience*, 13(2):330–45, 2013.

[42] M E Raichle, A M MacLeod, A Z Snyder, W J Powers, D A Gusnard, and G L Shulman. A default mode of brain function. *Proceedings of the National Academy of Sciences of the United States of America*, 98(2):676–682, 2001.

[43] N C Andreasen, D S O'Leary, T Cizadlo, S Arndt, K Rezai, G L Watkins, L L B Ponto, and R D Hichwa. Remembering the past: Two facets of episodic memory explored with positron emission tomography. *American Journal of Psychiatry*, 152(11):1576–1585, 1995.

[44] R N Spreng, R A Mar, and A S N Kim. The common neural basis of autobiographical memory, prospection, navigation, theory of mind, and the default mode: a quantitative meta-analysis. *Journal of cognitive neuroscience*, 21(3):489–510, 2009.

[45] M D Fox, A Z Snyder, J L Vincent, M Corbetta, David C Van E, and Marcus E Raichle. The human brain is intrinsically organized into dynamic, anticorrelated functional networks. *Proceedings of the National Academy of Sciences of the United States of America*, 102(27):9673–8, July 2005.

[46] M Marchetti and K Priftis. Brain-computer interfaces in amyotrophic lateral sclerosis: A metanalysis. *Clinical Neurophysiology : Official Journal of the International Federation of Clinical Neurophysiology*, 126(6):1255–63, 2015.

[47] R L Buckner, J R Andrews-Hanna, and D L Schacter. The Brain's Default Network. *Annals of the New York Academy of Sciences*, 1124(1):1–38, 2008.

[48] S Whitfield-Gabrieli and J M Ford. Default Mode Network Activity and Connectivity in Psychopathology. 8(1):49–76, 2012.

[49] J R Bach. Amyotrophic lateral sclerosis. Communication status and survival with ventilatory support. *American journal of physical medicine & rehabilitation / Association of Academic Physiatrists*, 72(6):343–349, 1993.

[50] H Schreiber, T Gaigalat, U Wiedemuth-Catrinescu, M Graf, I Uttner, R Muche, and A C Ludolph. Cognitive function in bulbar- and spinal-onset amyotrophic lateral sclerosis: A longitudinal study in 52 patients. *Journal of Neurology*, 252(7):772–781, 2005.

Chapter 4

A Cognitive BCI for Patients with ALS

A Cognitive Brain-Computer Interface for Patients with Amyotrophic Lateral Sclerosis

Matthias R. Hohmann[a,b], Tatiana Fomina[a,b], Vinay Jayaram[a,b], Natalie Widmann[b], Christian Förster[b], Jennifer Just[c,d], Matthis Synofzik[c], Bernhard Schölkopf[b], Ludger Schöls[c,d], Moritz Grosse-Wentrup[b]

[a]*International Max Planck Research School for Cognitive and Systems Neuroscience, Österbergstr. 3, 72074, Tübingen, Germany*
[b]*Max Planck Institute for Intelligent Systems, Department for Empirical Inference, Spemannstr. 38, 72076, Tübingen, Germany*
[c]*Hertie Institute for Clinical Brain Research, Department of Neurology, Hoppe-Seyler-Str. 3, 72076, Tübingen, Germany*
[d]*German Center for Neurodegenerative Diseases (DZNE), Otfried-Müller-Str. 23, 72076 Tübingen Germany*

Abstract

Brain-computer interfaces (BCIs) are often based on the control of sensorimotor processes, yet sensorimotor processes are impaired in patients suffering from amyotrophic lateral sclerosis (ALS). We devised a new paradigm that targets higher-level cognitive processes to transmit information from the user to the BCI. We instructed five ALS patients and twelve healthy subjects to either activate self-referential memories or to focus on a process without mnemonic content while recording a high-density electroencephalogram (EEG). Both tasks are designed to modulate activity in the default mode network (DMN) without involving sensorimotor pathways. We find that the two tasks can be distinguished after only one experimental session from the average of the combined bandpower modulations in the theta- (4–7 Hz) and alpha-range (8–13 Hz), with an average accuracy of 62.5% and 60.8% for healthy subjects and ALS patients, respectively. The spatial weights of the decoding algorithm show a preference for the parietal area, consistent with modulation of neural activity in primary nodes of the DMN.

Keywords: EEG, brain-computer interface, brain-machine interface, ALS, locked-in.

1. Introduction

1.1. Amyotrophic Lateral Sclerosis

Amyotrophic Lateral Sclerosis (ALS) describes a variety of conditions that have the progressive degeneration of upper and lower motor-neurons in common [1]. There is no known cure for ALS. The progressive paralysis leads to death due to respiratory failure within an average of three to five years [2]. While modern life-support technology like artificial respiration and nutrition allows for a prolonged life, it in turn also prolongs the psychological

---

*Corresponding author
Email address:* `matthias.hohmann@tuebingen.mpg.de` (Matthias R. Hohmann)

and social burden of being in a paralysed and eventually totally locked-in state. In this state, all voluntary muscle control is lost, including oculomotor functions [1, 3].

The crucial ability lost in 80 to 95% of ALS patients over the course of the disease is communication [4]. The inability to communicate emotions, thoughts, and needs is the most daunting problem that both ALS patients and the social environment inevitably have to face during the progress of the disease [5]. Establishing and maintaining communication may not prolong survival, but it greatly increases the quality of life for ALS patients [6].

1.2. Brain-Computer Interfaces

One way to enable communication via non-muscular modalities is a brain-computer interface (BCI). The term refers to a direct interface with the nervous system through a range of techniques, currently limited by technical and surgical constraints [7]. A BCI communication system delivers the messages or commands of an individual to the external world without peripheral nerves and muscles through the understanding of brain activity [3], the most commonly used of which is non-invasive electroencephalography (EEG). The acquired signals are processed and classified as digital commands to control an application [8].

BCIs have already been used successfully in clinical settings, e.g. for stroke rehabilitation, the treatment of mental illness, and early-stage ALS patients [9]. This has raised hopes that BCIs could also provide autonomy for and enable communication with late-stage ALS patients. However, this mission has proven to be very challenging, as BCIs are often based on motor- and sensory processes, such as the voluntary modulation of sensorimotor rhythms [10]. Patients suffering from ALS show degeneration of neurons in the primary motor cortex [11] and are impaired in their ability to modulate these rhythms in later stages of the disease [12]. Visual speller systems, like the P300 speller or the SSVEP system, require subjects to fixate on target stimuli through gaze. They can be used during the progress of the disease, but fail in the latest stages due to the loss of oculomotor control [13]. BCIs that rely on covert attention can be operated without gazing movements [14, 15, 16], but the retinal jitter that is necessary to perceive a visual stimulus could be affected by the disease as well. Circumventing the visual modality by porting the P300 speller to an auditory [8] or tactile setting [17], or using acoustic odd-ball BCIs for yes/no communication [18] have mostly been tested on healthy subjects and patients in earlier stages of the disease. One study reported a promising results when testing a word-based acoustic odd-ball paradigm in two later-stage ALS patients, however they were not completely locked-in [?]. The usefulness of slow cortical potentials [19] for establishing a reliable communication with completely locked-in patients remains unclear as well. A recent meta-study [20] addressed these issues and concludes that, to this day, no reliable EEG-based communication method has been established for completely locked-in patients.

Some of the cortical processes impaired in ALS can be avoided by training subjects via neurofeedback to self-regulate neural activity in cortical areas that subserve higher functions [21, 22]. One major issue with this approach is the amount of training that is needed for patients to successfully modulate activity. The need for extensive training decreases the feasibility of the system, especially for patients in later stages of the disease. Another issue is the use of visual stimuli, which only works if the patient is not yet completely locked-in. Additionally, if the training starts too late in the progress of the disease the patient may be unable to achieve a classification accuracy that is necessary for communication.

Finally, the state of consciousness in completely locked-in patients remains unclear. It has been argued that the long-term paralysis in the final stages of the disease extinguishes goal-directed thinking [23], and patients may reside in a state-of-mind similar to REM sleep [12].

1.3. The Current Work

We propose to employ a cognitive strategy for realising a BCI that targets higher cognitive functions without relying on neurofeedback-driven learning mechanisms. This cognitive strategy should fulfil three important criteria: First, it should target processes that are at the very basis of human nature and therefore be immediately accessible for everyone. Second, these processes should be generally unrelated to motor processes, circumventing the issues with previous BCIs in ALS patients. And third, they should remain accessible to ALS patient for as long as they possess the cognitive capacity for communication.

While most brain areas are eventually affected by ALS, with the possible exception of the occipital lobe, parietal and prefrontal areas appear to be affected later in the course of disease progression than sensorimotor regions [24]. Based on these findings, we chose to target the Default Mode Network (DMN), a large-scale cortical network that has first been discovered in PET- [25] and later in fMRI-recordings [26]. It consists of three major subdivisions: the medial prefrontal cortex (MPC); the temporoparietal junction (TPJ); and its most important hub, the posterior cingulate cortex, combined with the precuneus. The DMN has been connected to social behaviour, mood control, motivational drive, self-referential judgements, and recollection of prior experiences [27, 28, 29]. Therefore, it plays an important role in the human ability to generate "spontaneous cognition", like daydreaming or mind-wandering, which is a basic and non-motor related human ability.

Recently, the DMN has also been connected to consciousness in brain-damaged patients: Connectivity patterns within the DMN during resting-state have been found to be negatively correlated with the degree of clinical consciousness impairment. Participants in the study ranged from fully conscious healthy controls over locked-in patients with spinal cord injuries or stroke to minimally conscious and comatose patients [30]. While comatose and vegetative patients showed the least connectivity within the DMN, patients with spinal cord injuries and stroke damage showed almost no difference to healthy controls. Therefore, the successful modulation of brain activity in this network could serve as an indicator for the state of consciousness of a patient. Under the assumption that completely locked in ALS patients are not in a comatose, unconscious state and goal-directed thinking is still possible, we hypothesise that the DMN will still exhibit activity patterns as described in [30]. If this is not the case, attempts to communicate would probably be meaningless.

To target processes in the DMN, we devised a novel, stimulus-independent cognitive strategy that modulates the activation and deactivation of the DMN by taking its self-referential properties into account. Based on previous, stimulus-driven studies in fMRI, we instructed subjects to alternate between self-referential thoughts, which activate the DMN [31, 32, 33], and focusing on their breathing, which we expect to deactivate the DMN because it is devoid of self-referential mnemonics [26]. The current work investigates the hypothesis that this strategy elicits bandpower changes in the EEG over areas consistent with the DMN regions found in fMRI. These changes should be sufficiently strong to enable above chance-level decoding accuracies in healthy subjects and patients with ALS, without the need of any

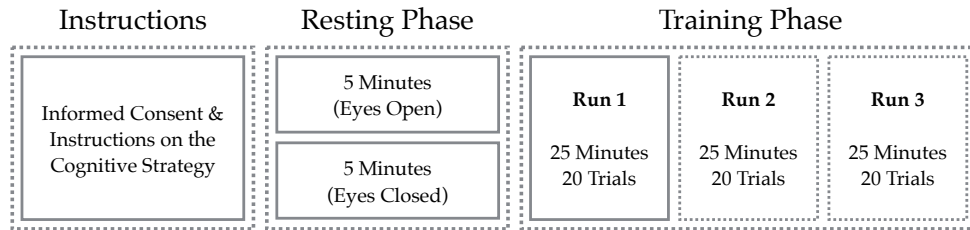| Instructions	Resting Phase	Training Phase		
Informed Consent & Instructions on the Cognitive Strategy	5 Minutes (Eyes Open) / 5 Minutes (Eyes Closed)	**Run 1** 25 Minutes 20 Trials	**Run 2** 25 Minutes 20 Trials	**Run 3** 25 Minutes 20 Trials

Figure 1: The experimental procedure. During all trials and the eyes open resting phase, a fixation cross appeared in the center of the screen. ALS patients were only asked to perform the two resting states and the first training run (depicted as boxes with solid borders).

subject training. A preliminary version of this work has been published recently in conference proceedings [34].

2. Methods

2.1. Experimental Paradigm

Healthy subjects were placed in a chair approximately 1.25 m away from a 17" LCD screen with a resolution of 1280x1024 pixels and a 60 Hz refresh rate. The background of the screen was black, with a white fixation cross appearing in the centre. Prior to the experimental session, two five-minute resting state EEGs were recorded. Subjects were asked to let their mind wander and to keep their eyes open in the first resting-state and closed in the second one.

After the resting-state sessions, subjects performed three experimental blocks with brief intermissions. Each experimental block consisted of ten trials in which the participants were asked to "remember a positive experience" and ten trials in which the participants were asked to "focus on their breathing", in pseudo-randomised order. We chose a trial time of 60 seconds to give participants enough time to concentrate on the high-level tasks that they were asked to do in each trial. Each trial began with 5.5±0.50 seconds rest, followed by a 60 second trial, in the beginning of which acoustic and visual instructions were given to indicate which of the two cognitive tasks should be performed. To ensure comprehension, both cognitive tasks were explained to participants in a briefing before the experiment. For ALS patients, the experimental paradigm remained the same. However, they were asked to only perform one experimental block. Figure 1 illustrates the paradigm.

2.2. Experimental Data

The study was conducted at the Max Planck Institute for Intelligent Systems in Tübingen, Germany. Recordings with ALS patients were conducted in their homes. Twelve healthy subjects (eight male and three female, mean age 29.3 ± 8.3 years) and five ALS patients (cf. Table 1) were recruited from the local community and in cooperation with the University Clinics Tübingen. Participants received 12 Euro per hour for their participation. One healthy subject was excluded due to noisy recordings. This left eleven healthy subjects for the final analysis. All participants were naive to the setup. They were informed by the experimenter about the procedure with standardised instructions and signed a consent form to confirm

Table 1: ALS Patient Data

Patient	Age	Sex	ALSFRS-R[1]	Impairment
P1	59	F	0	Residual eye-movements
P2	54	M	48	Mild limb impairments
P3	75	M	42	Mild limb impairments
P4	81	M	23	No limb functionality
P5	51	F	12	Locked-in, eye-movements

[1]Revised amyotrophic lateral sclerosis functional rating scale [35]. The rating scale was filled out after the recording session by the experimenter.

their voluntary participation in advance. For subject P1, informed consent was given by her legal guardian. The study was approved by the ethics committee of the Max Planck Society.

A 124-channel EEG was recorded at a sampling frequency of 500 Hz using actiCAP active electrodes and a QuickAmp amplifier (BrainProducts GmbH, Gilching, Germany). Electrodes were placed according to the extended 10-20 system with the left mastoid electrode as the initial reference. All recordings were converted to common average reference. The application was realised with the BCI2000 and BCPy2000 toolboxes [36].

2.3. EEG Analysis

We performed an offline analysis of the acquired data to attenuate confounding electromyographic activity, to investigate differentiability of the activity-patterns associated with self-referential thoughts and focus on breathing, and to analyse the spatial distribution as well as the dynamics of the induced bandpower changes.

2.3.1. Attenuation of EMG artifacts

EEG recordings are likely to be contaminated by scalp-muscle artifacts [37]. Subjects may have been able to involuntarily influence the EEG signal by altering the tonus of their scalp muscles. In order to identify such EMG confounds, we employed independent component analysis (ICA) [38]. The continuous data of one session was first reduced to 64 components by principal component analysis, and then separated into independent components (ICs) using the SOBI algorithm [39]. We then sorted the ICs according to their neurophysiological plausibility [40], manually inspected the topography, spectrum, and time-series of each component, and rejected those for which at least one of the following criteria applied: (1) Components displayed a monotonic increase in spectral power starting around 20 Hz. This is characteristic for muscle activity. (2) Eye-blinks were detectable in the time series. (3) The topography did not show a dipolar pattern. (4) The time series seemed to be contaminated by other sources of noise, like large spikes and 50 Hz line noise (adapted from [41]). The remaining ICs were reprojected onto the scalp. As discussed in [38], it is unreasonable to expect a complete removal of artifacts using ICA, but careful application "is a useful means of rejecting the most dubious results on the scalp".

153 *2.3.2. Preprocessing*

154 We restricted our analysis to the time-window of 4.5 to 60 seconds per trial, as instructions
155 were played back for the first two seconds and were shown on the screen for the first four
156 seconds of each trial. To reduce the feature space for later classification and to capture the
157 effect of self-referential processing, we restricted our analysis to the θ- and α-frequency bands
158 of the EEG signal. Mu et al. [42] found that self-referential processing correlates with θ
159 and α spectral power in a stimulus-driven task. θ-band activity is generally modulated by
160 memory load and retrieval of episodic information from long-term memory [43]. α-bandpower
161 is linked to inner-directed attention demand in self-referential processing [42]. In particular,
162 parietal α-power has been associated with the DMN in EEG studies [44]. As our classification
163 algorithm will be trained on all subjects simultaneously, we used standard boundaries for θ-
164 and α-bandpower. Based on [43], θ-bandpower ranges from 4 Hz to 7 Hz, and α-bandpower
165 was set to 7 Hz to 13 Hz. For each trial, we windowed every channel's time-series with a
166 Hann window. We then computed the trial-wise log-bandpower of the averaged, combined
167 θ- and α-range at every channel location using the Fourier transform. This served as the
168 124-dimensional feature-space.

169 *2.3.3. Pattern Classification*

170 Due to the long trial duration, the number of trials was limited to 60 and 20 for healthy
171 subjects and ALS patients, respectively. With a 124-dimensional feature space, standard
172 machine learning techniques are unlikely to learn a good decoder when trained on each
173 subject's data individually. We resolved this problem by using a transfer learning technique,
174 which is capable of simultaneously learning decoders for all subjects while accounting for
175 inter-individual differences [45]. In this framework, a linear regression model is learned for
176 each subject individually, while penalising deviations of the regression weights from a Gaussian
177 prior that is learned on the data of all other subjects. This leads to the following loss function,

$$
\min_{\boldsymbol{W},\boldsymbol{\mu},\boldsymbol{\Sigma}} LP(\boldsymbol{W},\boldsymbol{\mu},\boldsymbol{\Sigma};\boldsymbol{X},\boldsymbol{Y},\lambda) = \min_{\boldsymbol{W},\boldsymbol{\mu},\boldsymbol{\Sigma}} \frac{1}{\lambda}\sum_{s}\|\boldsymbol{X}_s\boldsymbol{w}_s - \boldsymbol{y}_s\|^2
$$
$$
+ \sum_{s}\frac{1}{2}\left[(\boldsymbol{w}_s - \boldsymbol{\mu})^{\mathrm{T}}\boldsymbol{\Sigma}^{-1}(\boldsymbol{w}_s - \boldsymbol{\mu})\right]. \tag{1}
$$

178 Here, $\boldsymbol{y}_s$ denotes a vector containing all trials' stimuli for one subject, which we represent
179 by $\{-1,1\}$ for the two cognitive tasks "focus on your breathing" and "remember a positive
180 memory", respectively. $\boldsymbol{X}_s$ denotes the feature matrix for subject s with dimensionality
181 [number of trials] $\times$ [number of features], in our case 60 trials (20 for patients) and one
182 bandpower-estimate at each of the 124 channels. $\boldsymbol{w}_s$ denotes the regression weights for each
183 subject, and $\boldsymbol{\mu}$ and $\boldsymbol{\Sigma}$ refer to the mean and the covariance matrix of the unknown Gaussian
184 prior over $\boldsymbol{w}$. Finally, λ refers to the importance of the subjects' individual information
185 relative to the prior. It is determined by a maximum likelihood estimation on the whole
186 dataset.

187 The prior is updated iteratively though an expectation-maximisation procedure in two
188 steps. First, we keep $\boldsymbol{\mu}$ and $\boldsymbol{\Sigma}$ constant and solve with respect to $\boldsymbol{w}_s$ for a given subject,

$$
\boldsymbol{w}_s = \left(\frac{1}{\lambda}\boldsymbol{\Sigma}\boldsymbol{X}_s^{\mathrm{T}}\boldsymbol{X}_s + \boldsymbol{I}\right)^{-1}\left(\frac{1}{\lambda}\boldsymbol{\Sigma}\boldsymbol{X}_s^{\mathrm{T}}\boldsymbol{y}_s + \boldsymbol{\mu}\right). \tag{2}
$$

In the second step, we update our information about the prior by updating its parameters $\boldsymbol{\mu}$ and $\boldsymbol{\Sigma}$,

$$\boldsymbol{\mu}^* = \frac{1}{S}\sum_s \boldsymbol{w}_s, \tag{3}$$

$$\boldsymbol{\Sigma}^* = \frac{\sum_s (\boldsymbol{w}_s - \boldsymbol{\mu})(\boldsymbol{w}_s - \boldsymbol{\mu})^{\mathrm{T}}}{\mathrm{Tr}\left(\sum_s (\boldsymbol{w}_s - \boldsymbol{\mu})(\boldsymbol{w}_s - \boldsymbol{\mu})^{\mathrm{T}}\right)} + \epsilon\boldsymbol{I}. \tag{4}$$

We add ϵI to (4), with ϵ set to $\frac{1}{10}$ of the smallest non-zero eigenvalue, to ensure a full rank matrix.

For each subject, we computed the parameters of the prior across all other subjects. We then used a five-fold cross-validation procedure within the test subject with a random separation of the data into folds while balancing the number of trials for each class in every fold, to obtain an estimate of the classification accuracy given the computed parameters. To account for the high variance of cross-validation with such few trials, we repeated this procedure 1000 times and averaged the classification accuracy across these repetitions.

2.3.4. Statistical Test on Decoding Accuracy

As discussed in [46], it cannot be assumed that the chance-level decoding accuracy matches the theoretical chance-level of 50% when performing cross-validation on a small number of trials. To test whether our strategy achieved above chance-level decoding accuracies, we compared the decoding accuracy during trial-time with the accuracy obtained on the pre-trial baseline. Specifically, we tested the null-hypothesis H0: trial-time classification accuracy = baseline classification accuracy by a two-tailed pair-wise t-test, given the mean classification-accuracy value of each subject during baseline and during trial-time.

2.3.5. Spatial Distribution

To investigate the spatial distribution of induced bandpower modulations, we averaged all 16 priors that were obtained by the transfer learning algorithm and multiplied it with the covariance matrix of the averaged 16 feature sets, as described by Haufe et al. [47]. This results in a topography that depicts the components within the feature space that are modulated by the cognitive strategy.

2.3.6. Dynamics of Induced Bandpower Changes and Timecourse of Classification Accuracy

In a further post-hoc analysis, we investigated the effect of our strategy on event-related (de-)synchronisation (ERD/ERS) during the course of a trial. We computed log-bandpower changes over time, relative to the last 3 seconds of the rest phase before each trial. We used a sliding window of one seconds with a step size of 100 ms to compute bandpower in frequencies from 1 to 40 Hz. We restricted this analysis to channel Pz due to its central parietal position over the posterior cingulate cortex.

Lastly, we investigated cumulative classification accuracy over the course of the trial. First, we employed the previously described pattern classification algorithm to train on the averaged, combined θ- and α-bandpower during the baseline and instruction phase of each trial, respectively. Second, we used an expanding window starting at 4.5 seconds, with an increment of one second, until it span the whole trial. We repeated the classification procedure

at each increment 100 times, with random splits of the data into training- and test set, and averaged the resulting accuracy across these repetitions.

3. Results

We rejected an average of 57 ICs ($\pm$ 1.7) per subject during artifact attenuation. Figure 2 shows the accuracy of the classification on the combined, averaged α and θ-bandpower for the ALS patients and healthy subjects in red and blue, respectively. ALS patients and healthy subjects achieved a decoding accuracy of 60.8% and 62.5%, respectively, with an across-group average of 62.0%. A two-tailed pair-wise t-test between trial-time and pre-trial baseline classification accuracies rejected the the null-hypothesis with $t = -3.87$, $p = 0.0015$ for the combined subject groups.
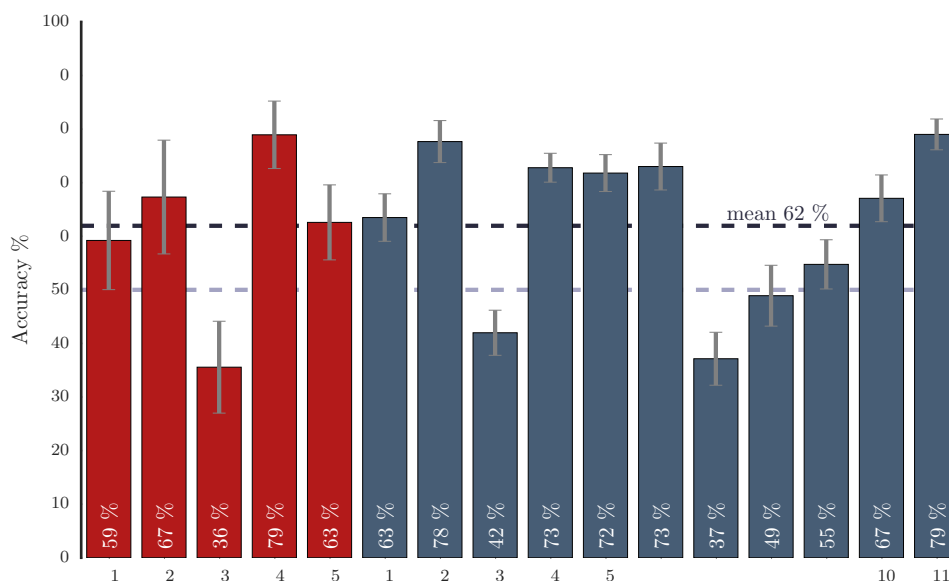
Figure 2: Classification accuracies for both patients and healthy subjects. The dashed grey line represents chance-level classification accuracy at 50%, the black reference line represents the mean classification accuracy of 62.0%. P1 to P5 are patients, S1 to S11 are healthy subjects.

Figures 3 shows the spatial distribution of bandpower modulation. We observe that the cognitive strategy leads to bandpower modulations that are concentrated over parietal areas.

The first row of Figure 4 shows the ERS/ERD patterns, averaged across all trials of the healthy subjects, at channel Pz for the self- and non-self-referential condition, respectively. In the self-referential condition, we observe a distinct ERS in the α-range and, to a lesser extent, in the β-range ($\sim$20 Hz), while the non-self-referential conditions shows an ERD first, followed by an ERS. All other frequencies display an ERD. In the self-referential condition, the α-ERS starts with stimulus presentation and remains roughly constant throughout the whole trial. In the non-self-referential condition, the α-bandpower first shows an ERD, until the effect turns into an ERS around 30 seconds. These different dynamics are also visible in the ERS/ERD differences between conditions (Figure 4, second row), in which an initial α-ERS diminishes at around 20 seconds. Subject-specific differences in ERD/ERS patterns
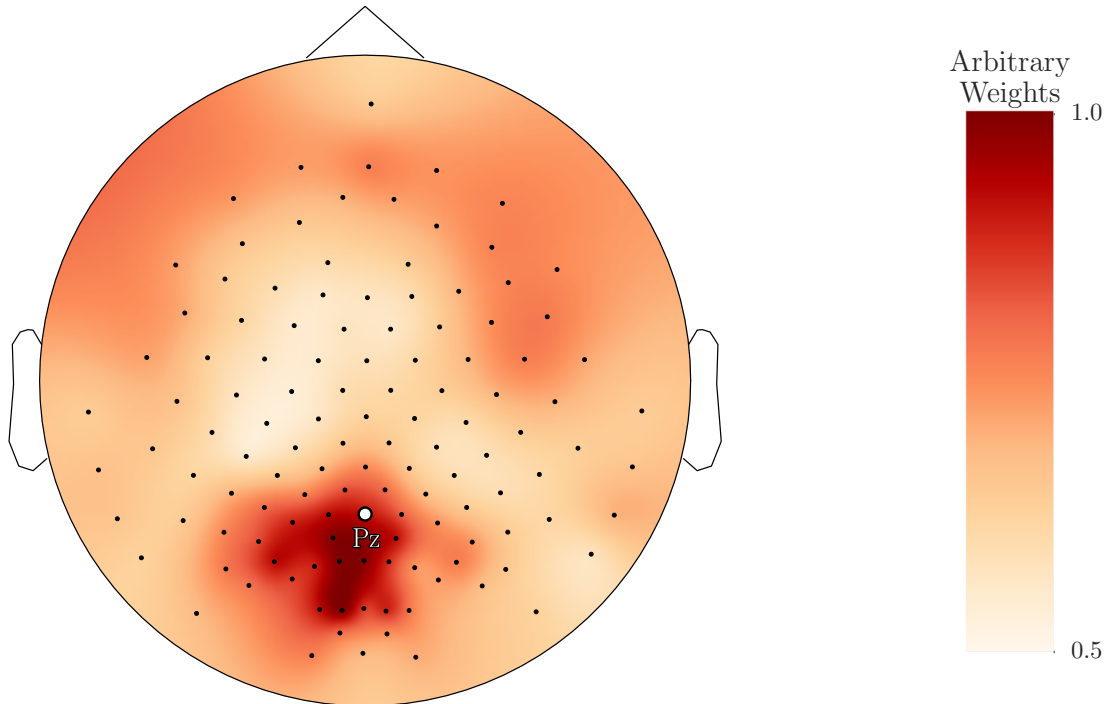
Figure 3: Classifier topography (see Section 2.3.5). A higher weight indicates a stronger modulation of combined θ- and α-power across conditions.

are shown in Figure 5. It is apparent that some subjects show a stronger α-ERS in the self-referential condition (S6, S9, and S11), while other subjects exhibit a stronger α-ERS in the non-self-referential condition (S4 and S5). The transfer learning approach, that we used for decoding, is flexible enough to accomodate these subject-specific differences, resulting in high classification accuracies in subjects S4 and S6 in spite of a reversed α-ERD/ERD.

The ALS patients exhibit a slightly different pattern (Figure 6). Both, the non- and the self-referential conditions, show a distinct ERS in the $\theta-$ and in the α-range. In contrast to the healthy subjects, the α-ERD is on average stronger in the non-self-referential condition throughout the whole time-course of a trial. As indicated by the patient-specific ERD/ERS shown in Figure 7, however, these observations are primarily driven by patient P1 (it is noteworthy that patient P1 is the only patient in this study with an ALS-FRS score of zero).

Figure 8 displays the classification performance over the course of the trial, based on the combined, averaged α- and θ-bandpower for the ALS patients and healthy subjects in red and blue, respectively. ALS patients achieved a peak decoding accuracy of 61.8% after 59 seconds trial-time. Healthy subjects achieved a peak accuracy of 62.4% after 55 seconds trial-time. Several differences in the course of classification performance can be seen between the two groups. Healthy subjects show a steep increase in performance shortly after the instruction phase, while the performance of ALS patients increases more gradually after about 35 seconds into the trial. Also, the standard error of measurement is noticeably smaller in healthy subjects compared to ALS patients.
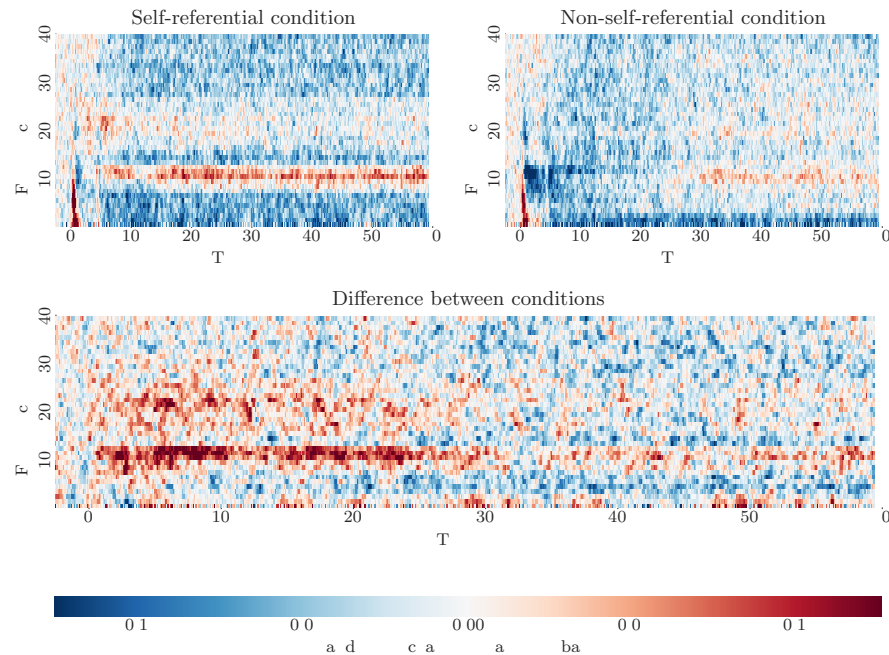
Figure 4: Average ERD/ERS in healthy subjects over the course of the trial. Time $t = 0$ denotes the presentation of the stimulus.

4. Discussion

The current study tested whether healthy subjects and ALS patients in various stages of the disease are able to use a cognitive paradigm for BCI control. Using a linear classifier in a transfer learning approach, we were able to successfully distinguish a self-referential from a non-self-referential condition with an average decoding of 62.5% and 60.8% for the healthy subjects and ALS patients, respectively. We found that the cognitive strategy primarily induced θ- and α-ERD/ERS over parietal areas. Most importantly, we found that even ALS patients in the latest stages of disease progression (P1 and P5) were capable of self-modulating activity in the the targeted areas without any training.

It has been argued that completely locked-in ALS patients reside in a state-of-mind similar to unconsciousness or REM sleep [23]. Therefore, they would be incapable of goal-directed thinking and hence unable to operate any BCI. In our current work, we targeted high-level cognitive processes that are associated with the DMN. This network has been related to the level of consciousness in clinical populations. We therefore hypothesised that a conscious state-of-mind is necessary to voluntarily modulate activity in this network. In agreement with our hypothesis, we found that neural activity between the two employed conditions significantly differed in both patients and healthy controls. This indicates that both groups were able to voluntarily modulate neural activity according to the experimental conditions. Importantly, we found a strong ERD/ERS in patient P1 with a ALS-FRS score of zero; this patient only retained minimal residual ocular control for communication. Based on this positive result, we argue that the unreliability of previous attempts to establish BCI control in late-stage ALS may have been caused by the employed paradigms that mostly relied on the
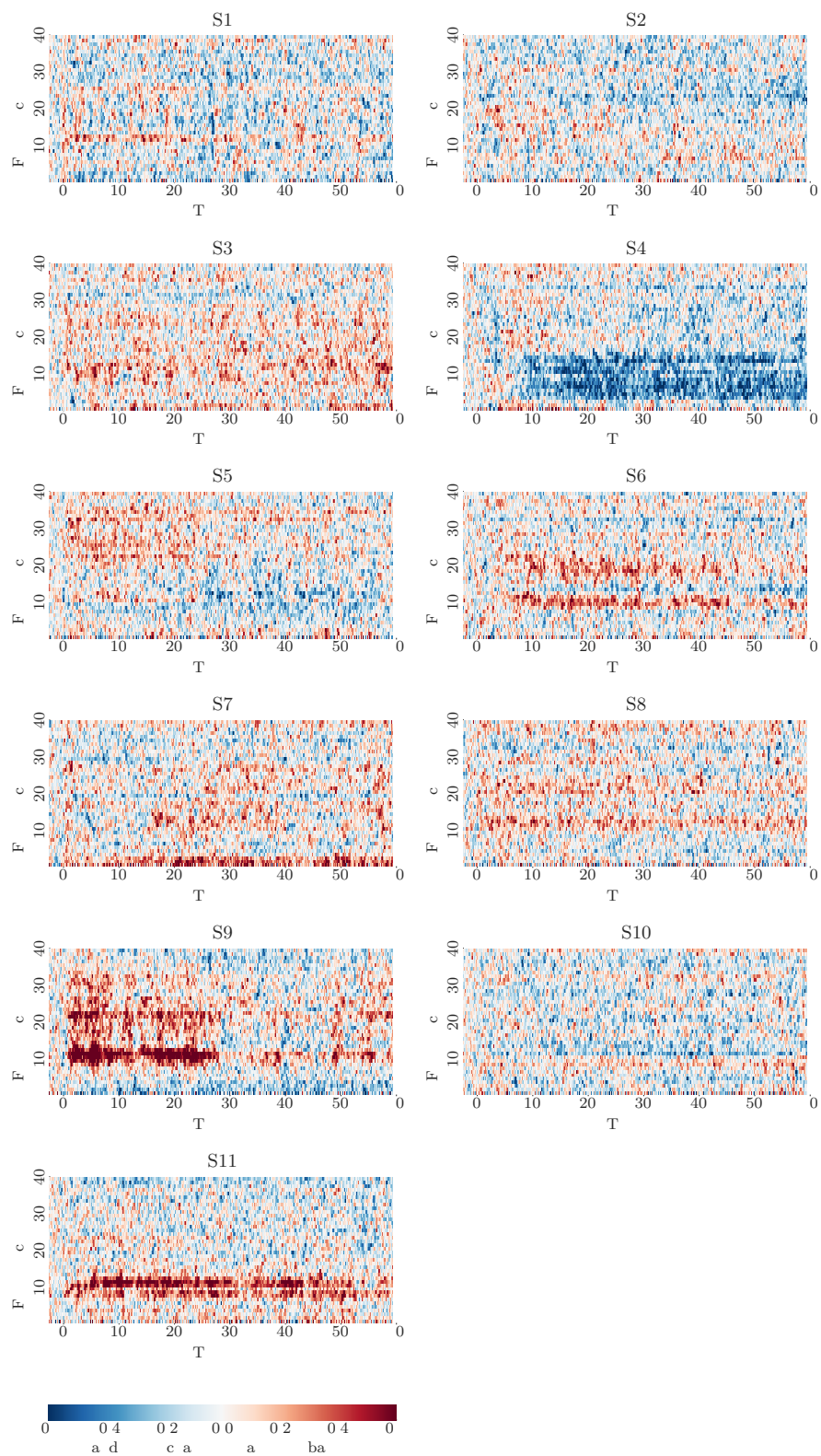
Figure 5: Bandpower differences between conditions for each healthy subject over the course of the trial. Time $t = 0$ denotes the presentation of the stimulus.
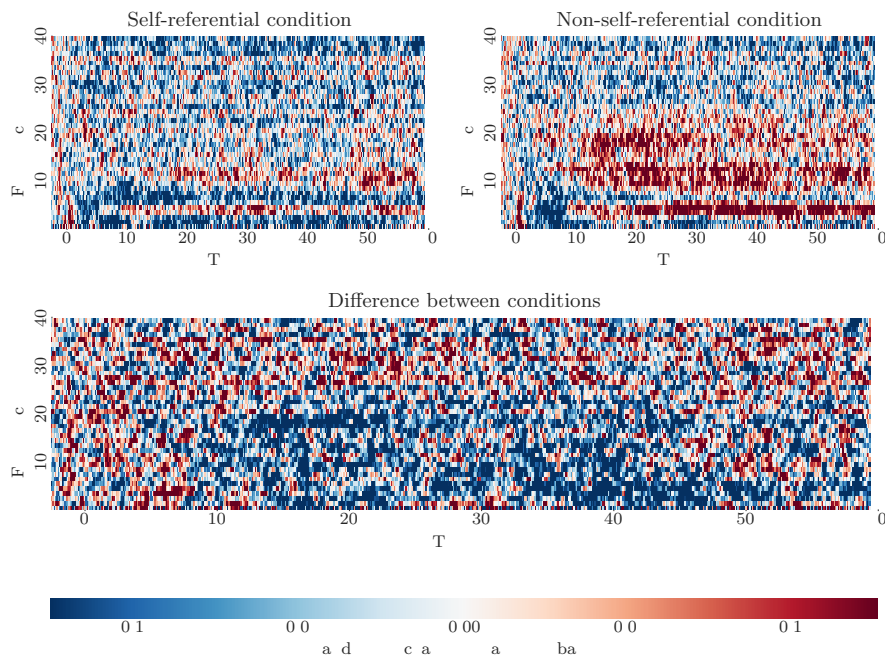
Figure 6: Average ERD/ERS in ALS patients over the course of a trial. Time $t = 0$ denotes the presentation of the stimulus.

subjects' responses to external stimuli or the modulation of SMRs. We point out, however, that previous fMRI studies found weakened activity in several regions of the DMN in ALS patients [48]. Specifically, areas that are involved in stimulus perception and recognition as well as in working memory were shown to be affected. This included the precuneus that may be responsible for the α-ERD/ERS elicited in this study. It thus remains an open question for how long late-stage ALS patients can maintain BCI control based on the cognitive paradigm introduced here.

We note that, due to the long trial time of 60 seconds and the decoding accuracies of 62.5% and 60.8% for the healthy subjects and ALS patients, respectively, the resulting information transfer rate (ITR) is low. Figure 8 indicates that this long trial-time is needed by patients to execute the cognitive strategy. While the maximum ITR of our novel paradigm is thus well below those achieved by other paradigms in healthy subjects, we note that the ITR is of secondary importance when working with severely paralysed patients in late stages of ALS. Instead, the primary challenge remains to establish any form of communication with completely locked-in ALS patients. Our work establishes a novel cognitive paradigm for achieving this goal.

The successful implementation of this novel cognitive strategy has a number of implications for further development of BCI systems for ALS patients. First, recordings were conducted with a 124-channel wet-electrode EEG system. Such conventional EEG systems are often only accessible in clinical environments. They are not very cost-efficient or portable. Also, nursing staff or family members of the ALS patient may not have the necessary expertise to setup such a conventional EEG system for online-communication. To create a communication method that is available to everyone, it would be beneficial to transfer the paradigm to a commercially
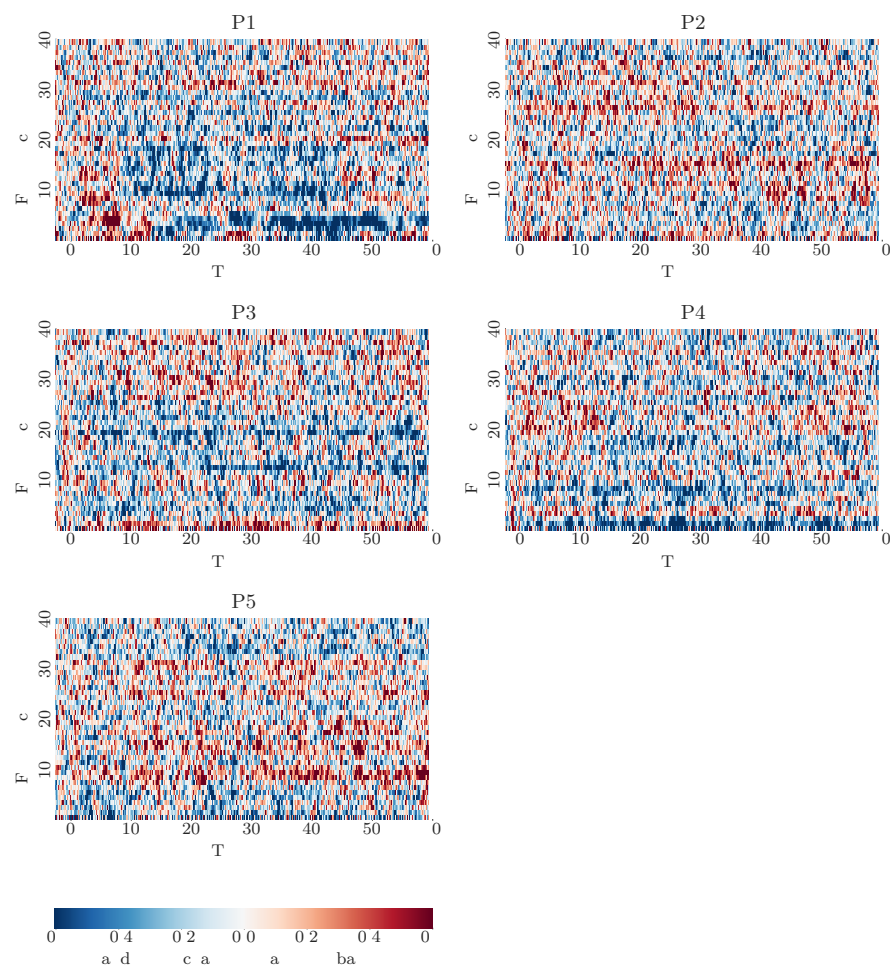
Figure 7: Bandpower differences between conditions for each ALS patient over the course of the trial. Time $t = 0$ denotes the presentation of the stimulus.
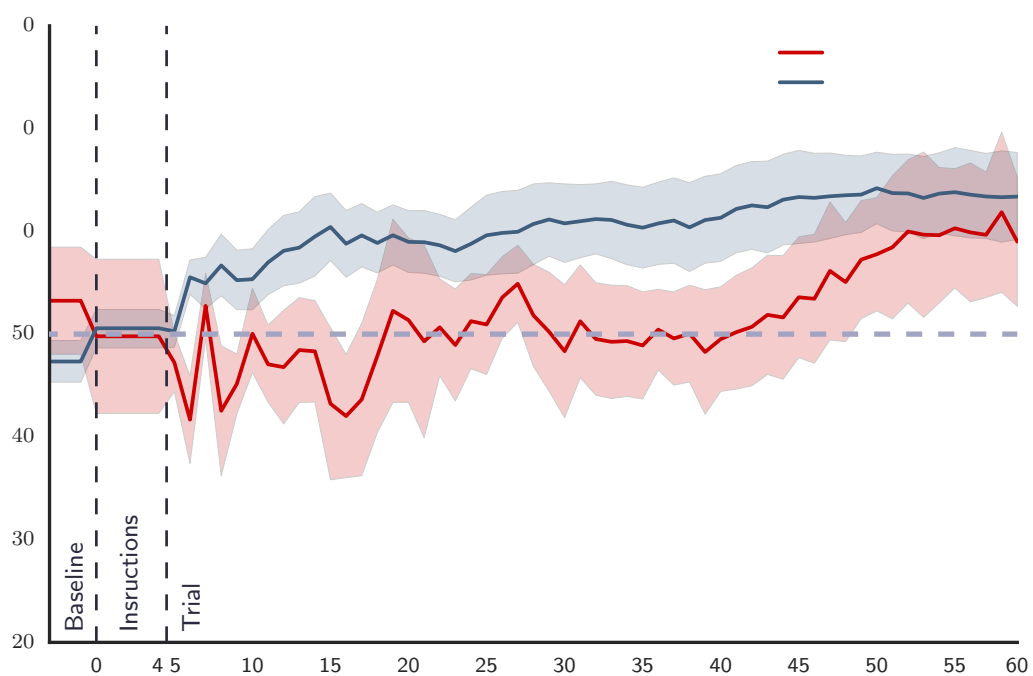
Figure 8: Mean classification performance over the course of the trial. Accuracy during baseline and instruction phase was computed with a single window. Accuracy during trialtime was computed with an expanding window, starting at 4.5 seconds, in steps of 1 second. The grey line represents chance-level. The shaded area around around the mean represents the standard error of measurement.

available, less expensive, and portable EEG system. As our novel paradigm primarily induces bandpower changes over parietal areas (cf. Figure 3), we expect that it can also be realised on a low-density and low-cost system that focuses on parietal areas only. Second, our strategy achieved classification accuracies above baseline without the need for prior subject training. Still, the results of the post-hoc analysis indicate that the induced effect varies between subjects. One reason for this finding could be the choice of the non-self-referential condition. Focusing on breathing has been shown to decrease overall activity in the DMN, but it also increases synchronisation within the DMN [49]. These two effects may be difficult to separate when investigating EEG bandpower-values, as an increase in synchronisation can lead to an increase in spectral-power, indistinguishable from the self-referential activation. Focusing on breathing could also be prone to distractions and mind-wandering, which in turn also increases DMN activity. A potential direction to address this problem in future studies could be the choice of a different non-self-referential strategy. One candidate could be a verbal spelling task, as verbal execution has been found to lower DMN activity [50]. It may also be sufficiently demanding to avoid involuntary mind-wandering.

References

[1] L. C. Wijesekera, P. N. Leigh, Amyotrophic lateral sclerosis, Orphanet Journal of Rare Diseases 4 (2009) 3.

[2] S. Aggarwal, M. Cudkowicz, ALS drug development: reflections from the past and a way forward, Neurotherapeutics : The Journal of the American Society for Experimental Neurotherapeutics 5 (2008) 516–27.

[3] J. R. Wolpaw, N. Birbaumer, D. J. McFarland, G. Pfurtscheller, T. M. Vaughan, Brain–computer interfaces for communication and control, Clinical Neurophysiology 113 (2002) 767–791.

[4] P. N. Leigh, The management of motor neurone disease, Journal of Neurology, Neurosurgery & Psychiatry 74 (2003) 32iv–47.

[5] A. Kübler, B. Kotchoubey, J. Kaiser, J. R. Wolpaw, N. Birbaumer, Brain-computer communication: unlocking the locked in, Psychological Bulletin 127 (2001) 358–375.

[6] J. R. Bach, Amyotrophic lateral sclerosis. Communication status and survival with ventilatory support, American Journal of Physical Medicine & Rehabilitation / Association of Academic Physiatrists 72 (1993) 343–9.

[7] J. D. Wander, R. P. N. Rao, Brain-computer interfaces: a powerful tool for scientific inquiry., Current Opinion in Neurobiology 25 (2014) 70–75.

[8] A. Kübler, A. Furdea, S. Halder, E. M. Hammer, F. Nijboer, B. Kotchoubey, A brain-computer interface controlled auditory event-related potential (P300) spelling system for locked-in patients, Annals of the New York Academy of Sciences 1157 (2009) 90–100.

[9] J. N. Mak, J. R. Wolpaw, Clinical Applications of Brain-Computer Interfaces: Current State and Future Prospects, IEEE Reviews in Biomedical Engineering 2 (2009) 187–199.

[10] G. Pfurtscheller, C. Neuper, Motor imagery and direct brain-computer communication, Proceedings of the IEEE 89 (2001) 1123–1134.

[11] K. Nihei, A. C. McKee, N. W. Kowall, Patterns of neuronal degeneration in the motor cortex of amyotrophic lateral sclerosis patients, Acta Neuropathologica 86 (1993) 55–64.

[12] N. Birbaumer, F. Piccione, S. Silvoni, M. Wildgruber, Ideomotor silence: the case of complete paralysis and brain-computer interfaces (BCI), Psychological Research 76 (2012) 183–191.

[13] L. Jacobs, D. Bozian, R. R. Heffner, S. a. Barron, An eye movement disorder in amyotrophic lateral sclerosis, Neurology 31 (1981) 1282–1287.

[14] F. Aloise, P. Aricò, F. Schettini, A. Riccio, S. Salinari, D. Mattia, F. Babiloni, F. Cincotti, A covert attention P300-based brain-computer interface: Geospell., Ergonomics 55 (2012) 538–51.

[15] P. Aricò, F. Aloise, F. Schettini, S. Salinari, D. Mattia, F. Cincotti, Influence of P300 latency jitter on event related potential-based brain-computer interface performance., Journal of Neural Engineering 11 (2014) 035008.

[16] M. Treder, N. Schmidt, B. Blankertz, Gaze-independent brain-computer interfaces based on covert attention and feature attention, Journal of Neural Engineering 8 (2011) 066003.

[17] A. M. Brouwer, J. B. F. van Erp, A tactile P300 brain-computer interface, Frontiers in Neuroscience 4 (2010) 19.

[18] F. Nijboer, A. Furdea, I. Gunst, J. Mellinger, D. J. McFarland, N. Birbaumer, A. Kübler, An auditory brain-computer interface (BCI), Journal of Neuroscience Methods 167 (2008) 43–50.

[19] A. Kübler, B. Kotchoubey, T. Hinterberger, N. Ghanayim, J. Perelmouter, M. Schauer, C. Fritsch, E. Taub, N. Birbaumer, The thought translation device: a neurophysiological approach to communication in total motor paralysis., Experimental Brain Research 124 (1999) 223–32.

[20] M. Marchetti, K. Priftis, Brain-computer interfaces in amyotrophic lateral sclerosis: A metanalysis., Clinical Neurophysiology : Official Journal of the International Federation of Clinical Neurophysiology 126 (2015) 1255–63.

[21] M. Grosse-Wentrup, B. Schölkopf, A brain-computer interface based on self-regulation of gamma-oscillations in the superior parietal cortex, Journal of Neural Engineering 11 (2014) 056015.

[22] M. J. Vansteensel, D. Hermes, E. J. Aarnoutse, M. G. Bleichner, G. Schalk, P. C. van Rijen, F. S. S. Leijten, N. F. Ramsey, Brain-computer interfacing based on cognitive control., Annals of Neurology 67 (2010) 809–16.

[23] A. Kübler, N. Birbaumer, Brain-computer interfaces and communication in paralysis: extinction of goal directed thinking in completely paralysed patients?, Clinical Neurophysiology : Official Journal of the International Federation of Clinical Neurophysiology 119 (2008) 2658–2666.

[24] H. Braak, J. Brettschneider, A. C. Ludolph, V. M. Lee, J. Q. Trojanowski, K. Del Tredici, Amyotrophic lateral sclerosis–a model of corticofugal axonal spread., Nature Reviews Neurology 9 (2013) 708–714.

[25] G. L. Shulman, J. A. Fiez, M. Corbetta, R. L. Buckner, F. M. Miezin, M. E. Raichle, S. E. Petersen, Common Blood Flow Changes across Visual Tasks: II. Decreases in Cerebral Cortex, Journal of Cognitive Neuroscience 9 (1997) 648–63.

[26] M. E. Raichle, a. M. MacLeod, A. Z. Snyder, W. J. Powers, D. a. Gusnard, G. L. Shulman, A default mode of brain function, Proceedings of the National Academy of Sciences of the United States of America 98 (2001) 676–682.

[27] J. R. Simpson, A. Z. Snyder, D. A. Gusnard, M. E. Raichle, Emotion-induced changes in human medial prefrontal cortex: I. During cognitive task performance, Proceedings of the National Academy of Sciences of the United States of America 98 (2001) 683–687.

[28] M. E. Raichle, The Brain's Default Mode Network, Annual Review of Neuroscience 38 (2015) 433–447.

[29] P. Fransson, G. Marrelec, The precuneus/posterior cingulate cortex plays a pivotal role in the default mode network: Evidence from a partial correlation network analysis, NeuroImage 42 (2008) 1178–1184.

[30] A. Vanhaudenhuyse, Q. Noirhomme, L. J. F. Tshibanda, M. A. Bruno, P. Boveroux, C. Schnakers, A. Soddu, V. Perlbarg, D. Ledoux, J. F. Brichant, G. Moonen, P. Maquet, M. D. Greicius, S. Laureys, M. Boly, Default network connectivity reflects the level of consciousness in non-communicative brain-damaged patients, Brain 133 (2010) 161–171.

[31] N. C. Andreasen, D. S. O'Leary, T. Cizadlo, S. Arndt, K. Rezai, G. L. Watkins, L. L. B. Ponto, R. D. Hichwa, Remembering the past: Two facets of episodic memory explored with positron emission tomography, American Journal of Psychiatry 152 (1995) 1576–1585.

[32] M. D. Greicius, B. Krasnow, A. L. Reiss, V. Menon, Functional connectivity in the resting brain: a network analysis of the default mode hypothesis, Proceedings of the National Academy of Sciences of the United States of America 100 (2003) 253–258.

[33] D. H. Weissman, K. C. Roberts, K. M. Visscher, M. G. Woldorff, The neural bases of momentary lapses in attention, Nature Neuroscience 9 (2006) 971–8.

[34] M. R. Hohmann, T. Fomina, V. Jayaram, N. Widmann, C. Förster, J. Müller vom Hagen, M. Synofzik, B. Schölkopf, L. Schölz, M. Grosse-Wentrup, A Cognitive Brain-Computer Interface for Patients with Amyotrophic Lateral Sclerosis, in: Proceedings of the 2015

IEEE International Conference on Systems, Man, and Cybernetics (SMC2015), Hong Kong.

[35] J. M. Cedarbaum, N. Stambler, E. Malta, C. Fuller, D. Hilt, B. Thurmond, A. Nakanishi, The ALSFRS-R: A revised ALS functional rating scale that incorporates assessments of respiratory function, Journal of the Neurological Sciences 169 (1999) 13–21.

[36] G. Schalk, D. J. McFarland, T. Hinterberger, N. Birbaumer, J. R. Wolpaw, BCI2000: A general-purpose brain-computer interface (BCI) system, IEEE Transactions on Biomedical Engineering 51 (2004) 1034–1043.

[37] A. J. Shackman, B. W. McMenamin, H. a. Slagter, J. S. Maxwell, L. L. Greischar, R. J. Davidson, Electromyogenic artifacts and electroencephalographic inferences, Brain Topography 22 (2009) 7–12.

[38] B. W. McMenamin, A. J. Shackman, L. L. Greischar, R. J. Davidson, Electromyogenic artifacts and electroencephalographic inferences revisited, NeuroImage 54 (2011) 4–9.

[39] A. Belouchrani, K. Abed-Meraim, J.-F. Cardoso, E. Moulines, A blind source separation technique using second-order statistics, IEEE Transactions on Signal Processing 45 (1997) 434–444.

[40] M. Grosse-Wentrup, S. Harmeling, T. Zander, J. Hill, B. Schölkopf, How to test the quality of reconstructed sources in independent component analysis (ICA) of EEG/MEG data, in: Proceedings - 2013 3rd International Workshop on Pattern Recognition in Neuroimaging, PRNI 2013, pp. 102–105.

[41] J. Onton, M. Westerfield, J. Townsend, S. Makeig, Imaging human EEG dynamics using independent component analysis., Neuroscience and Biobehavioral Reviews 30 (2006) 808–22.

[42] Y. Mu, S. Han, Neural oscillations involved in self-referential processing, NeuroImage 53 (2010) 757–768.

[43] W. Klimesch, EEG alpha and theta oscillations reflect cognitive and memory performance: A review and analysis, Brain Research Reviews 29 (1999) 169–195.

[44] G. G. Knyazev, EEG correlates of self-referential processing, Frontiers in Human Neuroscience 7 (2013) 264.

[45] V. Jayaram, M. Alamgir, Y. Altun, B. Schölkopf, M. Grosse-Wentrup, Transfer Learning in Brain-Computer Interfaces, IEEE Computational Intelligence Magazine (2015).

[46] D. Coyle, J. Stow, K. McCreadie, J. McElligott, Á. Carroll, Sensorimotor modulation assessment and brain-computer interface training in disorders of consciousness., Archives of Physical Medicine and Rehabilitation 96 (2015) S62–70.

[47] S. Haufe, F. Meinecke, K. Görgen, S. Dähne, J.-D. Haynes, B. Blankertz, F. Bießmann, On the interpretation of weight vectors of linear models in multivariate neuroimaging., NeuroImage 87 (2014) 96–110.

[48] B. Mohammadi, K. Kollewe, A. Samii, K. Krampfl, R. Dengler, T. F. Münte, Changes of resting state brain networks in amyotrophic lateral sclerosis, Experimental Neurology 217 (2009) 147–53.

[49] J. a. Brewer, P. D. Worhunsky, J. R. Gray, Y.-Y. Tang, J. Weber, H. Kober, Meditation experience is associated with differences in default mode network activity and connectivity, Proceedings of the National Academy of Sciences 108 (2011) 20254–20259.

[50] H. Koshino, T. Minamoto, K. Yaoi, M. Osaka, N. Osaka, Coactivation of the default mode network regions and working memory network regions during task preparation, Scientific Reports 4 (2014) 5954.

Chapter 5

EEG Correlates of Self-referential Processing are Altered in ALS

Electrophysiological Correlates of Self-referential Processing are Altered in ALS

Tatiana Fomina[1,2], Sebastian Weichwald[1], Ludger Schöls[3], Bernhard Schölkopf[1], and Moritz Grosse-Wentrup[1]

[1] Department Empirical Inference, Max Planck Institute for Intelligent Systems, Tübingen, Germany

[2] IMPRS for Cognitive and Systems Neuroscience, University of Tübingen, Tübingen, Germany

[3] Hertie Institute for Clinical Brain Research, Tübingen, Germany

E-mail: `tfomina@tuebingen.mpg.de`

September 2016

Abstract.

Self-referential processing is a key cognitive process, associated with the serotogenic system and the default mode network (DMN). Decreased levels of serotonin and reduced activations of the DMN observed in amyotrophic lateral sclerosis (ALS) suggest that self-referential processing might be altered in patients with ALS. Here, we investigate the effects of ALS on the electroencephalography (EEG) correlates of self-referential thinking. We find that EEG correlates of self-referential thinking differ between healthy individuals and those with ALS. In particular, thinking about themselves or others significantly modulates the bandpower in the medial prefrontal cortex (MPFC) in a healthy population, but not in ALS patients. This finding supports the view of ALS as a complex multisystem disorder that spreads beyond the motor cortices, and points towards possible alterations of consciousness in ALS patients.

Introduction

Amyotrophic lateral sclerosis (ALS) is a neurodegenerative disease that is characterised mainly by the loss of motor neurons [1]. Although ALS has long been believed to be a purely motor disease, there is a growing body of physiological evidence to suggest that neuronal degeneration in ALS is not limited to motor cortices and motor pathways [2]. In particular, Braak et al. related ALS to the buildup of pTDP-43 protein agglomerations [3]; they showed that these agglomerations spread from the motor cortices to nearby areas and, eventually, to most of the cortex. The broad effect of ALS was subsequently confirmed with a neuroimaging study by Schmidt et al. [4], who found alterations in functional and structural connectivity throughout the whole cortex. Given such widespread physiological alterations in the brain, it is not surprising that ALS is often accompanied by cognitive deficits [5]. Cases of impaired emotions [6] and pathological

laughing and crying [7] have been reported in ALS patients. Zimmeerman et al. found facial emotion recognition deficits in bulbar ALS [8]. Massman et al. examined 146 patients with a battery of neuropsychological tests [9] and found that ALS patients performed worse than healthy individuals in word generation, immediate free recall, attention and mental control tasks. They also found a correlation between the severity of ALS symptoms and cognitive impairment. Later studies found approximately half of the ALS patients that were examined to be cognitively impaired with alterations of memory, executive functions, judgment and reasoning [10–12]. Several studies have related the impaired cognitive functions to anatomical alterations in the prefrontal areas of the brain. [10, 13–16]. Ludolph et al. found that decreased verbal fluency in ALS correlated with reduced glucose metabolism in the prefrontal cortex [13]. Abrahams et al. later confirmed the connection between decreased verbal fluency and reduced activity in the prefrontal cortex by using positron emission tomography (PET) [14] and found white matter changes in the frontal areas of the brains of ALS patients [15]. Mantovan et al. related abnormal memory retrieval to frontal lobe dysfunction by using single photon emission computer tomography (SPECT) [16]. In addition to executive functions and memory retrieval, the prefrontal cortex is also involved in one of the main cognitive processes, namely self-referential thinking. Self-referential thinking, one of the key elements of self-awareness and consciousness, has not been investigated in ALS patients to date. Nevertheless, alterations in the prefrontal cortex (PFC) and the medial prefrontal cortex (MPFC) in particular [14,15] lead us to hypothesize that self-referential processing may be affected in the progress of ALS. This hypothesis is further supported by ALS patients having decreased serotonin concentrations [17,18], a neurotransmitter connected to self-referential processing [19] (Figure 1). In the following paragraphs, our motivation for this study is explained in further detail. Recent research suggests that ALS affects deep brain structures, including the serotogenic system (Figure 1). Dentel et al. found pathological agglomerates of pTDP-43 protein in the central serotogenic neurons of the brainstem (raphe nuclei) [17]. These areas are involved in the regulation of sleep-arousal [20,21], and their degeneration probably gives rise to the sleep disorders that are observed in ALS patients [22–24]. Moreover, the raphe nuclei release serotonin to the whole brain, and therefore one can expect the degeneration of raphe nuclei to correlate with decreased serotonin concentrations in the brain, which has indeed been observed in ALS [17,18]. Based on the serotonin's strong relation with locomotion (for a detailed review see [25]), Sandyk suggested a serotogenic model of ALS progression [25]. This model explains the ALS symptoms with degeneration of the serotonin projections in the motor cortices [17] and serotonin deficiency. Serotonin-innervated neurons outside of the motor cortices are involved in high cognitive processing and, in particular, self-referential thinking (Figure 1): Hahn et al. have shown that the intensity of self-referential thinking correlates with the concentrations of serotonin receptors in the default mode network (DMN) [19]. The DMN, which comprises the precuneus/posterior cingulate cortex, MPFC and the temporoparietal junction, is a resting-state network that is active in the absence of any cognitively demanding tasks [26], and it is involved

in self-referential processing [27]. Reduced serotonin projections in the DMN nodes and altered DMN activity in ALS [28] lead to the question of whether self-referential thinking is altered in ALS patients (Figure 1). Self-referential thinking is a cognitive
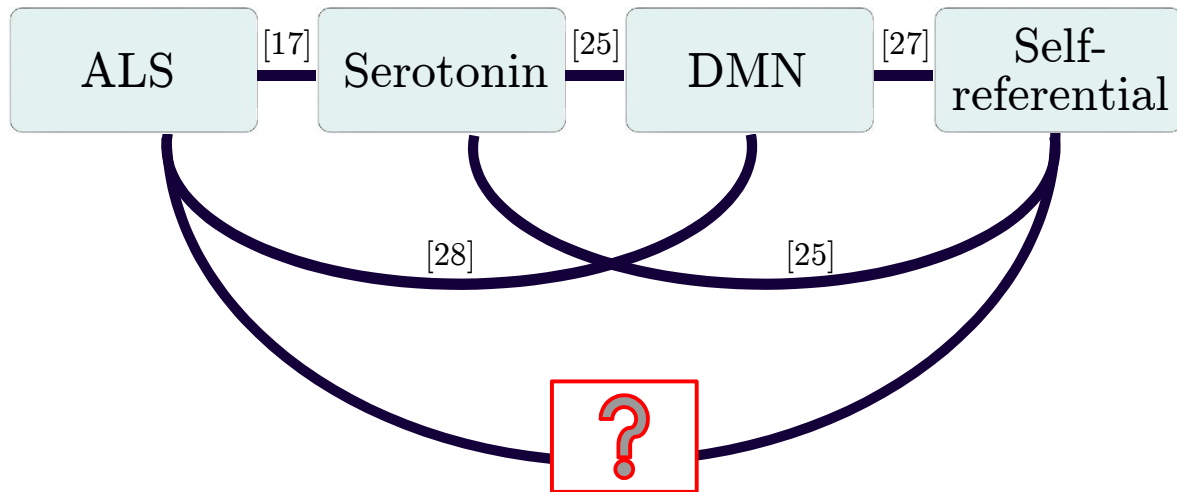

Figure 1. Motivation: Overview of the studies relating ALS and self-referential processing

process and has been widely studied in healthy subjects using different experimental techniques. Kelley et al. studied blood oxygen level-dependent (BOLD) brain activation, using functional magnetic resonance imaging (fMRI) while the subjects performed trait judgments about themselves and others; the study found that the subjects selectively engaged the MPFC for self-referential judgments [29]. In a following BOLD fMRI study, Heatherton et al. found that the right MPFC also differentiates thinking about oneself and close friends [30]. D'Argembeau et al. found the cerebral metabolism in the ventral MPFC (VMPFC) to correlate with the level of self-referential processing, comparing PET measurements acquired while the subjects were thinking about themselves, others, society or relaxing [31]. Later, Whitfield-Gabrieli et al. performed a similar BOLD fMRI study comparing self-referential activations to the DMN. They suggested that the VMPFC is related to self-referential thinking in the absence of attention to external stimuli and that the dorsal MPFC (DMPFC) is related to the consideration of psychological traits in people [32]. Several electroencephalography (EEG) studies have also targeted self-referential processes (for a detailed review see [33]). Esslen et al. compared EEG recordings during judgments about self and others and found, using time-series analysis combined with source-localisation LORETA methods, that the VMPFC is involved in self-referential thinking in pre-self-reflective time periods while the DMPFC is involved in reflective time periods [34]. Mu et. al conducted a similar study and found that event-related desynchronisation (ERD) is related to self-referential thinking in the centro-parietal beta (20–27 Hz), the fronto-central gamma (28–40 Hz) and the right parieto-occipital theta (5–7 Hz) [35]. Here, we investigate whether self-referential processing differs between ALS patients and healthy controls.

So that patients at various disease stages, ranging from early symptoms to completely locked-in state (CLIS) could be included in the analysis, we decided to use neuroimaging methods rather than behavioural methods, since the behavioural methods require two-way communication (for a review of methods see [36]). For example, a memory test that was used previously by Harvey et al. to study self-referential thinking in schizophrenic patients [37] requires the patients to answer questions and cannot be used with CLIS patients who cannot communicate in any way. In order to avoid unnecessary risks associated with transporting patients, we decided to use EEG, which allowed us to perform all the studies in the homes of the participants. We employed a widely used setup to induce different depths of self-referential processing, ranging from thinking of oneself to a close person to a celebrity [29, 31]. During the experiment, we asked the participants to make judgments about themselves and others. We added a control non-self-referential condition, for which we asked participants to count syllables. While we found a significant difference between log-bandpower EEG during self-referential and non-self-referential thinking both for healthy and ALS participants, we found a significant difference between different self-referential conditions for healthy participants; there was no significant difference between different self-referential conditions for ALS patients. Our findings suggest that the log-bandpower EEG correlates of self-referential processing differ between ALS patients and healthy controls.

Materials and Methods

Participants

EEG data were recorded from ten ALS patients (mean age 51.5 ± 11.7 years, ALSFRS-R scores [38]: 0,0,0,1,12,14,17,32,35,40 out of 48) and ten healthy participants (mean age 61.4 ± 6.4 years). All ALS and healthy participants were recruited from the local community, were native German speakers and were not diagnosed with any additional neurological diseases (apart from ALS). All recordings were carried out in the participants' homes. For safety reasons, it was recommended that severely paralysed and artificially ventilated ALS patients were not transported. Healthy participants were visited at their homes in order to make the conditions for ALS patients and healthy participants comparable. For severely paralysed ALS patients, all the recordings were performed in the constant presence of a caretaker. All participants or their legal representatives gave informed consent according to the guidelines set by the Max Planck Society and they received financial compensation for their participation. The study was approved by the Max Planck Society's Ethics Committee.

Hardware

EEG data were obtained using an EEG cap with 121 actiCAP active electrodes at a sampling frequency of 500 Hz and a QuickAmp amplifier (BrainProducts GmbH, Germany). The electrodes were placed according to the 10-5 system, using the electrode

located over the left mastoid (TPP9h in 10-5 system) as the initial reference. All recordings were converted to a common average reference.

Study design

The study design was based on similar fMRI [29, 30, 39] and EEG [35] studies with healthy participants. We presented the participants with adjectives, as stimuli, and asked them to make judgments about whether these adjectives described themselves, a friend or a celebrity; this resulted in three levels of self-referential processing depth. In order to identify the effects that were specific to self-referential processing and were not related to general cognitive decline or decreased attention, we introduced a fourth control condition that did not involve any self-referential thinking. In that condition, the participants were asked to count the syllables of the adjective that they were presented with. Prior to the experiment, the participants were asked to choose a close friend (referred as "Friend") and a celebrity (referred as "Celebrity"). Throughout the experiment, all stimuli were presented to the subjects aurally, through the CereProc text-to-speech system (CereProc Limited, United Kingdom). All stimuli were in German, and all participants, independent of their disease stage, received the same instructions. In the beginning of the experiment, two consecutive periods of resting state, each of five-minute duration (eyes-open and eyes-closed), were recorded. The subjects were instructed to relax and let their mind wander. In the eyes-open condition, they were additionally asked to fixate their eyes on a cross in the middle of a computer screen that was placed at a distance of 1.25 ± 0.2 m. The two resting-state datasets were used to determine the individual frequency bands, as described in [40]. The next part of the study consisted of 80 trials recorded in a single run. Each trial started with the word "Pause" (German, "Pause") being played. During this three second-long pause, the participants were instructed to relax. After the pause, the participants heard a cue: "Selbst" (German, "Self"), "Freund" (German, "Friend"), "Prominente" (German, "Celebrity") or "Zählen"(German, "Count"). Depending on the cue, the participants were asked either to make judgments about themselves, their friend or the celebrity, or to count the syllables of the adjective (Table 1). The adjective was then played and the participants were asked to make the appropriate judgement according to the cue that they had previously been given. All the adjectives were pseudo randomly drawn from a list of 100 German adjectives [41].

Each trial had a ten-second duration (3s pause + 2s cue + 5s adjective). Participants were asked to try to fixate their eyes on the cross and to move as little as possible for the duration of the experiment.

Data analysis

Individual frequency bands The θ and α boundaries were determined individually for each subject in both the eyes-open and eyes-closed resting conditions [40]. We employed the established observation that there is more power in the α frequency band in the eyes-

Cue	Activity
Self	Judge whether the following adjective characterises the participant themself
Friend	Judge whether the following adjective characterises the selected friend
Celebrity	Judge whether the following adjective characterises the selected celebrity
Count	Count syllables of the following adjective

Table 1. Experimental setup: Cues and corresponding activities

closed state than in the eyes-open state [40]. We computed the log-bandpower (fast Fourier transform (FFT) with a Hanning window of five-minute width) of the channel Oz, overlapped the two log-bandpower spectra and determined the intersections around the α peak. The upper θ (lower α) boundary was set, to the nearest integer, to the first intersection point before the α peak. The lower θ was set to the half of the upper θ (rounded up to the nearest integer). The upper α (lower β) boundary was set, to the nearest integer, to the first intersection point after the α peak. The upper β boundary was set to 30 Hz, the lower γ to 30 – 45 Hz and the upper γ to 55 – 85 Hz.

Independent component analysis artefact attenuation EEG recordings are often contaminated by muscle (EMG) [42] and ocular (EOG) artefacts [43]. We attenuated the effects of these artefacts by using second-order blind identification (SOBI) independent component analysis (ICA) [44]. Specifically, the data from each subject were first high-pass filtered with a third-order Butterworth filter with cutoff frequency of 0.1 Hz and separated into independent components (ICs). The ICs were then inspected visually and deemed to be cortical if they fulfilled the following criteria [45]: (i) the IC spectrum followed the cortical $\frac{1}{f}$-behaviour, (ii) the IC topography was dipolar, (iii) the IC time series contained no EOG-like activity (eyelid blinks, eye movements), and (iv) the IC time series contained no other artefacts (50Hz line noise, large spikes). Only the cortical ICs that satisfied one of these conditions were re-projected on the 121 electrodes in order to obtain clean data with the muscular, ocular and other artefacts attenuated. We obtained $18, 18 \pm 3, 12$ cortical ICs for healthy participants and $13, 6 \pm 2, 12$ cortical ICs for ALS patients the implications of different number of cortical ICs is discussed later in the Discussion section.

Beamforming Following the results of a previous fMRI study of healthy participants, in the present study we expect to see modulation in right MPFC [30]. The MPFC is situated on the inside between the two cerebral hemispheres, and thus is not directly accessible by EEG measurements taken on the surface of the scalp. The MPFC activity can be evaluated with a source localisation procedure. For this purpose, we first

generated a forward model for K = 15,028 dipoles spread over the cortex with the BrainStorm toolbox [46] for standardised electrode locations and a standardised three-shell spherical head model. There is no established method for localising the MPFC with EEG. Therefore, we manually selected the voxels that overlapped with areas that were found to be modulated with self-referential thinking in a previous fMRI study (Fig.2, [30]). We selected a larger area than that reported by Heatherton et al. in order to account for the lower spatial precision of EEG as compared to fMRI. Source localisation
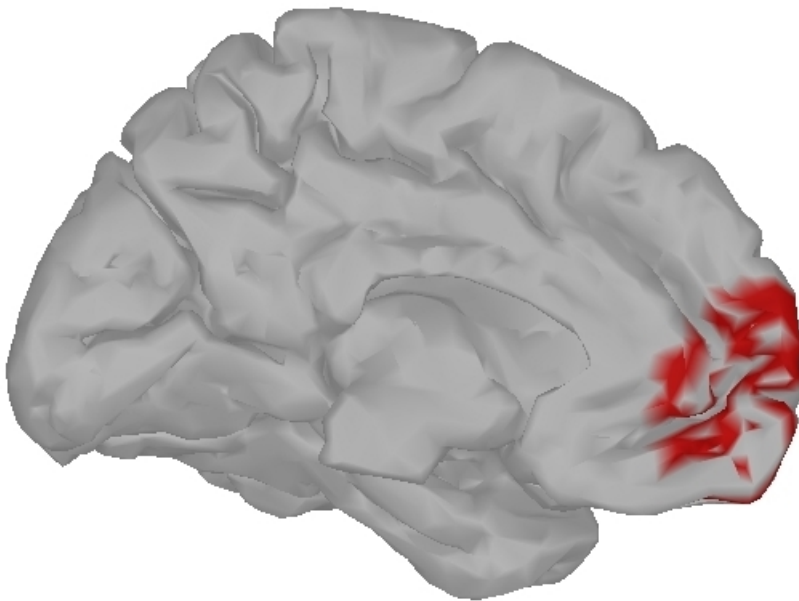
Figure 2. Beamformer target. Right hemisphere medial view: Voxels chosen for the beamformer are shown in red.

was performed with linearly constrained minimum variance (LCMV) beamforming [47]. LCMV beamforming is an adaptive spatial filter that attenuates the activity of the sources outside a region of interest (ROI), while preserving the activity from the sources within the ROI. The ROI activity $y[t]$ is estimated as the dot product between the spatial filter $\mathbf{w}^*$ and the EEG measurements at N electrode locations $\mathbf{x}[t] \in R^N$: $y[t] = \mathbf{w}^{*T}\mathbf{x}[t]$. The spatial filter is obtained by solving the optimisation problem

$$\mathbf{w}^* = \underset{\mathbf{w}}{\operatorname{argmin}}\{\mathbf{w}^T\Sigma_{EEG}\mathbf{w}\} \text{ s.t. } \mathbf{w}^T\mathbf{a} = 1, \tag{1}$$

which has the analytic solution [47]

$$\mathbf{w}^* = (\mathbf{a}^T\Sigma_{EEG}^{-1}\mathbf{a})^{-1}\mathbf{a}^T\Sigma_{EEG}^{-1}. \tag{2}$$

Here, $\Sigma_{EEG} \in R^{N \times N}$ is the spatial covariance matrix of the EEG data computed for every subject from the experimental data (pre-filtered for 1–100 Hz with 3rd-order

Butterworth filter); $\mathbf{a} \in \mathbb{R}^N$ is the average topography of the MPFC dipole projections on the scalp, which are provided by the forward model.

Statistical testing   We computed the log-bandpower estimates of the beamformed signal from the MPFC for every subject and every trial, as now described. Each five-second window after the adjective presentation onset was multiplied with a Hann window, an FFT was performed, and the log-bandpower was calculated and averaged over the individual frequency bands (θ, α, β, low γ, high γ). For visualisation purposes (Fig. 3), we averaged the log-bandpower over the trials and subjects for each group (healthy and ALS). We performed the same averaging for log-bandpower in the individual frequency bands and then subtracted the averaged log-bandpower in the control condition from the averaged log-bandpower in every other condition for every frequency band (Fig. 3, inset). We performed analysis of variance (ANOVA) on the log-bandpower averaged over the individual frequency bands using a general linear factorial model. The band power was analysed for healthy subjects and for ALS patients separately in an n-way mixed ANOVA, with condition ("self", "friend", "celebrity") and frequency band (θ, α, β, low γ, high γ) as within-subjects variables and subject as a between-subjects variable. All tests of significance were performed at $\alpha = .05$. For control, we performed the same calculations with the four conditions ("self", "friend", "celebrity", "count"). This allowed us to identify the effects that were specific to self-referential processing and to exclude possible confounding due to the inability of participants to follow the instructions due to general cognitive decline, lack of concentration, misunderstanding of instructions, falling asleep during the experiment, etc. After testing our hypothesis, we performed an additional post-hoc exploratory analysis. Specifically, we pointed a beamformer at each of the 15,028 dipoles, computed the log-bandpower estimates for every subject and trial (pre-multiplied with the five-second width Hann window) and performed ANOVA, as described above.

Results

First, we analysed the differences between the self-referential and control conditions in order to ensure that the participants were able to follow the instructions. Both healthy participants and ALS patients showed modulations of MPFC log-bandpower for different conditions, with less log-bandpower in the control non-self-referential condition than in the self-referential conditions (Fig. 3). We performed an ANOVA to test whether the log-bandpowers averaged over the individual frequency bands (Fig. 3, inset) were significantly different for the self-referential ("self", "friend", "celebrity") and control ("count") conditions. A significant main effect of the condition ("self", "friend", "celebrity", "count") on bandpower was found both for healthy participants ($F(3, 3983) = 9.17$, $p = 0.0000$) and for ALS patients ($F(3, 3999) = 5.94$, $p = 0.0005$). This agrees with previous EEG, fMRI and PET studies with healthy participants [29–34], which also found that MPFC activity differs between self-referential and
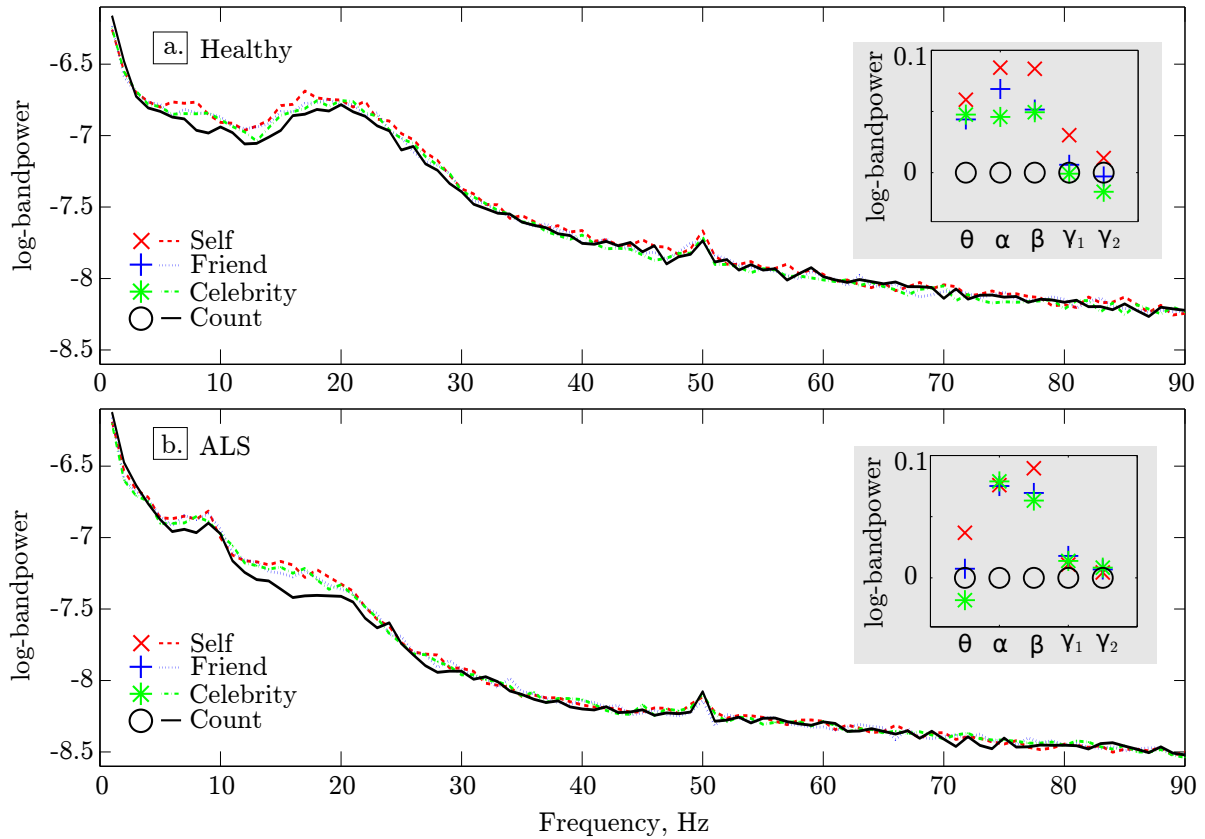
Figure 3. Mean MPFC log-bandpower for the conditions "self", "friend", "celebrity", "count" for a. healthy participants and b. ALS patients. Inset plot shows for every frequency band the modulation of the mean log-bandpowers in the self-referential conditions relative to the control ("count") condition. The mean log-bandpower is averaged over subjects and trials for every frequency band. γ_1 indicates low γ and γ_2 indicates high γ.

non-self-referential processing. This also suggests that both healthy participants and ALS patients engage the MPFC differently for self-referential and non-self-referential (control) tasks. Thus, both groups were able to understand and follow the experimental tasks. To investigate the effect of the degree of self-referentiality on the MPFC EEG, we omitted the control ("count") condition and performed the ANOVA again. We found that a main effect of the self-referential conditions ("self", "friend", "celebrity") on bandpower remained significant for healthy participants $F(2, 2984) = 4.03$, $p = 0.0179$. This agrees with previous EEG, fMRI and PET studies with healthy participants [29–34], which also found significant modulation of the MPFC by different degrees of self-referential processing. However, a main effect of the self-referential conditions ("self", "friend", "celebrity") on bandpower was not significant for ALS patients: $F(2, 2984) = 1.26$, $p = 0.2837$. These results suggest that there are differences in the MPFC activations between healthy individuals and ALS participants in self-referential processing. After testing our hypothesis, we further investigated whether brain regions beyond the MPFC are involved in self-referential processing in ALS patients. For this,
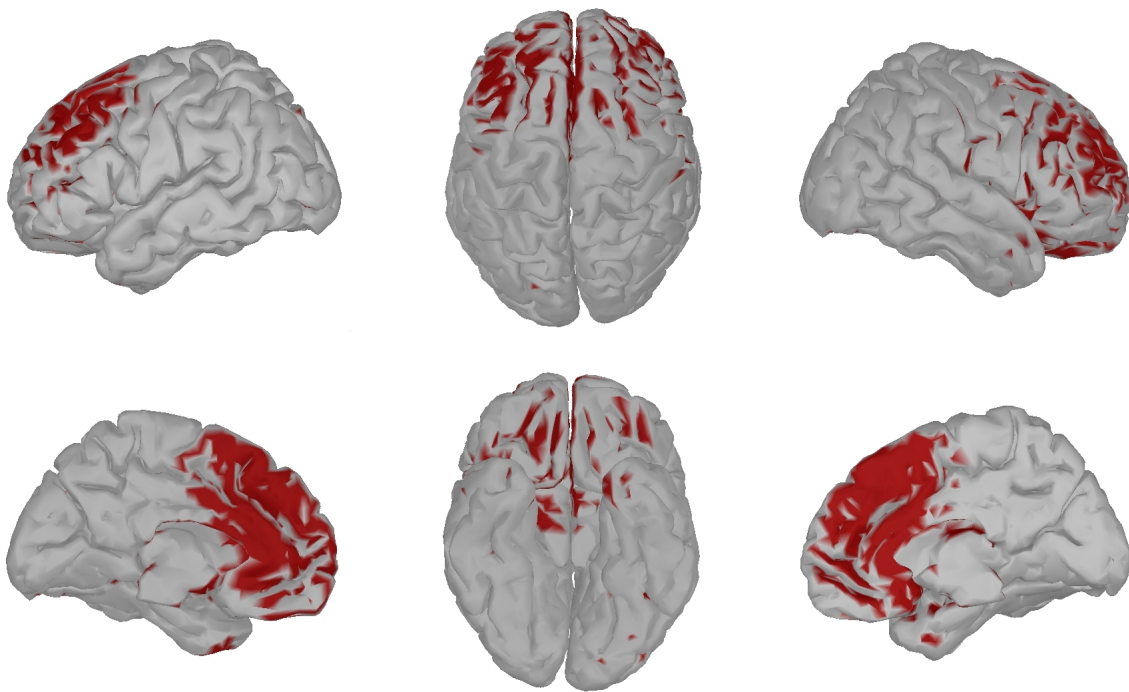
Figure 4. Healthy controls: p-value brain map. Color shows voxels with $p < 0.05$
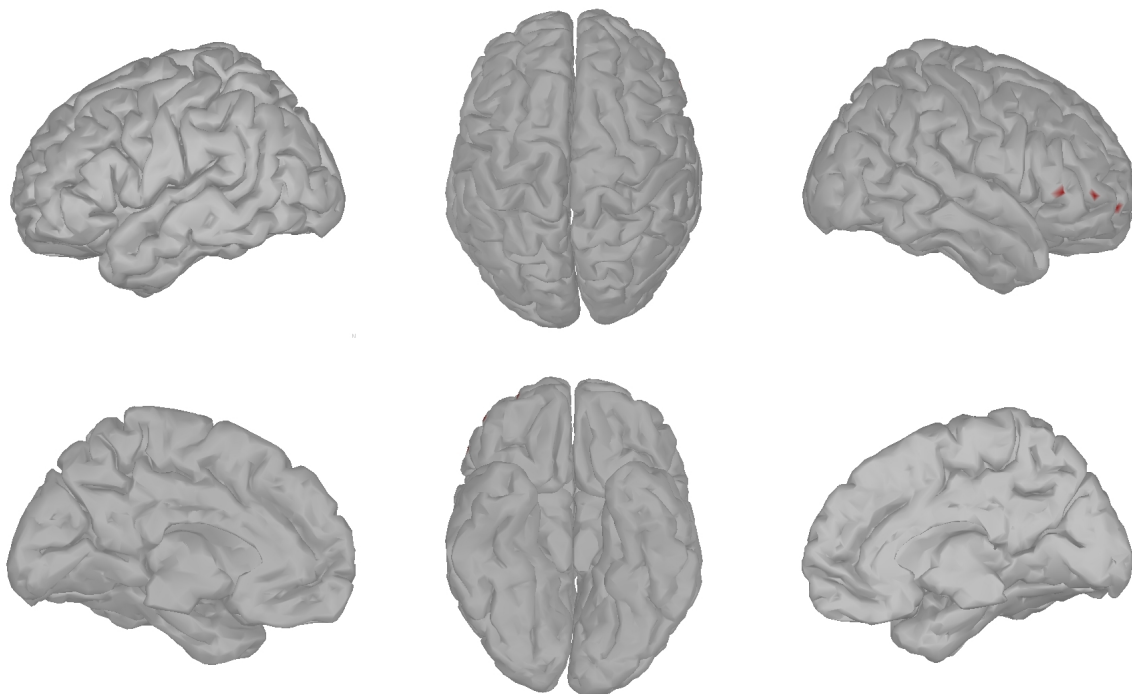

Figure 5. ALS patients: p-value brain map. Color shows voxels with $p < 0.05$

we performed an ANOVA on log-bandpowers in three self-referential conditions ("self", "friend", "celebrity") for all brain voxels. Figs. 4 and 5 show brain areas of healthy controls and ALS patients for which the main effect of the self-referential condition on

log-bandpower has a p-value below 5% (without correction for multiple comparisons). For the healthy controls, the *p*-value falls below 5% in the MPFC, with the DMPFC being more prominent. The latter agrees with a previous fMRI study that found the DMPFC to correlate specifically with trait judgments [32]. For ALS patients, no brain region showed *p*-values below 5%. This observation suggests that there is an effect of depth of self-referential processing on EEG of healthy controls, but not on EEG of ALS patients. We did not correct for multiple comparisons in this exploratory analysis. As such, one can expect 5% of the tested voxels to show false-positive results. We observed more than 10% of the voxels to be statistically significant for healthy controls and less than 5% for ALS patients, which means no cortical area of ALS patients gives rise to EEG log-bandpower being significantly modulated by the depth of self-referential processing.

Discussion

Our study broadens the scope of cognitive abnormalities in ALS patients. Impaired memory functions and emotion processing have been observed previously in non-demented ALS patients [5, 48, 49]. In combination, these cognitive deficits can give rise to impaired self-awareness (anosognosia) [36]. We tested the hypothesis of altered self-referential processing in ALS, and indeed we found alterations of the EEG correlates of self-referential processing in ALS patients when compared to healthy controls. The observed results cannot be explained simply by impaired attention [49] or the inability of patients to understand a given task. Both patients and healthy participants showed significantly distinct levels of activation in the MPFC for self-referential and counting conditions. This suggests that both groups understood and were able to perform the task. Thus, the alterations in neural processing that were detected by EEG were specific to self-referential processing and might indicate that ALS patients have difficulties in distinguishing themselves from others. Our results agree with the serotogenic model of ALS progression [25] that discussed in the Introduction (Fig. 1). However, we cannot exclude the possibility that the alterations to self-referential processing were caused not by ALS directly, but rather by other confounding factors. For example, long-term paralysis and inability to act and communicate can change the way one sees oneself and others. Birbaumer et al. suggested that the inability to act leads to thought-extinction [50]. Such thought extinction might be specific to thoughts about oneself, as one cannot observe one's own actions any more, but one can still observe the actions of others. This hypothesis was proposed by Heilman et al. , who argued that the lack of sensory feedback and the inability to observe one's own body acting can cause anosognosia [51]. Depression might also contribute to alterations in self-referential thinking [52]. Although none of the participants in this study had been diagnosed with depression, it should be noted that depression diagnosis with CLIS patients is not possible and, thus depression cannot be excluded. Nevertheless, previous studies found no correlation between depression and cognitive impairment in

ALS [9]; another study showed that depression is relatively rare in ALS patients [53]. Our results may have been confounded by the preprocessing steps. In particular, we observed fewer cortical ICs for ALS patients than for healthy controls. As such, it would have been possible to have rejected the IC connected with self-referential thinking for ALS patients. Nevertheless, this would mean that such IC follows the criteria for cortical ICs in healthy participants, but not in ALS patients; this would support our hypothesis that EEG correlates of self-referential thinking are altered in ALS. Altered self-referential processing and lack of self-awareness is associated with a number of neurodegenerative and psychiatric disorders [36]: schizophrenia [37, 54], Alzheimer disease [55, 56], frontotemporal dementia (FTD) [36]. In fact, anosognosia is so common in FTD, that it is used as a major criterion for diagnosis of FTD [57]. Physiologically, FTD is characterised by degeneration of frontal areas that leads to cognitive processing disruption. FTD often co-occurs with ALS and shares genetic correlates with ALS [2, 58]. Although it is usually considered to be an independent disease, there might be a continuum between ALS and FTD, with symptoms of each individual disease being more or less pronounced in different patients [2, 5, 10, 59]. Our results support the theory of an ALS-FTD continuum since we found alterations in EEG that were related to self-referential processing in ALS patients who had not been diagnosed with FTD. None of the participants in the present study had been diagnosed with FTD, and neither the experimenters nor the family reported any abnormalities in the behaviour of the patients. We speculate that EEG correlates of self-referential processing are able to detect changes in the brain at sub-clinical stages of the disease, before they become apparent from the exhibited behaviour. Tsermentseli et al. and Portet et al. previously reported similar observations whereby they found changes in the BOLD fMRI signal and ERPs both in the cognitively impaired patients and in those who showed no signs of cognitive impairment [5, 10]. Tsermentseli et al. suggested that neuroimaging alterations precede clinical symptoms in the cognitive domain. Similarly, anatomical alterations precede the decline of motor functions; muscle atrophy develops only when at least one third of the motor neurons are affected [60]. A longitudinal study of 52 patients with sporadic ALS over an 18-month period showed that cognitive deficits progress more slowly than motor deficits [48]. In this case, cognitive deficits, and especially deficits in self-referential thinking, might develop in many ALS patients in the late stages of the disease, in particular after entering the CLIS stage when, due to the lack of communication means, they cannot be detected any more with conventional behavioural tests and questionnaires. With self-referential processing being a key component of consciousness [61], the question arises whether the consciousness of the CLIS ALS patients is also altered. Alterations to consciousness [62] might explain the decreased activation of the DMN observed in ALS patients [28] and the difficulty of communication attempts using Brain-Computer Interfaces (BCI) in CLIS ALS patients [63]. Future studies should address the problem of consciousness in CLIS ALS patients. Even though established fMRI methods for consciousness estimation exist [62], it can be difficult to use these methods with CLIS patients for safety reasons.

EEG methods for consciousness estimation, for example entropy estimation, should be used to determine the level of consciousness of CLIS ALS patients [64]. The issue of consciousness in CLIS ALS has implications not only for ALS research and for the developers of BCI systems, but more importantly for patients and their families. This knowledge can affect the patient's perspective on their disease and influence their end-of-life decisions.

Acknowledgements

References

[1] K Nihei, A C McKee, and N W Kowall. Patterns of neuronal degeneration in the motor cortex of amyotrophic lateral sclerosis patients. *Acta Neuropathologica*, 86(1):55–64, June 1993.

[2] W Robberecht and T Philips. The changing scene of amyotrophic lateral sclerosis. *Nature reviews. Neuroscience*, 14(4):248–64, 2013.

[3] H Braak, J Brettschneider, A C Ludolph, V M Lee, J Q Trojanowski, and K Del Tredici. Amyotrophic lateral sclerosis–a model of corticofugal axonal spread. *Nature reviews. Neurology*, 9(12):708–14, 2013.

[4] R Schmidt, E Verstraete, M A de Reus, J H Veldink, L H van den Berg, and M P van den Heuvel. Correlation between structural and functional connectivity impairment in amyotrophic lateral sclerosis. *Human Brain Mapping*, 35(9):4386–4395, 2014.

[5] S Tsermentseli, P N Leigh, and L H Goldstein. The anatomy of cognitive impairment in amyotrophic lateral sclerosis: More than frontal lobe dysfunction. 48(2):166–182, 2012.

[6] S McCullagh, M Moore, M Gawel, and A Feinstein. Pathological laughing and crying in amyotrophic lateral sclerosis: An association with prefrontal cognitive dysfunction. *Journal of the Neurological Sciences*, 169(1-2):43–48, 1999.

[7] N T Olney, M S Goodkind, C Lomen-Hoerth, P K Whalen, C A Williamson, D E Holley, A Verstaen, L M Brown, B L Miller, J Kornak, R W Levenson, and H J Rosen. Behaviour, physiology and experience of pathological laughing and crying in amyotrophic lateral sclerosis. In *Brain*, volume 134, pages 3455–3466. Oxford University Press, 2011.

[8] E K Zimmerman, P J Eslinger, Z Simmons, and A M Barrett. Emotional perception deficits in amyotrophic lateral sclerosis. *Cognitive and behavioral neurology : official journal of the Society for Behavioral and Cognitive Neurology*, 20(2):79–82, 2007.

[9] P J Massman, J Sims, N Cooke, L J Haverkamp, V Appel, and S H Appel. Prevalence and correlates of neuropsychological deficits in amyotrophic lateral sclerosis. *Journal of neurology, neurosurgery, and psychiatry*, 61(5):450–5, 1996.

[10] F Portet, C Cadilhac, J Touchon, and W Camu. Cognitive impairment in motor neuron disease with bulbar onset. *Amyotrophic lateral sclerosis and other motor neuron disorders : official publication of the World Federation of Neurology, Research Group on Motor Neuron Diseases*, 2(1):23–9, 2001.

[11] C Lomen-Hoerth, J Murphy, S Langmore, J H Kramer, R K Olney, and B Miller. Are amyotrophic lateral sclerosis patients cognitively normal? *Neurology*, 60(7):1094–1097, 2003.

[12] G M Ringholz, S H Appel, M Bradshaw, N A Cooke, D M Mosnik, and P E Schulz. Prevalence and patterns of cognitive impairment in sporadic ALS. *Neurology*, 65(4):586–590, 2005.

[13] A C Ludolph, K J Langen, M Regard, H Herzog, B Kemper, T Kuwert, I G Böttger, and L Feinendegen. Frontal lobe function in amyotrophic lateral sclerosis: a neuropsychologic and positron emission tomography study. *Acta neurologica Scandinavica*, 85(2):81–9, 1992.

[14] S Abrahams, L H Goldstein, J J Kew, D J Brooks, C M Lloyd, C D Frith, and P N Leigh. Frontal lobe dysfunction in amyotrophic lateral sclerosis. A PET study. *Brain : a journal of neurology*, 119 (Pt 6:2105–20, 1996.

[15] S Abrahams, L H Goldstein, J Suckling, V Ng, A Simmons, X Chitnis, L Atkins, S C R Williams, and P N Leigh. Frontotemporal white matter changes in amyotrophic lateral sclerosis. *Journal of Neurology*, 252(3):321–331, 2005.

[16] M C Mantovan, L Baggio, G Dalla Barba, P Smith, E Pegoraro, G Soraru, P Bonometto, and C Angelini. Memory deficits and retrieval processes in ALS. In *European Journal of Neurology*, volume 10, pages 221–227, 2003.

[17] C Dentel, L Palamiuc, A Henriques, B Lannes, O Spreux-Varoquaux, L Gutknecht, F René, A Echaniz-Laguna, J L Gonzalez De Aguilar, K P Lesch, V Meininger, J P Loeffler, and L Dupuis. Degeneration of serotonergic neurons in amyotrophic lateral sclerosis: A link to spasticity. *Brain*, 136(2):483–493, 2013.

[18] L Dupuis, O Spreux-Varoquaux, G Bensimon, P Jullien, L Lacomblez, F Salachas, G Bruneteau, P F Pradat, J P Loeffler, and V Meininger. Platelet serotonin level predicts survival in amyotrophic lateral sclerosis. *PLoS ONE*, 5(10), 2010.

[19] A Hahn, W Wadsak, C Windischberger, P Baldinger, A S Hflich, J Losak, L Nics, C Philippe, G S Kranz, C Kraus, M Mitterhauser, G Karanikas, S Kasper, and R Lanzenberger. Differential modulation of the default mode network via serotonin-1a receptors. *Proceedings of the National Academy of Sciences*, 109(7):2619–2624, 2012.

[20] C M Portas, B Bjorvatn, and R Ursin. Serotonin and the sleep/wake cycle: Special emphasis on microdialysis studies, 2000.

[21] C B Saper, T E Scammell, and J Lu. Hypothalamic regulation of sleep and circadian rhythms. *Nature*, 437(7063):1257–1263, 2005.

[22] I Arnulf, T Similowski, F Salachas, L Garma, S Mehiri, V Attali, V Behin-Bellhesen, V Meininger, and J P Derenne. Sleep disorders and diaphragmatic function in patients with amyotrophic lateral sclerosis. *American journal of respiratory and critical care medicine*, 161(3 Pt 1):849–56, 2000.

[23] S R. Soekadar, J Born, N Birbaumer, M Bensch, S Halder, A R Murguialday, A Gharabaghi, F Nijboer, B Scholkopf, and S Martens. Fragmentation of slow wave sleep after onset of complete locked-in state. *Journal of Clinical Sleep Medicine*, 9(9):951–953, 2013.

[24] R M Ahmed, R E A Newcombe, Amanda J Piper, S J Lewis, B J Yee, M C Kiernan, and R R Grunstein. Sleep disorders and respiratory function in amyotrophic lateral sclerosis. *Sleep Medicine Reviews*, 26:33–42, 2016.

[25] R Sandyk. Serotonergic mechanisms in amyotrophic lateral sclerosis. *The International journal of neuroscience*, 116(7):775–826, July 2006.

[26] M E Raichle, A M MacLeod, A Z Snyder, W J Powers, D A Gusnard, and G L Shulman. A default mode of brain function. *Proceedings of the National Academy of Sciences of the United States of America*, 98(2):676–682, 2001.

[27] R L Buckner, J R Andrews-Hanna, and D L Schacter. The Brain's Default Network. *Annals of the New York Academy of Sciences*, 1124(1):1–38, 2008.

[28] B Mohammadi, K Kollewe, A Samii, K Krampfl, R Dengler, and T F Münte. Changes of resting state brain networks in amyotrophic lateral sclerosis. *Experimental Neurology*, 217(1):147–153, 2009.

[29] W M Kelley, C N Macrae, C L Wyland, S Caglar, S Inati, and T F Heatherton. Finding the self? An event-related fMRI study. *Journal of cognitive neuroscience*, 14(5):785–794, 2002.

[30] T F Heatherton, C L Wyland, C N Macrae, K E Demos, B T Denny, and W M Kelley. Medial prefrontal activity differentiates self from close others. *Social cognitive and affective*

neuroscience, 1(1):18–25, 2006.

[31] A D'Argembeau, F Collette, M Van Der Linden, S Laureys, G Del Fiore, C Degueldre, A Luxen, and E Salmon. Self-referential reflective activity and its relationship with rest: A PET study. *NeuroImage*, 25(2):616–624, 2005.

[32] S Whitfield-Gabrieli, J M Moran, A Nieto-Castanon, C Triantafyllou, Rebecca Saxe, and J D E Gabrieli. Associations and dissociations between default and self-reference networks in the human brain. *NeuroImage*, 55(1):225–232, 2011.

[33] G G Knyazev. EEG correlates of self-referential processing. *Frontiers in human neuroscience*, 7(June):264, 2013.

[34] M Esslen, S Metzler, R Pascual-Marqui, and L Jancke. Pre-reflective and reflective self-reference: A spatiotemporal EEG analysis. *NeuroImage*, 42(1):437–449, 2008.

[35] Y Mu and S Han. Neural oscillations involved in self-referential processing. *NeuroImage*, 53(2):757–768, 2010.

[36] H J Rosen. Anosognosia in neurodegenerative disease. *Neurocase : case studies in neuropsychology, neuropsychiatry, and behavioural neurology*, 17(3):231–241, 2011.

[37] P O Harvey, J Lee, W P Horan, K Ochsner, and M F Green. Do patients with schizophrenia benefit from a self-referential memory bias? *Schizophrenia Research*, 127(1-3):171–177, 2011.

[38] J M. Cedarbaum, N Stambler, E Malta, C Fuller, D Hilt, B Thurmond, and A Nakanishi. The ALSFRS-R: A revised ALS functional rating scale that incorporates assessments of respiratory function. *Journal of the Neurological Sciences*, 169(1-2):13–21, 1999.

[39] H C Lou, B Luber, M Crupain, J P Keenan, M Nowak, T W Kjaer, H Sackeim, and S H Lisanby. Parietal cortex and representation of the mental Self. *Proceedings of the National Academy of Sciences*, 101(17):6827–6832, 2004.

[40] W Klimesch. EEG alpha and theta oscillations reflect cognitive and memory performance: a review and analysis. *Brain Research Reviews*, 29(2–3):169–95, 1999.

[41] P Schönbach. Likableness ratings of 100 German personality-trait words corresponding to a subset of Anderson's 555 trait words. *European Journal of Social Psychology*, 2(3):327–333, 1972.

[42] I I Goncharova, D J McFarland, T M Vaughan, and J R Wolpaw. EMG contamination of EEG: Spectral and topographical characteristics. *Clinical Neurophysiology*, 114(9):1580–1593, 2003.

[43] D Hagemann and E Naumann. The effects of ocular artifacts on (lateralized) broadband power in the EEG. *Clinical Neurophysiology*, 112(2):215–231, 2001.

[44] A Belouchrani, K Abed-Meraim, JF Cardoso, and E Moulines. A blind source separation technique using second-order statistics. *IEEE Transactions on Signal Processing*, 45(2):434–444, 1997.

[45] M Grosse-Wentrup and B Schölkopf. High γ-power predicts performance in sensorimotor-rhythm brain-computer interfaces. *Journal of neural engineering*, 9(4):046001, August 2012.

[46] J C Mosher, S Baillet, F Darvas, D Pantazis, E K Yildirim, and R M Leahy. Brainstorm electromagnetic imaging software. In *5th International Symposium on Noninvasive Functional Source Imaging within the Human Brain and Heart (NFSI 2005)*, 2005.

[47] B D van Veen, W van Drongelen, M Yuchtman, and A Suzuki. Localization of brain electrical activity via linearly constrained minimum variance spatial filtering. *IEEE Transactions on Bio-Medical Engineering*, 44(9):867–880, 1997.

[48] H Schreiber, T Gaigalat, U Wiedemuth-Catrinescu, M Graf, I Uttner, R Muche, and A C Ludolph. Cognitive function in bulbar- and spinal-onset amyotrophic lateral sclerosis: A longitudinal study in 52 patients. *Journal of Neurology*, 252(7):772–781, 2005.

[49] E H Pinkhardt, R Jürgens, W Becker, M Mölle, J Born, A C Ludolph, and H Schreiber. Signs of impaired selective attention in patients with amyotrophic lateral sclerosis. *Journal of neurology*, 255(4):532–8, 2008.

[50] N Birbaumer, F Piccione, S Silvoni, and M Wildgruber. Ideomotor silence: the case of complete paralysis and brain-computer interfaces (BCI). *Psychological Research*, 76(2):183–91, 2012.

[51] K M Heilman, a M Barrett, and J C Adair. Possible mechanisms of anosognosia: a defect in self-awareness. *Philosophical transactions of the Royal Society of London. Series B, Biological*

sciences, 353(1377):1903–1909, 1998.

[52] Y I Sheline, D M Barch, J L Price, M M Rundle, S N Vaishnavi, A Z Snyder, M Mintun, S Wang, R S Coalson, and M E Raichle. The default mode network and self-referential processes in depression. *Proceedings of the National Academy of Sciences of the United States of America*, 106(6):1942–7, 2009.

[53] A J Averill, E J Kasarskis, and S C Segerstrom. Psychological health in patients with amyotrophic lateral sclerosis. *Amyotrophic Lateral Sclerosis : Official Publication of the World Federation of Neurology Research Group on Motor Neuron Diseases*, 8(4):243–54, 2007.

[54] D S Lehrer and J Lorenz. Anosognosia in Schizophrenia : Hidden in. *Innovations in clinical neuroscience*, 11(5-6):10–7, 2014.

[55] E Salmon, P Ruby, D Perani, E Kalbe, S Laureys, S Adam, and F Collette. Two aspects of impaired consciousness in Alzheimer's disease, 2005.

[56] S E Starkstein. Anosognosia in Alzheimer's disease: Diagnosis, frequency, mechanism and clinical correlates, 2014.

[57] D Neary, J S Snowden, L Gustafson, U Passant, D Stuss, S Black, M Freedman, A Kertesz, P H Robert, M Albert, K Boone, B L Miller, J Cummings, and D F Benson. Frontotemporal lobar degeneration: a consensus on clinical diagnostic criteria. *Neurology*, 51(6):1546–1554, 1998.

[58] J Grosskreutz, J Kaufmann, J Frädrich, R Dengler, H-J Heinze, and T Peschel. Widespread sensorimotor and frontal cortical atrophy in Amyotrophic Lateral Sclerosis. *BMC neurology*, 6:17, 2006.

[59] M J Strong, C Lomen-Hoerth, R J Caselli, E H Bigio, and W Yang. Cognitive impairment, frontotemporal dementia, and the motor neuron diseases. In *Annals of Neurology*, volume 54, 2003.

[60] G Wohlfahrt. Collateral regeneration in partially denervated muscle. *Neurology*, 7:124–134, 1957.

[61] G M Edelman. Naturalizing consciousness: a theoretical framework. *Proceedings of the National Academy of Sciences of the United States of America*, 100(9):5520–5524, 2003.

[62] A Vanhaudenhuyse, Q Noirhomme, L J F Tshibanda, M A Bruno, P Boveroux, C Schnakers, A Soddu, V Perlbarg, D Ledoux, J F Brichant, G Moonen, P Maquet, M D. Greicius, S Laureys, and M Boly. Default network connectivity reflects the level of consciousness in non-communicative brain-damaged patients. *Brain*, 133(1):161–171, 2010.

[63] M Marchetti and K Priftis. Brain-computer interfaces in amyotrophic lateral sclerosis: A metanalysis. *Clinical Neurophysiology : Official Journal of the International Federation of Clinical Neurophysiology*, 126(6):1255–63, 2015.

[64] J D Sitt, J R King, I El Karoui, B Rohaut, F Faugeras, Alexandre Gramfort, L Cohen, M Sigman, S Dehaene, and L Naccache. Large scale screening of neural signatures of consciousness in patients in a vegetative or minimally conscious state. *Brain*, 137(8):2258–2270, 2014.

Chapter 6

Identification of the DMN with EEG

Identification of the Default Mode Network with Electroencephalography

Tatiana Fomina[1,2], Matthias Hohmann[1,2], Bernhard Schölkopf[1], and Moritz Grosse-Wentrup[1]

Abstract— **The Default Mode Network (DMN) is a brain resting-state network that is closely linked to consciousness and neuropsychiatric disorders. The DMN is routinely identified with functional magnetic resonance imaging (fMRI) or positron emission tomography (PET). However, both of these methods impose restrictions on the groups of patients that can be examined. We show that the DMN can also be identified by electroencephalography (EEG). Instructing subjects to alternate between self-referential memory recall and focusing on their breathing induces a spatial pattern of spectral band power modulation in the θ- and α-band (4–16 Hz) that is consistent with the DMN pattern observed with PET and fMRI. Since EEG is a portable, cheap, and safe technology, our work enables the characterization of DMN alterations in patient groups that are difficult to study with fMRI or PET.**

I. INTRODUCTION

The brain is composed of large-scale cortical networks that are intimately linked to high-level cognition [1], [2]. Among these networks, the default mode network (DMN) [3], comprising the precuneus/posterior cingulate cortex, medial prefrontal cortex, and the temporoparietal junction, is of particular interest, because it has been linked to neuropsychiatric disorders [4] and to the degree of consciousness [5].

A variety of neuroimaging techniques have been used to analyse the DMN. Functional Magnetic Resonance Imaging (fMRI) or Positron Emission Tomography (PET) are routinely used to identify the DMN, either by contrasting resting-state to task-induced DMN deactivation levels [3], [6] or by a functional connectivity analysis on resting-state recordings [7]. Several attempts have been also made to recover the DMN from magnetoencephalographic recordings (MEG) [8], [9]. Using resting-state data, De Pasquale et al. identified MEG correspondents of DMN with a topography of interregional band power correlations in the θ- (3.5–7 Hz), α- (8–13 Hz), and β- (14–25 Hz) band [8]. Brookes et al. identified MEG signatures of DMN activity by amplitude envelope correlations in the α-band (8–13 Hz) [9].

However, fMRI, PET and MEG are difficult to perform on certain groups of patients, such as severely paralysed patients in late stages of amyotrophic lateral sclerosis (ALS), that are dependent on artificial ventilation systems and thus cannot be easily put into the MRI, PET, or MEG scanners. In contrast, EEG is a portable, safe (non-invasive), cheap, and widespread technology, that can be used at the patient's home. EEG-based DMN characterisation would enable the investigation of alterations in DMN activity in a wide range of patients groups that are difficult to examine with other methods. In particular, the connectivity within the DMN is negatively correlated with the degree of consciousness impairment and thus could be used to distinguish the conscious state from the vegetative state in CLIS [5] patients, for whom the degree of consciousness cannot be concluded from behaviour due to the absence of communication.

Previous attempts to identify the DMN with EEG were only partially successful. Knyazev et al. partially reproduced DMN spatial features by first estimating current source density, then applying independent component analysis (ICA), and comparing the resulting resting-state α band (8–12 Hz) activation of the obtained ICs to that during social cognition tasks [10]. However, spatial overlap of the identified EEG-based DMN pattern with that of the fMRI-based DMN was restricted to only one node of the DMN (precuneus/posterior cingulate cortex). This prevented an analysis of the connectivity within the DMN, which is relevant for characterizing the degree of consciousness [5].

We devised a novel behavioural paradigm that allows us to obtain an EEG-based DMN pattern more similar to the regions identified by fMRI. We instructed healthy subjects to alternate between two experimental conditions, recalling of positive autobiographical memories and focusing on breathing, and then computed dynamic Statistical Parametric Maps (dSPM) [11] from high density EEG recordings in the two conditions. Comparing source level activations, we found θ- and α band power changes in the medial prefrontal cortex, the posterior cingulate cortex, and the temporoparietal junction - a pattern that is highly consistent with the DMN.

II. METHODS

A. Subjects

EEG data was recorded from eleven healthy subjects (eight male and three female, mean age 29.3 $\pm$ 8.3 years). All subjects gave informed consent to participate in the study according to guidelines set by the Max Planck Society and received 12 Euro per hour for their participation. The study was approved by an ethics committee of the Max Planck Society.

[1]Tatiana Fomina, Matthias Hohmann, Bernhard Schölkopf, Moritz Grosse-Wentrup are with Max Planck Institute for Intelligent Systems, Spemannstrae 41, 72076 Tübingen, Germany tfomina@tuebingen.mpg.de, matthias.hohmann@tuebingen.mpg.de, bs@tuebingen.mpg.de, moritzgw@tuebingen.mpg.de

[2]Tatiana Fomina, Matthias Hohmann are with the IMPRS for Cognitive and Systems Neuroscience, University of Tübingen, Österbergstr. 3, D-72074 Tübingen, Germany

B. Experimental Data

All data was recorded with 124 active electrodes at 500 Hz sampling frequency using actiCAP active electrodes and a BrainAmp amplifier (both provided by BrainProducts GmbH, Gilching, Germany). Electrodes were placed according to the extended 10-20 system, with the electrode P7P as the initial reference. All recordings were converted to common average reference. The stimuli presentation was realised with the BCI2000 and BCPy2000 toolboxes [12].

First, two resting states (eyes-open and eyes-closed) were recorded. For each resting state, subjects were placed in front of a computer screen at a distance of 1.25 ± 0.2 m and were instructed to relax and let their mind wander for five minutes. In the eyes-open condition, they were additionally asked to fixate on a cross in the middle of the screen. After that, the EEG in the conditions of self-reflective thoughts and breathing was recorded in three blocks with a short break (1-5 minutes) in between. Each block consisted of ten trials for each condition presented in pseudo-randomized order, resulting in 30 trials for each condition. In the beginning of each trial, instructions appeared on the screen, asking subjects either to recall positive autobiographic memories or to concentrate on their breathing. Simultaneously, the same instructions were read out by a male voice. After four seconds, the instructions disappeared and subjects performed the announced task while fixating on the white cross. After one minute, the word "Pause" appeared on the screen, indicating the end of the trial. The pause lasted for 5.5 ± 0.5 seconds, then the new trial began.

Due to technical problems, subject 9 had different number of trials per condition (27 and 33 trials). For that subject only the first 27 trials for each condition were used for the analysis.

C. Data analysis

1) Preprocessing: We used the time window 4–30 seconds of each trial and restricted our analysis to a combination of θ and α frequency bands (4–16 Hz, individually adjusted for each subject). The lower θ boundary was set to 4 Hz for all the subjects, while the upper α boundary was determined individually for each subject by determining the intersection of the spectral power of channel Oz between eyes-open and eyes-closed resting states [13]. For subject 5, the eyes-closed recordings were corrupted by noise, so the upper boundary of the individual α band was set to 14 Hz. The data was then bandpass-filtered with a 3rd order Butterworth filter in the θ- and in the α- frequency band, respectively, and downsampled to 50 Hz.

2) Dynamic Statistical Parametric Mapping: To project the sensor activations on the source level, we applied dSPM, a noise-normalized minimum norm estimate, to the preprocessed data. [11]. First, the forward model $\mathbf{x}[t] = A\mathbf{s}(t)$ was computed, with the matrix A specifying the projection of $K = 15028$ current dipoles spread over the cortex $\mathbf{s}[t] \in R^K$ on the $N = 124$ electrodes $\mathbf{x}[t] \in R^N$. We generated the forward model with the BrainStorm toolbox [14], using standardized electrode locations and a standardized three-shell spherical head model. Then, the activity of each source was estimated from the measurements of the electrical potential on the surface of the scalp at N electrode locations as described in [11]:

$$\tilde{\mathbf{s}}(t) = W\mathbf{x}(t), \text{ with } W = \Sigma A^T (A\Sigma A^T + C)^{-1}. \quad (1)$$

Here, Σ is the spatial covariance of the dipole strength vector $\Sigma = \mathbf{s}(t)\mathbf{s}(t)^T$, approximated by the identity matrix, and C is the sensor noise covariance matrix, computed individually for each subject from their eyes-open resting-state data The estimated time series $\tilde{\mathbf{s}}(t)$ were then normalized by the noise variance, leading to noise normalized activity estimate $\tilde{\mathbf{z}_\mathbf{i}}(t)$ at each time point t and location i [11]:

$$\tilde{\mathbf{z}_\mathbf{i}}(t) = \frac{\tilde{\mathbf{s}}_i(t)}{\sqrt{\mathbf{w}_i C \mathbf{w}_i^T}}, \quad (2)$$

where $\mathbf{w}_i$ is the ith row of the unmixing matrix W. We then estimated a noize-normalized current dipole power at each time point t and location i [11]. We made no assumptions on dipole orientation and thus averaged three dipoles for each location:

$$\tilde{\mathbf{q}_\mathbf{i}}(t) = \frac{\sum\limits_{j \in G_i} \tilde{\mathbf{s}}_i^2(t)}{\sum\limits_{j \in G_i} \mathbf{w}_i C \mathbf{w}_i^T}, \quad (3)$$

where G_i is the set of indices of dipoles located at i. As a last step, we averaged the current dipole power over the 4–30 seconds of each trial.

3) Statistical testing: We computed the signed coefficient of determination (signed R^2) for every subject and source to evaluate condition-induced differences between band power, averaged across the θ- and the α-band (4–16 Hz). To test the null-hypothesis H_0: $R^2 = 0$ that there is no difference between the two conditions on the group level we first estimated p-values for each subject. For that we randomly permuted the condition labels of the trials 10^3 times. We then counted the instances in which the resulting $|R^2_{HO}|$ exceeded $|R^2|$ and estimated the probability that $|R^2_{HO}| > |R^2|$. We thereby obtained a p-value for each of the $K = 15028$ sources and $M = 11$ subjects. Then, we computed the empirical cumulative distribution function (CDF) of these p-values across subjects for each source and quantified its deviations from a uniform CDF with support from zero to one by integrating the differences between the two CDFs. We drew samples from the uniform CDF 10^3 times. This enabled us to estimate the probability of observing the obtained p-values under H_0, because by construction p-values from a null-distribution are uniformly distributed between zero and one. As a last step, we corrected the significance level using a false discovery rate (FDR) of $\alpha_{FDR} = 0.05$ [15] to compensate for the multiple comparisons for each of the K cortical sources.

To plot the results, we averaged the signed R^2 across subjects and set the signed $R^2 = 0$ for the sources for which we could not reject the null-hypothesis.
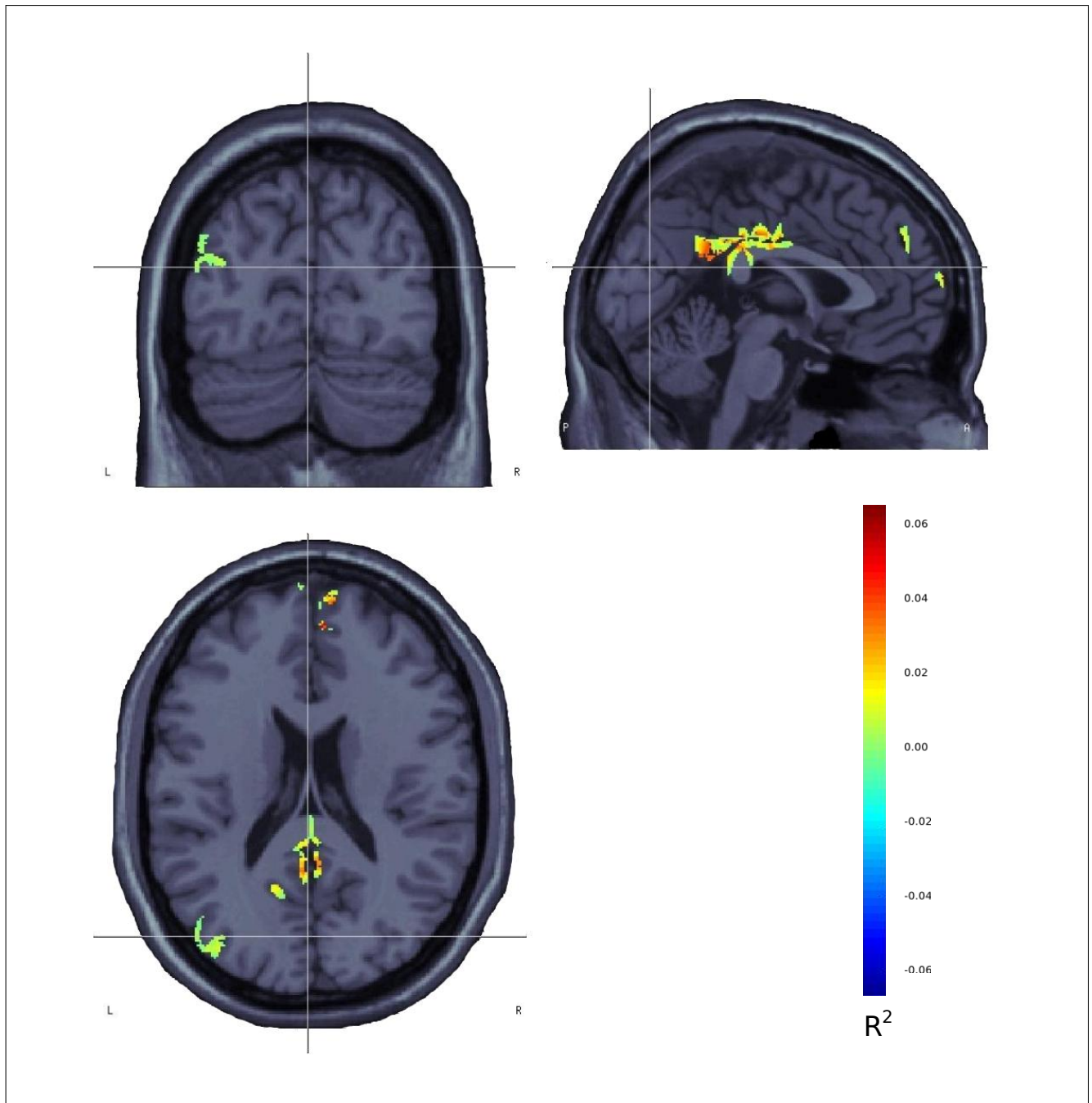
Fig. 1. The Default Mode Network (DMN) identified with EEG. Signed R^2 between recalling of the positive autobiographical memories condition and focusing on breathing condition, averaged over the subjects for significant sources only (FDR corrected at 0.05). Orange shows positive correlation with the autobiographical memories condition, while blue areas are positively correlated with focusing on breathing.

III. RESULTS

Figure 1 displays the sources that we found to show a statistically significant modulation on the group-level. We find the most prominent modulation of band power in the posterior cingulate cortex, which constitutes a hub of the DMN [16]. In addition, we observe band power modulation in the medial prefrontal cortex and in the left temporo-parietal junction. With the exception of the right temporo-parietal junction, our method thus identifies the core areas of the DMN [3].

IV. DISCUSSION

Using the cognitive strategy of alternation between autobiographical memories and focusing on breathing, we identified a pattern of EEG band power modulation that is highly consistent with the DMN as characterized by PET [6], [18] and fMRI [3], [7], [17]. This is of particular significance for two reasons. First, this EEG-based identification of the DMN enables us to study oscillatory properties of the DMN that are not accessible by PET or fMRI. And second, our work makes it feasible to study DMN alterations in patient

groups that are difficult to study by with PET, fMRI and MEG, such as severely paralysed patients in late stages of ALS.

We note, however, that the EEG-based DMN nodes are smaller than those found by fMRI, despite the fact that fMRI has a higher spatial resolution. One potential reason for this observation is the low spatial resolution of EEG source localization methods. Due to inter-subjects differences in head shape and cortex folding, the spatial overlap between individual DMN patterns may be smaller than each individual DMN pattern on its own. On the group level, this may lead to a spatial underestimation of the DMN. This problem could be addressed by using individualised EEG forward models derived from structural MRI scans.

The difference between the two conditions arises from the properties of the DMN: self-referential thoughts, such as autobiographical memories, activate the DMN [6], [18], while task-related activity free from self-referential thoughts and memories, such as focusing on the breathing, induces DMN deactivation [3]. To capture the effect of self-referential processing, we restricted our analysis to the θ and α frequency bands (4-16 Hz), following the previous work of Mu et al. who correlated self-referential processing with spectral power in the θ and in the α range [19]. We combined the two bands, since PET and fMRI analysis are not frequency-specific and the DMN pattern obtained with those methods is likely to consist of neurons oscillating in different frequency ranges. Our choice of tasks, however, could also lead to underestimation of the extent of the DMN. While focusing on breathing has been shown to deactivate the DMN, it also increases synchronization within the DMN [20]. Because EEG is sensitive to synchronized oscillations, the increase in synchronisation may lead to an increase in the spectral power that is not distinguishable from changes in activation levels of the involved cortical areas. Further refining the behavioural paradigm may alleviate this problem.

Future studies need to investigate if EEG-based connectivity measures between nodes of the DMN correlate with levels consciousness in similar ways to fMRI-based connectivity patterns [5]. The EEG-based identification of the DMN brings a new exciting possibility of DMN characterisation to groups of patients that are difficult to study with other methods.

ACKNOWLEDGMENT

REFERENCES

[1] S. L. Bressler and V. Menon, "Large-scale brain networks in cognition: emerging methods and principles," Trends in Cognitive Sciences, vol. 14, no. 6. pp. 277-290, 2010.

[2] V. Menon, "Large-scale brain networks and psychopathology: A unifying triple network model," Trends in Cognitive Sciences, vol. 15, no. 10. pp. 483-506, 2011.

[3] M. E. Raichle, A. M. MacLeod, A. Z. Snyder, W. J. Powers, D. A. Gusnard, and G. L. Shulman, "A default mode of brain function.," Proceedings of the National Academy of Sciences of the United States of America, vol. 98, no. 2, pp. 676-682, 2001.

[4] S. Whitfield-Gabrieli and J. M. Ford, "Default Mode Network Activity and Connectivity in Psychopathology," Annual Review of Clinical Psychology, vol. 8, no. 1. pp. 49-76, 2012.

[5] A. Vanhaudenhuyse, Q. Noirhomme, L. J. F. Tshibanda, M. A. Bruno, P. Boveroux, C. Schnakers, A. Soddu, V. Perlbarg, D. Ledoux, J. F. Brichant, G. Moonen, P. Maquet, M. D. Greicius, S. Laureys, and M. Boly, "Default network connectivity reflects the level of consciousness in non-communicative brain-damaged patients," Brain, vol. 133, no. 1, pp. 161-171, 2010.

[6] R. N. Spreng, R. A. Mar, and A. S. N. Kim, "The common neural basis of autobiographical memory, prospection, navigation, theory of mind, and the default mode: a quantitative meta-analysis.," Journal of Cognitive Neuroscience, vol. 21, no. 3, pp. 489-510, 2009.

[7] M. D. Greicius, B. Krasnow, A. L. Reiss, and V. Menon, "Functional connectivity in the resting brain: a network analysis of the default mode hypothesis.," Proceedings of the National Academy of Sciences of the United States of America, vol. 100, no. 1, pp. 253-258, 2003.

[8] F. de Pasquale, S. Della Penna, A. Z. Snyder, C. Lewis, D. Mantini, L. Marzetti, P. Belardinelli, L. Ciancetta, V. Pizzella, G. L. Romani, and M. Corbetta, "Temporal dynamics of spontaneous MEG activity in brain networks.," Proceedings of the National Academy of Sciences of the United States of America, vol. 107, no. 13, pp. 6040-5, Mar. 2010.

[9] M. J. Brookes, M. Woolrich, H. Luckhoo, D. Price, J. R. Hale, M. C. Stephenson, G. R. Barnes, S. M. Smith, and P. G. Morris, "Investigating the electrophysiological basis of resting state networks using magnetoencephalography.," Proceedings of the National Academy of Sciences of the United States of America, vol. 108, no. 40, pp. 16783-8, Oct. 2011.

[10] G. G. Knyazev, J. Y. Slobodskoj-Plusnin, A. V. Bocharov, and L. V. Pylkova, "The default mode network and EEG alpha oscillations: An independent component analysis," Brain Research, vol. 1402, pp. 67-79, 2011.

[11] A. M. Dale, A. K. Liu, B. R. Fischl, R. L. Buckner, J. W. Belliveau, J. D. Lewine, and E. Halgren, "Dynamic Statistical Parametric Mapping," Neuron, vol. 26, no. 1. pp. 55-67, 2000.

[12] G. Schalk, D. J. McFarland, T. Hinterberger, N. Birbaumer, and J. R. Wolpaw, "BCI2000: A general-purpose brain-computer interface (BCI) system," IEEE Transactions on Biomedical Engineering, vol. 51, no. 6, pp. 1034-1043, 2004.

[13] W. Klimesch, "EEG alpha and theta oscillations reflect cognitive and memory performance: a review and analysis.," Brain research. Brain research reviews, vol. 29, no. 2-3, pp. 169-95, Apr. 1999.

[14] J. Mosher, S. Baillet, F. Darvas, D. Pantazis, E. Yildirim, R. Leahy, Brainstorm electromagnetic imaging software, in: 5th International Symposium on Noninvasive Functional Source Imaging within the Human Brain and Heart (NFSI 2005), 2005.

[15] Y. Benjamini and Y. Hochberg, "Controlling the False Discovery Rate: A Practical and Powerful Approach to Multiple Testing," Journal of the Royal Statistical Society. Series B (Methodological), vol. 57, no. 1, pp. 289-300, 1995.

[16] P. Fransson and G. Marrelec, "The precuneus/posterior cingulate cortex plays a pivotal role in the default mode network: Evidence from a partial correlation network analysis," NeuroImage, vol. 42, no. 3, pp. 1178-1184, 2008.

[17] A. Vanhaudenhuyse, A. Demertzi, M. Schabus, Q. Noirhomme, S. Bredart, M. Boly, C. Phillips, A. Soddu, A. Luxen, G. Moonen, and S. Laureys, "Two distinct neuronal networks mediate the awareness of environment and of self.," Journal of Cognitive Neuroscience, vol. 23, no. 3, pp. 570-578, 2011.

[18] N. C. Andreasen, D. S. O'Leary, T. Cizadlo, S. Arndt, K. Rezai, G. L. Watkins, L. L. B. Ponto, and R. D. Hichwa, "Remembering the past: Two facets of episodic memory explored with positron emission tomography," American Journal of Psychiatry, vol. 152, no. 11, pp. 1576-1585, 1995.

[19] Y. Mu and S. Han, "Neural oscillations involved in self-referential processing," NeuroImage, vol. 53, no. 2, pp. 757-768, 2010.

[20] J. A. Brewer, P. D. Worhunsky, J. R. Gray, Y.-Y. Tang, J. Weber, and H. Kober, "Meditation experience is associated with differences in default mode network activity and connectivity," Proceedings of the National Academy of Sciences, vol. 108, no. 50. pp. 20254-20259, 2011.

Acknowledgements